STREAM FLOW AND SEDIMENT YIELD MODELING: THE CASE OF ROBI JIDA WATERSHED, UPPER BLUE NILE BASIN, ETHIOPIA.

M.Sc. THESIS

BELSTI DEGU NURIE

HAWASSA UNIVERSITY, HAWASSA, ETHIOPIA

OCTOBER, 2024

STREAM FLOW AND SEDIMENT YIELD MODELING: THE CASE OF ROBI JIDA WATERSHED, UPPER BLUE NILE BASIN, ETHIOPIA.

BELSTI DEGU NURIE

A THESIS SUBMITTED TO

THE DEPARTMENT OF HYDRAULIC AND WATER RESOURCES ENGINEERING,

FACULTY OF BIOSYSTEMS AND WATER RESOURCES ENGINEERING,

INSTITUTE OF TECHNOLOGY, SCHOOL OF GRADUATE STUDIES

HAWASSA UNIVERSITY

HAWASSA, ETHIOPIA

IN PARTIAL FULFILLMENT OF THE

REQUIREMENTS FOR THE

DEGREE OF

MASTER OF SCIENCE IN HYDRAULIC AND WATER RESOURCES ENGINEERING

(SPECIALIZATION: HYDRAULIC ENGINEERING)

OCTOBER, 2024

SCHOOL OF GRADUATE STUDIES

HAWASSA UNIVERSITY ADVISORS' APPROVAL SHEET

This is to certify that the thesis entitled "**Stream Flow and Sediment Yield Modeling; the case of Robi Jida Watershed, Upper Blue Nile Basin, Ethiopia"** submitted in partial fulfillment of the requirements for the degree of Master's with specialization in Hydraulic Engineering, the Graduate Program of the Department of Hydraulic and Water Resources Engineering, Hawassa University, institute of technology and has been carried out by **Belsti Degu Nurie ID. No.GPHydr R/0004/14**, under my/our supervision. Therefore, we recommend that the student has fulfilled the requirements and hence hereby can submit the thesis to the department.

Approved by:

Major Advisor Shemelies Asseffa (Ph.D.)	_____	_____
Name	Signature	Date
Co-Advisor Mebiratu Esubalew (M.Sc.)	_____	_____
Name	Signature	Date

SCHOOL OF GRADUATE STUDIES

HAWASSA UNIVERSITY EXAMINERS' APPROVAL SHEET

We, the undersigned, members of the Board of Examiners of the final open defense by Belsti Degu Nurie have read and evaluated his thesis entitled "**Stream Flow and Sediment Yield Modeling; the case of Robi Jida Watershed, Upper Blue Nile Basin, Ethiopia"**, and examined the candidate. This is, therefore, to certify that the thesis has been accepted in partial fulfillment of the requirements for the degree of Masters of Science in Hydraulic and Water Resources Engineering specializing in Hydraulic Engineering.

Name of Chairperson	Signature	Date
Name of Major Advisor	Signature	Date
Name of Co-Advisor	Signature	Date
Name of Internal Examiner	Signature	Date
Name of External Examiner	Signature	Date
SGS Approval	Signature	Date

Final approval and acceptance of the thesis is contingent upon submitting the final copy to the School of Graduate Studies (SGS) through the Department/School Graduate Committee (DGC/SGC) of the candidate's department.

Stamp of SGS **Date: _____**

ACKNOWLEDGEMENT

Above all, I would like to thank the creator and governor of the world, ‘almighty God’, for his mother, St. Virgin Mary, all his angels and saints for their priceless and miraculous gift of giving me life, who showered their generous grace and wisdom, and who made it possible to begin and finish this work successfully.

My first and foremost heartfelt thanks go to my esteemed Advisor, **Shemelies Asseffa (Ph.D.)**, for his valuable guidance, scientific and innovative advice, positive criticism, support, and recommendations throughout my thesis work. Without his constant supervision and timely help, this thesis would not have been possible. I have learned, explored, and advanced from him. I am thankful to my second Advisor, **Mebiratu Esubalew (M.Sc.)**, for his very kindness and willingness to help me in any way possible and for his support of data science and documentation.

My second great gratitude goes to different institutions, including the National Meteorological Service Agency of Ethiopia, and the Minister of Water and Energy. I would also like to acknowledge Alage ATVET College for the financial support and the opportunity to do my Master's Degree during the last three years.

I am grateful to Mr Bantamlak Kasse for his valuable suggestions, constructive comments, and support throughout my thesis preparation. Finally, I would like to thank my friends and staff members of Hawassa University and Alage ATVET College for helping me during my work. Your assistance and support are greatly appreciated. I remain grateful to all of you who directly or indirectly contributed information to the success of my thesis work.

TABLE OF CONTENTS

LIST OF FIGURES

LIST OF TABLES

LIST OF TABLES IN APPENDIXES

LIST OF FIGURES IN APPENDIXES

DECLARATION

I hereby declare that this MSc thesis is my original work and has not been presented for a degree award in any other university, and all sources of material used for this thesis have been duly acknowledged.

Name: Belsti Degu Nurie

Signature: _____

Date of Submission: _____

Place: Hawassa University

LIST OF ABBREVIATIONS AND ACRONYMS

ATVET	Agricultural Technical, Vocational and Educational Training
Arc GIS	Aeronautical Reconnaissance Coverage Geographic Information System
BMPs	Best management practices
DEM	Digital Elevation Model
EHRS	Ethiopian Highland Reclamation Study
EMI	Ethiopian Meteorological Institute
GIS	Geographic Information System
GLUE	Generalized Likelihood Uncertainty Estimation
HRU	Hydrologic Response Unit
LULC	Land Use/ Land Cover
M.A.S.L	Meter above sea level
MCMC	Markov Chain Monte Carlo
MoWE	Ministry of Water and Energy
MUSLE	Modified Universal Soil Loss Equation
SCS	Soil Conservation Service
SSA	Sub-Saharan Africa
SUFI-2	Sequential Uncertainty Analysis Fitting version 2
SWAT-CUP	SWAT Calibration and Uncertainty Procedure
SWAT	Soil and Water Assessment Tool
SWC	Soil and Water Conservation
SWCP	Soil and Water Conservation Practices
USDA-ARS	United States Department of Agriculture –Agriculture Research Service
USDA-SCS	United States Department of Agriculture Soil Conservation Service
USLE	Universal Soil Loss Equation
WGEN	Weather Generator

ABSTRACT

*Soil erosion, streamflow, and sediment studies are crucial for supporting the agricultural sector through watershed planning and management practices. This study aimed to model stream flow and sediment yield in the Robi Jida watershed in the Upper Blue Nile Basin, Ethiopia, and identify best management scenarios with the records of suspended sediment concentration. The historical records of the meteorological, hydrological, and suspended sediment concentration data were used for the hydrological modeling. Sediment yield data was generated from the discharge-sediment rating curve equation using the suspended sediment concentration data. Spatially, 30*30 m DEM, 90*90m soil, and 30*30m resolution land use/land cover data were used as input for the hydrological model. In this study, the Soil and Water Assessment Tool (SWAT) model was used to model streamflow and sediment yield. The model performance in simulating streamflow and sediment yield was evaluated through sensitivity analysis, calibration, and validation processes. Period from 1994 to 2010 was used for calibration and 2011 to 2018 was used for validation. During calibration the model performance statics R^2, NSE, and PBIAS were obtained (0.80, 0.70), (0.80, 0.70), and (-4.8, 1.1) for stream flow and sediment yield respectively, and similarly for model validation R^2, NSE, PBIAS as obtained (0.77, 0.72), (0.77, 0.71), (-4.7, -5.7) respectively. Therefore, the result indicated that the SWAT model performed well and the estimated average annual sediment yield of the Robi Jida watershed was 6.42 tons/ha/year. Based on the average annual simulated sediment yield, identified 9 sub-watersheds are critical whose annual sediment yield limit ranges above the tolerable limit were identified and prioritized for effective watershed management. Therefore applying and evaluating the different management scenarios, filter stripe 1m and 5m, vegetative contour strip, soil/stone bund, terracing, and contouring resulted in a 19.15%, 35.01%, 47.13%, 57.09%, 73.37%, and 52.81% decrease in the average annual sediment yield, respectively. Therefore, soil/stone bund and terracing scenarios demonstrated the highest potential for reducing sediment yield and showed promising results as effective best management practices in the Robi Jida watershed.*

Keywords: SWAT model; Sediment Yield; Sediment rating curve; Simulation; and BMPs.

1. INTRODUCTION

1.1 Background

The Blue Nile River in Ethiopia supplies more than 60% of total discharge to the Nile River and originates in the Ethiopian highlands and flows to Sudan, where it meets the White Nile at Khartoum to form the Main Nile, traveling north to Egypt and finally into the Mediterranean Sea (Gebrekristos, 2015).

The upper Blue Nile River basin suffers from erosion and desertification problems that undesirably reduce soil fertility and agricultural productivity (Ali et al., 2014). Soil erosion is a serious global environmental problem (Kenderessy and Lieskovský, 2014) and a major watershed problem in many developing countries. There may be many derived from the watershed, sediment from the riverbed and banks will be transported with the flow as sediment transport, either in suspension or as bed load and ultimately, this sediment is redeposited and causes problems in downstream areas (Awulachew et al., 2008). It is accelerated by human mismanagement of land resources, which results in soil and land degradation and reduces forest and agricultural productivity (García-Orenes et al., 2012) induced by man's impact on a landscape, to remove the forest cover. Therefore soil erosion is among the most serious mechanisms of land degradation and soil fertility decline (Asmamaw and Mohammed, 2019). Soil erosion results in decreased soil fertility in the upper catchments and increase sedimentation in reservoirs and irrigation canals downstream (Gebrekristos, 2015).

Erosion and sedimentation are sequential phenomena that occur in the watershed and affect sustainable water resource planning and management. While erosion starts in the watershed, it creates suitable conditions for sediment accumulation based on soil erosion phases. Sedimentation is by product of erosion and happens when the flow velocity is decelerated by any flow retardation force (Tesfu, 2015). In addition, the rainfall-runoff-sediment relationship is an essential component in the process of evaluating water resources and is considered a central problem in hydrology. Many parameters affect runoff, such as rainfall, soil primitive wetness, earth surface material, geomorphology watershed, evaporation, infiltration rainfall distribution, rainfall duration, and so on (Remesan et al., 2009).

The presence of steep slopes, changes in land use and land cover, and inappropriate use of land (overgrazing, poor farming systems, etc.) are the main factors for intensive erosion. Soil

erosion has different effects like declining agricultural productivity due to the removal of fertile soil from the land (Aga et al., 2018) and reduction of the reservoir capacity due to sedimentation (Moges et al., 2018). The presence of recorded suspended sediment concentration data helps to characterize the basin or watershed in sediment yield, identify hotspot areas, and plan soil and water conservation practices. Nowadays, several dams are built for different purposes in Ethiopia, but, those dams are not functioning throughout their design period due to sedimentation (Moges et al., 2018). One of the reasons for the decline of agricultural productivity and reservoir capacity in Ethiopia was the inaccurate estimation of erosion and sedimentation in the planning and design stage (Moges, 2021). So, it is necessary to show the relevance of runoff and sediment management on water resource projects.

Records of suspended sediment concentration are limited in Ethiopia. This limited sediment concentration record presents challenges for planning and management options like stream flow and sediment yield modeling (Womber et al., 2021). So, accurate estimation of stream flow and sediment yield modeling is crucial for the planning and management of hydraulic structures constructed across a river, determining the capacity of reservoirs by estimating dead storage, reducing entering sediment into the reservoir by constructing sediment traps, and conducting watershed management in a watershed.

The main aim of this study is to model stream flow and sediment yield generated from the Robi Jida watershed using the Soil and Water Assessment Tool (SWAT) to understand the hydrological processes of different parts of this study area. Therefore, the purpose of this study was to investigate the stream flow and sediment distribution patterns in the Robi Jida watershed using the SWAT model for better water and land resource management.

1.2 Statement of the Problem

There is a significant knowledge gap regarding the importance of proper runoff, erosion, streamflow, and sediment management in water resource projects. The primary factors contributing to intense erosion and sedimentation are changes in land use/land cover and improper land practices. Researchers have conduct streamflow and sediment yield modeling in the Upper Blue Nile basin, identify erosion-prone areas, or implement effective soil and water conservation strategies. Nevertheless, this study face limitations when applied to small watersheds.

To address these issues, this research aim to bridge the understanding gap in streamflow and sediment yield modeling, specifically within the Robi Jida watershed. By collecting daily streamflow and sediment data and creating a sediment rating curve, the study aims to pinpoint erosion-prone areas within the watershed. This data will then guide the development of targeted erosion and sediment control strategies, known as Best Management Practices (BMPs).

This study aims to understand and predict the movement of water and sediment within the Robi Jida watershed. By utilizing the Soil and Water Assessment Tool (SWAT) and incorporate data on suspended sediment concentration, the researchers estimated streamflow and sediment yield at various sub-watershed levels. Analyzing spatial and temporal trends in this data would help identify areas most susceptible to erosion. This information is crucial for prioritizing and implementing effective soil and water conservation (SWC) practices throughout the watershed.

1.3 Objective of the Study

1.3.1 General Objective

The main objective of this study is to model stream flow and sediment yield in the Robi Jida watershed by using the SWAT hydrological model.

1.3.2 Specific Objectives

The specific objectives of the study are:

- ✓ To estimate the average annual sediment yield of Robi Jida watershed,
- ✓ To assess the spatial variability of sediment yield and identify erosion-vulnerable sub-catchments, and
- ✓ To determine appropriate best management scenarios to reduce sediment yield of the Robi Jida watershed.

1.4 Research Questions

The research questions for this study are:

- ✓ How much sediment yield is produced from the Robi Jida watershed annually?
- ✓ Which sub-catchment of Robi Jida is sensitive to excessive erosion?
- ✓ Which sediment management scenarios are best for the erosion-exposed areas in the Robi Jida watershed?

1.5 Scope of the Study

In this study, the modeling of stream flow and sediment yield from the Robi Jida watershed is up to the entrance of Jemma River. The land use land cover, soil, slope, meteorological, and hydrological data were used for stream flow and sediment simulation in the SWAT model. In addition; this study assessed the spatial variability of sediment yield, identified erosion-vulnerable sub-catchments, and conducted best management scenarios in the watershed for proper soil and water conservation (SWC) management options.

1.6 Significance of the Study

This study provided awareness of stream flow and sediment yield modeling in the Robi Jida watershed and understanding how stream flow and sediment yield modeling is important in water resources management practice in the watershed, which would help watershed managers, agricultural producers, and policymakers, but the resources have different problems. For instance, land resources are eroded due to different factors, which cause a reduction in soil fertility and crop production. As a result, resources like water and land need proper management practices to feed the coming generation. Moreover, it may help in the development of adaptive measures for water resources; it may reduce unnecessary losses from the water cycle. In addition, modeling stream flow and sediment yield, assessing the spatial variability of sediment yield, and identifying erosion-vulnerable sub-catchments in the Robi Jida watershed are the objectives of the study to conduct watershed management planning options to reduce the amount of soil loss from the watershed and are used as an input for designing water resources structures in the Robi Jida watershed for different purposes.

2. LITERATURE REVIEW

2.1 Land Degradation, Soil Erosion, and Sediment Yield in the World

Land degradation is an environmental phenomenon that negatively affects the land. As a result of land degradation social, environmental, and economic imbalances have also evolved across the world (Mahata & Sharma, 2021). One of the finite, non-renewable resources on the earth is also thought to be soil. It takes between 200 and 1000 years for 2.5 cm of topsoil to form in agriculture (Pimentel et al., 1995). Past and present human intervention in the utilization and manipulation of environmental resources is having unexpected consequences. The earth's soils are being washed away, rendered sterile, or contaminated with toxic materials at a rate that cannot be sustained (Mahata & Sharma, 2021). Erosion is a common global phenomenon that depletes land surfaces of soil, which harms the productivity of ecosystems that are all-natural, including agricultural, forest, and rangeland ecosystems (Lal and Stewart, 1990; Pimentel et al., 1995).

Sedimentation is a critical process that impacts river ecosystems and water quality globally. It involves the deposition of eroded material like rock fragments, soil, and organic matter, affecting water bodies and habitats. Human activities, such as damming rivers, deforestation, and agricultural practices, significantly influence sedimentation rates and the quality of deposited sediment, impacting ecosystems and water quality (Tundu et al., 2018)

Therefore overall, sedimentation poses significant challenges to river systems and reservoirs worldwide, affecting water quality, ecosystem health, and the sustainability of water resources. Addressing sedimentation issues requires a multifaceted approach that considers the complex interactions between human activities, natural processes, and the environment to ensure the long-term health and resilience of aquatic ecosystems.

2.2 Land Degradation and Soil Erosion in Sub-Saharan Africa

In tropical Africa, particularly Sub-Saharan Africa, soil erosion and land degradation are major issues that are generally acknowledged to be more severe than in non-tropical regions. Excessive levels of soil erosion occur throughout Sub-Saharan Africa, primarily as a result of the combination of arid, highly erosive climates, vulnerable, highly erodible soils, steep gradients, and inadequate management of natural resources. Its primary challenge is distinguishing between soil erosion imposed on by humans and that which is essentially

background-level and driven by biophysical, geomorphic, topographic, and climatic factors (Kiage, 2013).

The primary cause of soil degradation in Sub-Saharan Africa (SSA) is the expansion and intensification of agriculture in efforts to feed its growing population (Tully et al., 2015). Land degradation in the form of soil erosion and nutrient depletion presents a threat to food security and sustainability of agricultural production in Sub-Saharan Africa (SSA) and in the developed country (Kassie et al., 2008).

Some studies suggested that sub-Saharan African agriculture was inherently unsustainable, and indicated losses of productivity due to erosion and declines in soil fertility at continental (Lal, 1995; Stoorvogel & Smaling, 1990). Many African pastoralists and farming households especially in Sub-Saharan Africa (SSA) respond to declining land productivity by abandoning their existing degraded pasture and cropland and moving to new lands for grazing and cultivation. Even if rural households choose to stay on degraded land, their declining productivity will be unable to support growing rural populations (Barbier, 2000). Many raised the idea that farmers were accountable for the higher rates of soil degradation and proposed that, to understand the various forms that African agriculture can intensify, more focus should be placed on farmers' skills and adaptability. It is also important to examine the various ways that systems develop rather than assuming that they will go in a particular direction, (Mazzucato & Niemeijer, 2000). Also, soil degradation in SSA leads to changes in ecosystem services on-site as well as off-site, the continuing land degradation that increasingly threatens the food security of the rural poor requires urgent action (Tully et al., 2015).

2.3 Land Degradation and Soil Erosion in the Ethiopian Highlands

It is possible to attribute Ethiopia's soil degradation directly to previous highland farming methods. Soil erosion is hastened by deforestation and farming practices in the highlands, as well as by the dissected topography, large sections with slopes above sixteen percent, and heavy rainfall (Badege, 2014). In the Ethiopian highlands, continuous soil erosion and sediment redistribution constitute a danger to water resources and yields from agriculture. The development of physically based distributed models and the growing availability of spatial hydrometeorological data allowed for the multisite calibration of the SWAT model, which was then used to determine the spatial distribution of erosion hotspots and evaluate the impact of the watershed on land management practices (Lemma et al., 2019).

The highlands of Ethiopia, having the most agricultural potential, suffer from substantial land degradation due to soil erosion caused by heavy runoff and deforestation, resulting in a steady decline in land and labor productivity (Haile & Fetene, 2012). In the Ethiopian Highlands, erratic and intensive rainfalls during the rainy season generate several peak runoff events, exposing steeply sloped areas to potentially severe soil erosion (Addis et al., 2016). Many environmentalists, policymakers, and researchers agree that land degradation mainly caused by soil erosion has been one of the chronic problems in Ethiopia.

The Ethiopian Highland Reclamation Study (EHRS) estimated that the average annual soil loss from arable land was 100 tons/ha and the average productivity loss on cropland was 1.8% (Asmamaw & Mohammed, 2019). According to the assessment of land degradation in Ethiopia (Taddese, 2001),1900 million tons of soil is annually eroded from the highlands. The highest rate of erosion was found in Wollo, Gondar, Gojam, and Shewa. The estimated soil loss due to sheet and rill erosion ranges between 201-300 tons $ha^{-1}year^{-1}$. This is on average, equivalent to 2.5 cm depth of soil from a hectare of land. As a consequence of land degradation, the productive capacity of the soils in the Ethiopian highlands is reducing at a rate of 2-3% annually (Taddese, 2001). The north and northeastern highland parts of the country have seen the greatest damage to their soil resources due to soil degradation.

2.4 Impact of Soil Erosion and Sedimentation in Ethiopia

Soil erosion and nutrient depletion have been two of the major environmental issues in the Ethiopian highlands, which provide over 86% of the water for the Nile River. Severe soil erosion and sedimentation were caused by high population pressure that only relied on natural resources, inadequate land management, and poverty. The Transboundary Rivers, which rise in the Ethiopian highlands, are thought to transport 1.3 billion tons of sediment annually to their neighboring nations, whereas the Blue Nile alone transports 131 million tons annually (Kidane & Alemu, 2015).

Water-induced soil material displacement can have several detrimental effects. High rates of soil erosion lead to the sedimentation and degrading of adjacent and surrounding water bodies in the downstream direction. The productivity of the soil is decreased when the part of the typically fertile topsoil is removed. In severe situations, however, the rooting depth of crops may become limited due to deforestation, desertification, unexpected shifts in climate, waterlogging, salinization, erosion, and loss of organic matter components (Mahata & Sharma, 2021).

Due to decreased agricultural soil fertility, land degradation has a detrimental effect on Ethiopia's economy as well as agricultural productivity. Land degradation is a widespread issue in Ethiopia that has catastrophic effects on the nation's ecological setting, sociocultural environment, and other agricultural aspects (Abebaw, 2019).

2.5 Siltation and Sedimentation on Reservoir Efficiencies

Throughout the world, several millions of hydraulic structures like small ponds exist for water supply, irrigation, and flood control or to control water quality downstream. Transported particles accumulate in these ponds as a result of the reduced flow velocity (Verstraeten et al., 2000).

The sediments that are transported in different ways to dam reservoirs/ponds decrease water storage capacity and shorten the reservoir/pond life span (Ilci et al., 2019). So sedimentation is becoming a major problem for small-scale irrigation dams in Ethiopia. The federal and regional Governments and donors have invested heavily in those interventions. However, Dam based small-scale irrigation schemes are often promoted because of the associated benefits such as lower investment costs, ease in maintenance, the possibility of end-users being able to have more control of the water they need, requiring very little in terms of water management issues, their potentially less negative environmental impact (Moges, 2021). However, those benefits might be outweighed if proper care is not given to issues related to dam sedimentation (Haregeweyn et al., 2006; Tamene et al., 2006).

Moges (2021), investigated seven small dams mainly used for irrigation in Northern Ethiopia (2 in the Tekeze Basin and 5 in the Upper Blue Nile Basin), namely Serenta and Maiambelay in Tekeze, and Shina, Selamko, Koga, Tebi, and Anjeb in Upper Blue Nile Basin. The average annual total capacity loss due to sedimentation for all dams is approximately 2.97% with individual values ranging between 1.5% and 11.5%. And also (Moges, 2021), expressed that globally, water reservoirs lose approximately 1% of their entire capacity annually to sedimentation, indicating the fact that sedimentation in those small-scale irrigation dams is very serious. Equivalently, those dams have lost from 0.17 to 3.10 million m^3 of water from their available storage. This information may occasionally be deceptive, suggesting that the amount of water lost or stored is insignificant to the overall amount of storage. However, following significant sediment deposition and the rising of the original reservoir bed, the maximum outlet level of most dams, at which water can be discharged naturally, is only a

few meters below the level of the natural reservoir. This means that after the outlet is blocked by silt, the remaining water is utterly unreachable by natural methods.

2.6 Hydrological Model

Modeling is defined as the process of organizing, synthesizing, and integrating parts into a realistic representation of the prototype. According to Yesuf et al., (2015), a model is a simplified representation of the real world system. The goal of using a model is to create baseline characteristics when data is lacking and to simulate long-term effects that are challenging to quantify, particularly in ecological modeling.

The hydrological models are tools that describes the physical processes controlling the transformation of rainfall to runoff. The focus of these models is to establish a relationship between various hydrological components like precipitation, evapotranspiration, surface runoff, groundwater flow, and soil water movement. It is important for a wide range of applications, including water resources planning, development, and management programs at the small catchment or basin level (Sitotaw et al., 2021), flood prediction and design, and coupled systems modeling including, for example, water quality, hydro-ecology, and climate. According to Admas et al. (2022), modeling soil erosion, sediment yield, and runoff are crucial for managing reservoir capacity, water quality, and watershed soil productivity.

However, because of resource limitations and the restricted variety of measurement methods, there are constraints on the availability of spatial-temporal data. This creates a need to extrapolate information from existing measurements over space and time. Additionally, it is necessary to evaluate the potential hydrological impacts of future system responses, such as those resulting from climate change and land management practices (Pechlivanidis et al., 2011). Sediment yield, which is the outcome of soil erosion along with sediment transport and deposition processes, is influenced by multiple factors. However, the processes that determine sediment yield are typically not linearly related to the same controlling variables. Hydrological models offer a different method for enhancing the understanding of sediment transport and deposition through overland flow, enabling more accurate predictions and forecasts. As a result, sediment yield modeling has become more widely used to assess the effects of variables that influence sediment dynamics at the basin level (Chakraparni, 2005).

Nowadays, several hydrological models are available that help to detect land use/land cover change and characterize a watershed based on runoff, sediment, nutrients, and soon.

Hydrological models are classified into different classes based on spatial representation as lumped, distributed, and semi-distributed.

Lumped models: Parameters of lumped hydrologic models do not vary spatially within the basin and thus, basin response is evaluated only at the outlet, without explicitly accounting for the response of individual sub-basins and the parameters of lumped models often do not represent the physical features of hydrologic processes and usually involve a certain degree of empiricism (Cunderlik, 2003). Also, Lumped models treat the watershed as a single unit, with state variables that represent averages over the watershed area (Pechlivanidis et al., 2011). The rational method for estimating peak runoff is an example of a lumped hydrological model (Cunderlik, 2003).

Distributed models: Parameters of distributed models are fully allowed to vary in space at a resolution usually chosen by the user and its approach attempts to incorporate data concerning the spatial distribution of parameter variations together with computational algorithms to evaluate the influence of this distribution on simulated precipitation-runoff behavior, by discretizing the watershed into several grids and solving the equations for the state variable associated with every element or grid (Cunderlik, 2003; Xu et al., 2006). The European hydrological system model (MIKE 11/ SHE) is an example of a distributed model. Semi-distributed models have been suggested to combine the advantages of both types of spatial representations (Cunderlik, 2003).

Semi-distributed models: Parameters of semi-distributed (simplified distributed) models are partially allowed to vary in space by dividing the basin into several smaller sub-basins and its examples are the Soil and water assessment tool (SWAT), hydraulic engineering center hydrologic modeling system (HEC- HMS), TOPMODEL (Cunderlik, 2003).

2.7 Selection of Model

The selection of a particular model is a key issue in getting satisfactory results for a given problem. Currently, numerous hydrological models are simulating the hydrological process at different spatial and temporal scales. The criteria for selecting the model type is always project-dependent since every project has its specific requirement. Some criteria are also user-dependent, such as the personal preference for a graphic user interface, a computer operation system, input/output management, and structure. Regardless of the SWAT model's ability to minimize errors resulting from the assumption of lumped, stationary, and linear systems, catchment modeling in a data-scarce environment and SWAT model with

minimal uncertainties can efficiently predict catchment runoff and sediment yield (Ayele et al., 2017).

The choice of the hydrologic model may depend on many selection criteria, including the character (e.g., relevant spatial and temporal scale, acceptable level of error, and uncertainty for alternative screening vs. detailed design (Clark et al., 2008)) of the water resource management issue. Moreover, the extent of variability physical characteristics (such as; land use, elevation, and geology) that affects key hydrological processes (like evapotranspiration, snow accumulation and melt, or groundwater recharge and discharge) can play a crucial role in the choice of hydrologic models (Surfleet et al., 2012).

For this study, the reason for the selection of the SWAT model is physically based, spatially distributed, and belongs to the public domain the model has been tested in different tropical watersheds to be used to model stream flow and sediment yield, particularly in the watershed have proven the suitability of such a model (Andualem and Yonas, 2008; Setegn et al., 2010) and reported to be capable to well explaining watershed hydrological processes like the study by Asres & Awulachew (2010), SWAT based runoff and sediment yield modeling in a case study of the Gumera watershed in the Blue Nile basin can be cited as examples, which additionally justify the possible use of the model in the small sub-watershed area. Therefore the fundamental selection criteria of the models are required model outputs are important for the needed purpose and therefore to be estimated, hydrological processes need to be modeled to estimate the desired outputs adequately and, the availability of input data.

2.8 Estimation of Sediment Yield

According to Kothyari & Jain (1997), estimation of sediment yield is needed for studies of reservoir sedimentation, river morphology, soil and water conservation planning, water quality modeling, and design of efficient erosion control structures. Also, Sediment yield is defined as the total sediment outflow from a watershed measurable at a point of reference during a specified period. However, sediment outflow from the watershed is induced by processes of detachment, transportation, and deposition of soil materials by rainfall and runoff, Therefore determination of the suspended sediment amount on the rivers is crucial importance since it directly affects the design and operation of many water resources structures (Cigizoglu,2004).

Estimating sediment yield is essential for various applications, including the design of reservoirs and dams, sediment and pollutant transport in water bodies, the design of stable

channels and debris basins, post-flood cleanup efforts, habitat protection for fish and wildlife, assessment of watershed management impacts, and environmental impact evaluations (Cigizoglu, 2008). Fine sediment has long been identified as an important vector for the transport of nutrients and contaminants such as heavy metals and microorganisms. Suspended sediment is important in its own right since its presence or absence exerts an important control on geo-morphological and biological processes in rivers and estuaries (Walling & Collins, 2016).

Different researches were carried out in modeling stream flow and sediment yield in the Upper Blue Nile basin (Nadew, 2018), modeling stream flow and sediment yield in Beles watershed, Upper Blue Nile, (Asres & Awulachew, 2010) they have used the SWAT model to estimate the sediment yield, and runoff and to establish the spatial distribution of sediment yield in the Gumera watershed. The result of this study showed that the model simulated average annual sediment yield ranging from 11 to 22ton $ha^{-1}yr^{-1}$. (Setegn et al., 2010) they have also used the SWAT model to estimate sediment yield from the Anjeni watershed. The result of this study showed that the model simulated average annual sediment yield was estimated as 24.6ton $ha^{-1}yr^{-1}$. Previous studies on the Upper Blue Nile Basin specifically Megech watershed sediment modeling using the SWAT model and the simulated mean annual sediment yield getting into the Megech reservoir was estimated as 12.33ton $ha^{-1}yr^{-1}$(Assfaw, 2019). And also (Abebe et al., 2022; Addis et al., 2016; Awulachew et al., 2008; Ayalew & Bharti, 2020; Ayele et al., 2017; Betrie et al., 2011; Easton et al., 2010; Lemann et al., 2016; Setegn, 2008; Sitotaw et al., 2021) are studied on stream flow and sediment yield modeling on upper blue Nile basin using SWAT models.

2.9 Extending Limited Sediment Records Using Sediment Rating Curve

Sediment rating curves display the rate of sediment transport as a function of stream flow and the rate of sediment transport is given in terms of sediment discharge or as a flux-averaged concentration (Aga et al., 2018; Warrick, 2015), and sediment concentration is converted to load to make the rating curve relation in ton $days^{-1}$ with flow (m^3s^{-1}).

Several studies have been conducted in extending limited sediment records for estimating the sediment yield generated from a watershed for watershed management and reduction of reservoir sedimentation using different hydrological (Aga et al., 2018; Assfaw, 2019). To generate sediment load for areas of limited continuous observation data, the use of a rating curve is recommended (Asselman, 2000). The sediment rating curve is especially used by

engineers and hydrologists to estimate the life expectancy of dams, while scientists use it to study depositional and erosional environments (Syvitski et al., 2000). For example, the sediment rating curve is applied to assess the sediment concentration rating in the upper Blue Nile Basin (Moges et al., 2015), and to revise the sediment budget in Lake Tana, Ethiopia (Ayele et al., 2017), in addition (Asres & Awulachew, 2010; Lemma et al., 2019) are using sediment rating curve to extend the limited records in the upper blue Nile basin.

2.10 Identifying Hotspot Areas for Land Management Practices

Land management strategies or practices are needed that protect soil erosion in agricultural watershed to achieve sustainable land use planning (Saha et al., 2019). Increasing population and climate change combined with a limited capacity of the people to respond to shocks has increased land degradation, which has resulted in major physical, social, and economic crises in many areas and communities of Ethiopia (Mengistu et al., 2015). Therefore, a coordinated effort and better organization are essential to conserve and enhance the productive capacity of agricultural soils. Effective soil conservation strategies and policy measures are necessary to address the rising rates of soil degradation seen in Ethiopia, as well as to rehabilitate affected areas and restore them for productive use (Sonneveld et al., 2001).

Understanding soil erosion processes plays a pivotal role in lowering the current rates of soil loss by planning, designing, and implementing appropriate conservation strategies (Tamene & Vlek, 2007). Identifying soil erosion hot-spot areas of a watershed/basin and isolating best management practices (BMPs) for soil erosion-prone sub-watersheds are imperative for effective soil loss reduction and lessening its on-site and off-site effects (Admas et al., 2022). It has different applications for land management practices. It helps to conduct soil and water conservation practices for highly eroded areas in reducing gully formation, increasing land coverage by plantation, and reducing soil fertility decline in a watershed. It also, reduces the efforts of stakeholders, in conducting soil and water conservation structures (Setegn et al., 2009).

Excessive soil loss and sediment yield in the highlands of Ethiopia are the primary factors that accelerate the decline of land productivity, water resources, operation and function of existing infrastructure, as well as soil and water management practices. Best Management Practices (BMPs) are a group of practices applied to control soil loss and sediment transport (Betrie et al., 2011) that help improve crop productivity through sediment loss reduction and soil moisture retention (Addis et al., 2020). Combining BMPs is necessary since a single

BMP is insufficient to create effective watershed management systems. The best mix of BMPs is difficult to determine, nevertheless, since it necessitates a methodical study that enables the approaches' efficacy assessments. Watershed models are commonly employed in this context to forecast the long-term effects of BMP applications on the watershed. According to several studies, the Soil and Water Assessment Tool (SWAT) model is regarded as a flexible model that combines several procedures to enable efficient watershed management worldwide (Betrie et al., 2011; Cooper, 2010; López-Ballesteros et al., 2019).

A study of the rates at which soil forms in Ethiopia's several agro-ecological zones shows that the range of negligible and acceptable soil loss levels for each zone was 0-5ton/ha/year and 5-11 ton/ha/year respectively and 11- 15ton/ha/year medium and above 15ton/ha/year are higher (Asres & Awulachew, 2010; Berihun et al., 2020; Dibabaa & Ebsab, 2022; Kefay et al., 2022; Lemma et al., 2019; Setegn et al., 2009) and generally summarized in table 2.1 below. According to the spatial variability of sediment source and sediment rate/erosion level, the BMP scenarios were developed. Identified and selected scenarios were also applied to the SWAT model for simulating and identifying the effects of these best management practices on the sediment yield of the watershed.

Table 2-1: General hot spot area classification based on sediment yield.

No	Soil loss in ton/ha/year	Erosion categories	Sources
1	0-5	Very low	(Asres & Awulachew, 2010; Berihun et al., 2020; Dibaba et al., 2021; Gashaw et al., 2019; Haregeweyn et al., 2015; Kefay et al., 2022; Lemma et al., 2019) (Asmamaw & Mohammed, 2019)
2	5-11	Low	
3	11-18	Medium	
4	18-30	High	
5	>30	Very high	

2.11 Soil erosion and Sediment Reduction Measure

Soil and water preservation actions are classified into structural measures (check dams, terracing, contouring, stone bunds and graded channel), agronomic measures (mulching, strip cropping, contour farming, mix cropping) and vegetative measures such as grassed waterways, filter strips and reforestation (Douglas-Mankin, Srinivasan, and Arnold 2010).

According to (Srinivasan et al. 2012) Soil and water protection actions are classified into two groups such as structural (grassed waterways, terraces, contouring and filter strips) and non-structural (no tillage, contour farming, conservation tillage, strip tillage).

Land management techniques are frequently used to reduce sediment yields at the watershed scale (Zantet et al. 2023). According to, investigation of (Hurni and Zeleke 2018) Soil erosion occurs mainly during the rainy season in the form of water erosion. Rills, gullies, and brown rivers full of sediment show that a lot of soil particle is transported and lost from agricultural production in agricultural land, the dominant forms of soil erosion are rill erosion and sheet erosion. To reduce soil erosion from the watershed, the following best management practices were used in Ethiopia: for instance, a vegetative contour strip, soil/stone bund, contour farming, slope terracing, and zero-free grazing, mulching, grassed waterways, filter strips, fanya juu, and reforestation (Hurni and Zeleke 2018). For this study the selected sediment management practices and the studies conducted by different researchers were discussed below.

A. Filter Strips

Filter strips are strips of dense vegetation placed along the channel's edge to reduce overland flow velocity and sediment input into the channel but not affect surface runoff in the SWAT model (Arnold, Kiniry, Srinivasan, Williams, Haney, et al. 2012). Incorporating filter strips on subbasins prone to sediment production can help reduce sediment yield. However, the effectiveness of these filter strips diminishes as their width increases beyond 30 meters, with additional widths beyond that point providing little further reduction in sediment output.(Gharabaghi, Rudra, and Goel 2006). The SWAT model includes parameters for managing sediment yield, such as a flag to indicate the presence of filter strips (VFSI), the ratio of field area to filter strip area (VESRATIO), the portion of the hydrologic response unit that drains to the most concentrated 10% of the filter strip area (VFS_CON), and the fraction of flow within 10% of most concentrated filter strip is fully channelized (VFS_CH). (Waidler et al. 2011). Nepal and Parajuli (2022) assessed vigitative filter strips management practices, specifically adjusting parameters, such as VFSI, VESRATIO, and VFS_CON within the SWAT model's operations management parameter in the Mississippi watershed. These parameters were adjusted to 1, 40, and 0.5, respectively, within the operations management parameter of the SWAT model, resulting in a 25% decrease in sediment yield. Adationaly, the study of Betrie et al. (2011) on Blue Nile Basin using SWAT model reports,

applying filter strips has also reduced the average annual sediment yield at the outlet point by 44%.

B. Vegetated Filter Strips

Vegetated sieve floorings necessity install along the edge of the channel segment to reduce the entrance of sediment, nutrients, pesticides, and bacteria in surface runoff (Kondolf et al. 2014). A filter strip is represented by width of the edge of field filter strips.(Anon 2008), vegetated filter strips are designed to treat sheet flow from adjacent surfaces and slowing runoff velocities and filtering out sediment and other pollutants. According to(Amaru Ayele and Gebremariam 2020), application of filter strips proposed middle Awash Dam watershed, Ethiopia using SWAT model has reduced regular yearly sediment harvest at outlet by 25.8%. The study of Andualem and Gebremariam (2015) conducted on Gilgel Abbay watershed, Ethiopia; found that applying filter strips on the study watershed can reduce 23.74% of the regular yearly sediment harvest at the outlet. Also, the study of Betrie et al. (2011) on Bluenile Sink by means of SWAT model reports, applying filter strips has also reduced the regular yearly sediment harvest at the outlet by 44%.

C. Stone/Soil Bund

In the highlands of Ethiopia, application of stone/soil bunds as a tactic to lessen erosion and sediment production regarded as a beneficial practice. By decreasing slopes and boosting watershed abstractions, the application of stone/soil bunds decreases overland flow and sediment loss (Addis et al., 2016). Reduced runoff, sheet scour, and slope length are goals of this approach. The impacts of creating stone/soil bunds on steep slope is simulated by varying parameters such as the length of slope (SLSUBBSN), steepness of slope (HRU_SLP), soil conservation services (SCS) curve number (CN_2), and erosion control practice factor (USLE_P) for key sub-basins (Gashaw et al., 2021; Lemann et al., 2018).

D. Terracing

When the slope steepness and slope length reduced by the application of terraces, the highest overflow degree and erosive power of runoff are reduced consistently (Parajuli and Acharya 2012). A promenade is a ground ridge, built crossways the field slope usually on the contour (Sanchez, Couto, and Buol 1982). To simulate terracing conservation practice in SWAT model, (CN_II), USLE practice (USLE_P) factor and the slope length (SLSUBBSN) could be adjusted based on cover type, hydrologic condition and hydrologic soil groups (Srinivasan et al. 2012). Studies of (CN and FM 2015) assessment of agricultural upkeep practices on

ecology services in Sasumua crunch, Kenya by means of SWAT model shows the application of parallel terracing reduced residue harvest for the critical affected sub basins by 85%. Study conducted by Maharjan. Simulates five different land management practice case using SWAT model. The study decided that application of terracing on the critically affected sub basins is the most effective land management practice to decrease residue harvest with an average of 78.6%. Another study conducted by (Amaru Ayele and Gebremariam 2020) using SWAT model on proposed middle Awash Dam watershed applying terraces reduced 83.3% of regular yearly sediment harvest for the critically affected sub basins.

E. Contouring

Application of contouring can minimize the formation of rills and reduce erosion by reducing surface runoff and giving a chance to infiltrate by impounding water in a small depression (Srinivasan et al. 2012). According to (Srinivasan et al. 2012), contouring tillage and contour planting provides protection against erosion from storms of low to moderate intensity, but little or no protection against occasional severe storms that causes excessive break-overs of contoured rows.

The study of (Kim and Gilley 2008) shows contouring can reduce at least 50% of regular yearly sediment harvest for treated sub basins. The study conducted by (Amaru Ayele and Gebremariam 2020) shows applying contouring on proposed middle Awash Dam watershed can reduced 61.1% of regular yearly sediment harvest for critical sediment source sub basins.

Contouring is particularly effective when rainfall amounts and intensities are low, when ridges are high, and Small ridges resulting from field operations increase surface storage and roughness, reducing runoff and sediment losses (Czapar et al. 2014). Contouring practice can simulated in SWAT model operation managment by adjusting curve number (CONT_CN) and USLE practice factor (CONT_P) (Arnold et al. 2012; Zantet et al. 2023).The study of Bitew & Kebede.(2023), found that the application of contour farming in the Blue Nile Basin reduced sediment yield by 43.6%.The study (Leta et al. 2023) successfully reduced average sediment yield by 39.5% in the critical subbasin of the Nashe watershed through the application of contouring sediment management practices in the Upper Blue Nile basin.

3. MATERIALS AND METHODS

3.1 Description of the Study Area

3.1.1 Location of the study area

Robi Jida watershed is part of the upstream areas of the Blue Nile River Basin, and the outlet point of the watershed is located about 90km northwest of Addis Ababa and close to Muke Turi Town. Geographically, it is found between 9°10′ and 9°40′N latitudes and 39°00′ and 39°20′E longitudes in Figure 3.1. It is situated in two administrative regions, i.e., Oromia and Amhara. The Amhara region, which includes two Woredas, Hageremariamna Kesem, and Siya Debirna Wayu, and Wuchalena Jido, Abichuna Gne'a, Kembibit, and Berehan Aleltu Woredas, were among those in the Oromia region. The topography is rugged, with hills and valleys having altitudes ranging from 2474 m a.s.l at the lowest point to 3156 m a.s.l at the highest point.

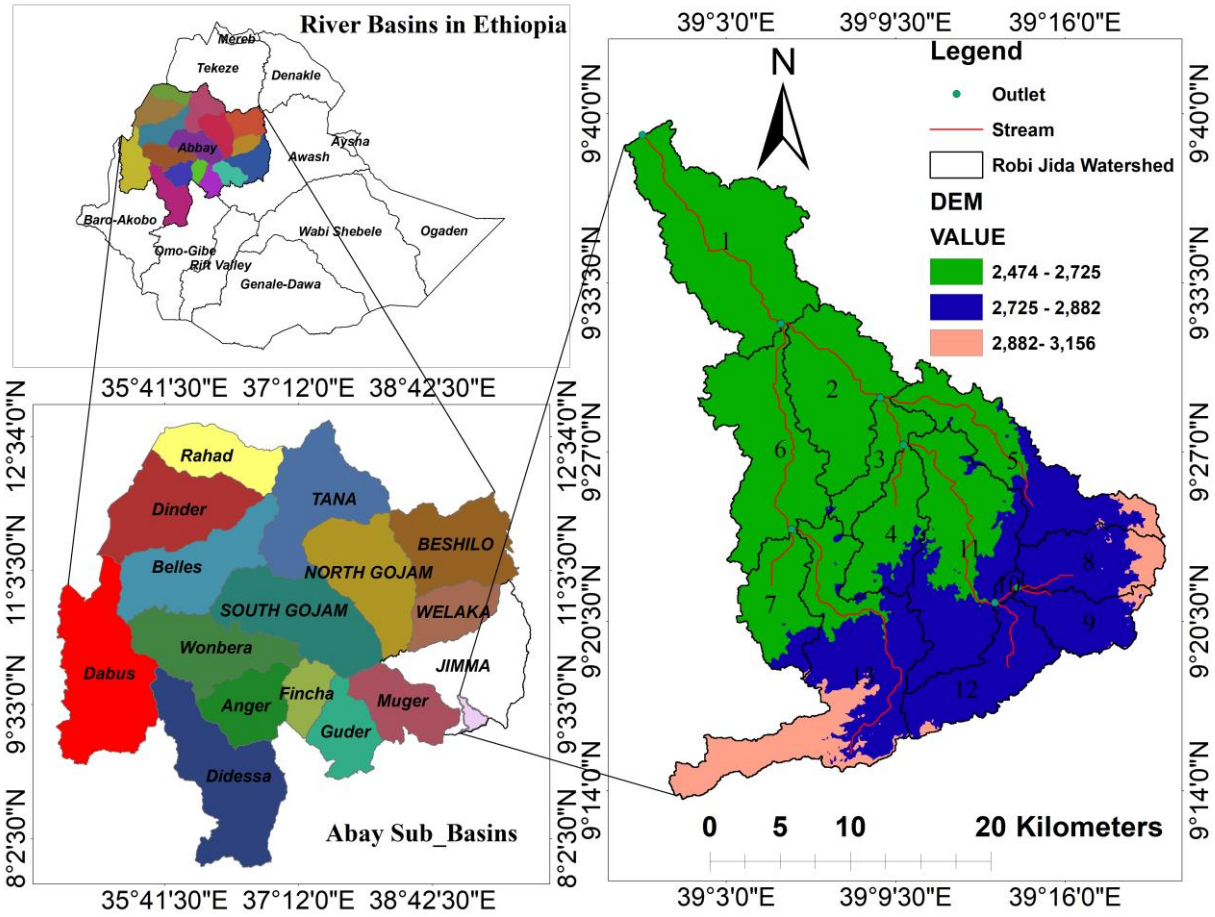

Figure 3-1: Location map of the study area.

3.1.2 Topography

The Robi Jida watershed is part of the Jemma sub-basin in the Blue Nile River basin and covers an area of about 762.74 km^2. Administratively, the major part of the Robi Jida watershed is in the Oromia regional state and a small part in the Amhara regional state. It is a diversified watershed in terms of topography, climate, land use, and socio-economics. Based on Berhanu et al.(2013), the slope grade is to divide the Robi Jida watershed into five slope classes as shown in Figure 3.2; 31.40% of the total area is flat (0–3%), whereas 54.70% of the entire areas are characterized as gently sloping (3%–8%). The remaining land slopes are divided into sloping, moderately sloping, and steep, which covered areas of 12.65% (8%–15%), 1.24% (15%–30%), and (0.01%) greater than 30%, respectively. Therefore the majority of the slope of the watershed is within the range of 3%-8% and is gently sloping and area coverage of each slope class is shown in Table 3.1.

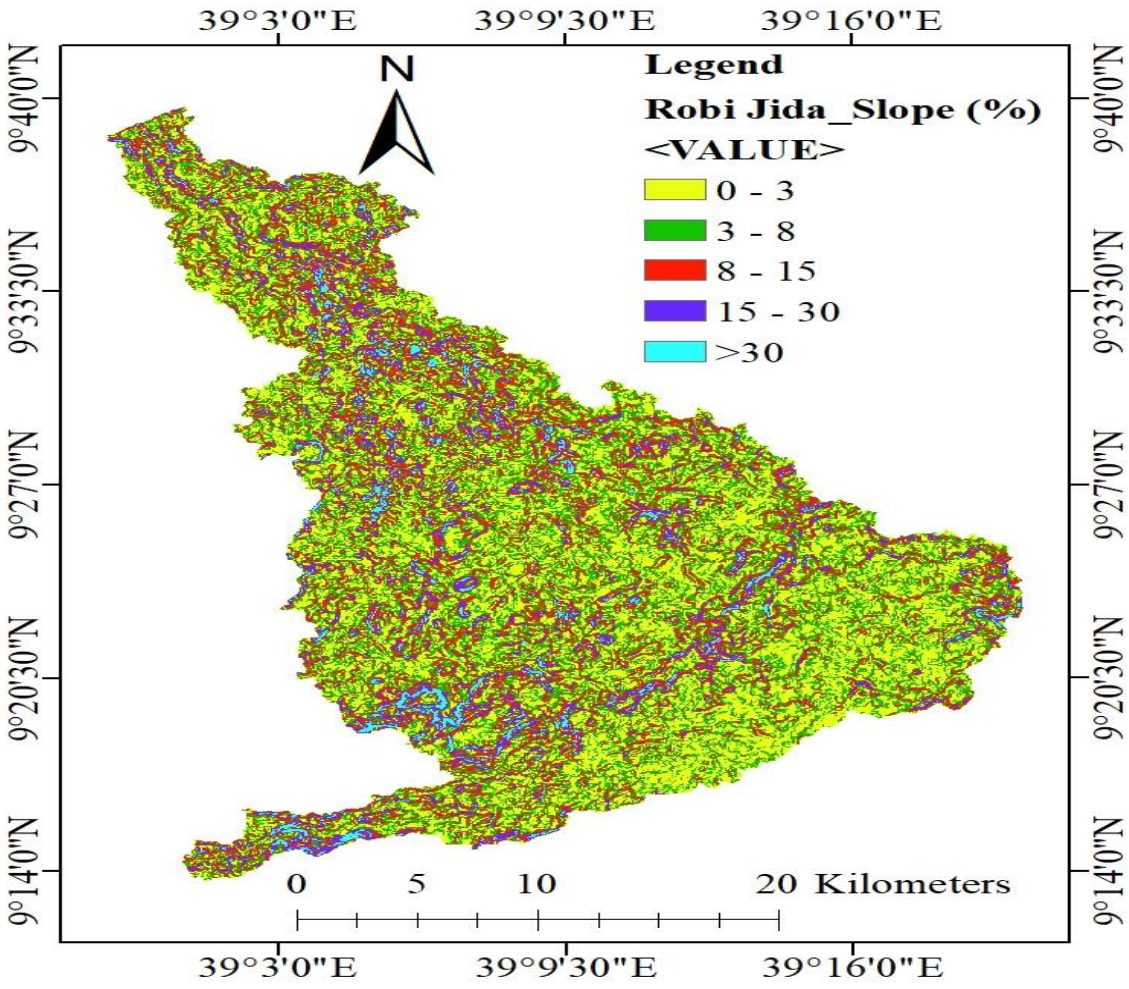

Figure 3-2: Slope class map of the Robi Jida watershed.

Table 3-1: Slope class of the Robi Jida watershed.

No.	Slope class	Description	Area (km^2)	Percent (%)
1	0-3%	Flat	239.47	31.40
2	3%-8%	Gently sloping	417.16	54.70
3	8%-15%	Sloping	96.45	12.65
4	15%-30%	Moderately sloping	9.45	1.24
5	>30%	Steep	0.06	0.01

3.1.3 Climate

According to Gorfu & Ahmed (2011); Taye et al.(2018), agro ecological zonation in Ethiopia has two facets, namely the traditional and elaborated agro ecological zones. The traditional zones include Bereha, Kolla, Woina Dega, Wurch, and Kur climate zones based on altitude and temperature. Bereha refers to hot lowlands less than 500 meters; Kolla refers to lowlands between 500 and 1,500 meters; Woina Dega refers to midlands between 1,500 and 2,300 meters; Dega refers to highlands between 2,300 and 3,200 meters; Wurch refers to highlands between 3,200 and 3,700 meters; and Kur refers to highland areas above 3,700 meters. Since the elevation of the Robi Jida watershed lies between 2474 meters and 3156 meters, it is characterized by Dega according to the mentioned climate zone.

The rainfall pattern within the study area is distinctively unimodal with peak rainfall located between July and August and the minimum rainfall occurs in January, February, October November, and December. The mean monthly annual rainfall distribution of the Robi Jida watershed of the surrounding stations for 30-year data from 1992 to 2021 is indicated in Figure 3.3. As shown from this figure the mean monthly rainfall records were observed from 6 mm to 323 mm and a mean annual rainfall varies from 705mm to 1,346 mm in the watershed. The mean annual point rainfall and annual rainfall of the surrounding station are available in Appendix Table 1 and Appendix Table 2 respectively.

The mean annual monthly maximum and minimum temperature range varies from 19.38 ^oC to 23.34 ^oC and 6.54^oC to 9.83 ^oC respectively in the surrounding station of the Robi Jida watershed also shown in Figure 3.4 below.

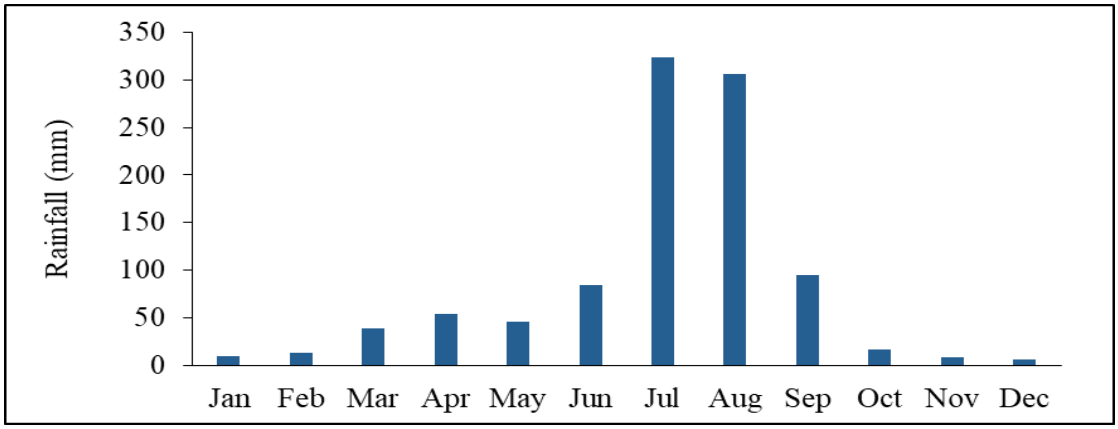

Figure 3-3: Mean monthly rainfall distribution of the Robi Jida watershed (1992 - 2021)

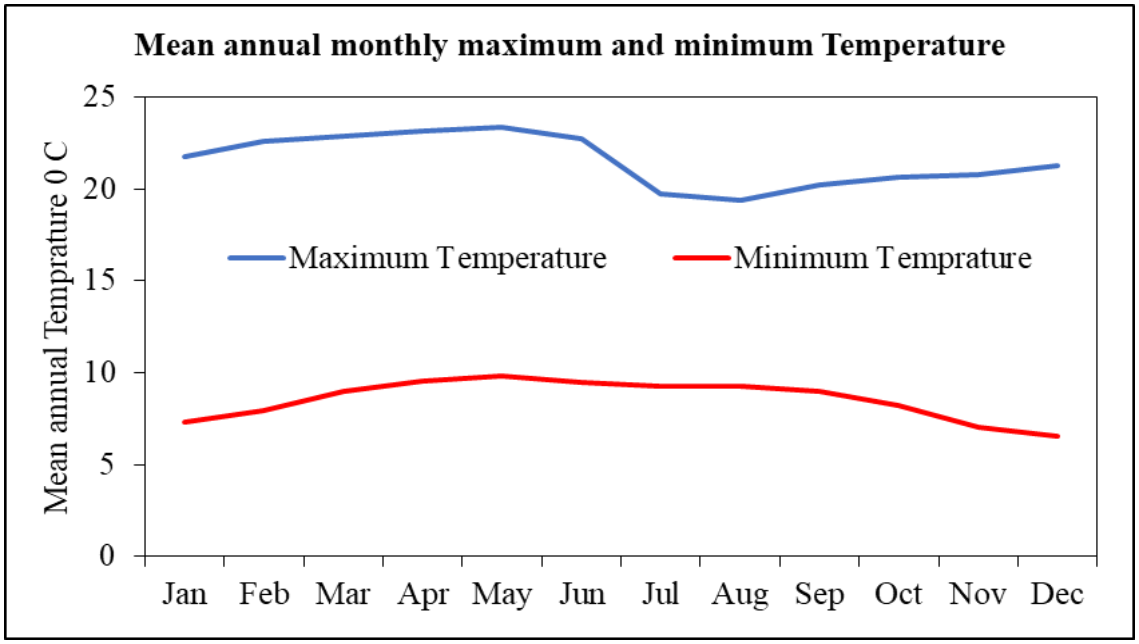

Figure 3-4: Mean monthly maximum and minimum temperature of Robi Jida watershed.

3.1.4 Land use /land cover and soil of the Study Area

The terms land use and land cover are often used interchangeably, even though the distinction between the two is important. The spatial coverage of the land use and land cover in the Robi Jida watershed is shown in Figure 3.5A. The major land use and land cover classes of the watershed are agriculture (94.85%), settlement (3.16%), rangeland (1.97%), and the remaining are forest and water bodies as shown in Table 3.2. Also, the Ministry of Water and Energy characterized the soils in the Robi Jida watershed as Eutric Cambisols, Eutric Vertisols, and Chromic Luvisols, and their spatial coverage is shown in Figure 3.5B

below. The soil classification of the dominant soil of the Robi Jida watershed is Eutric Vertisols as shown in Table 3.2 below.

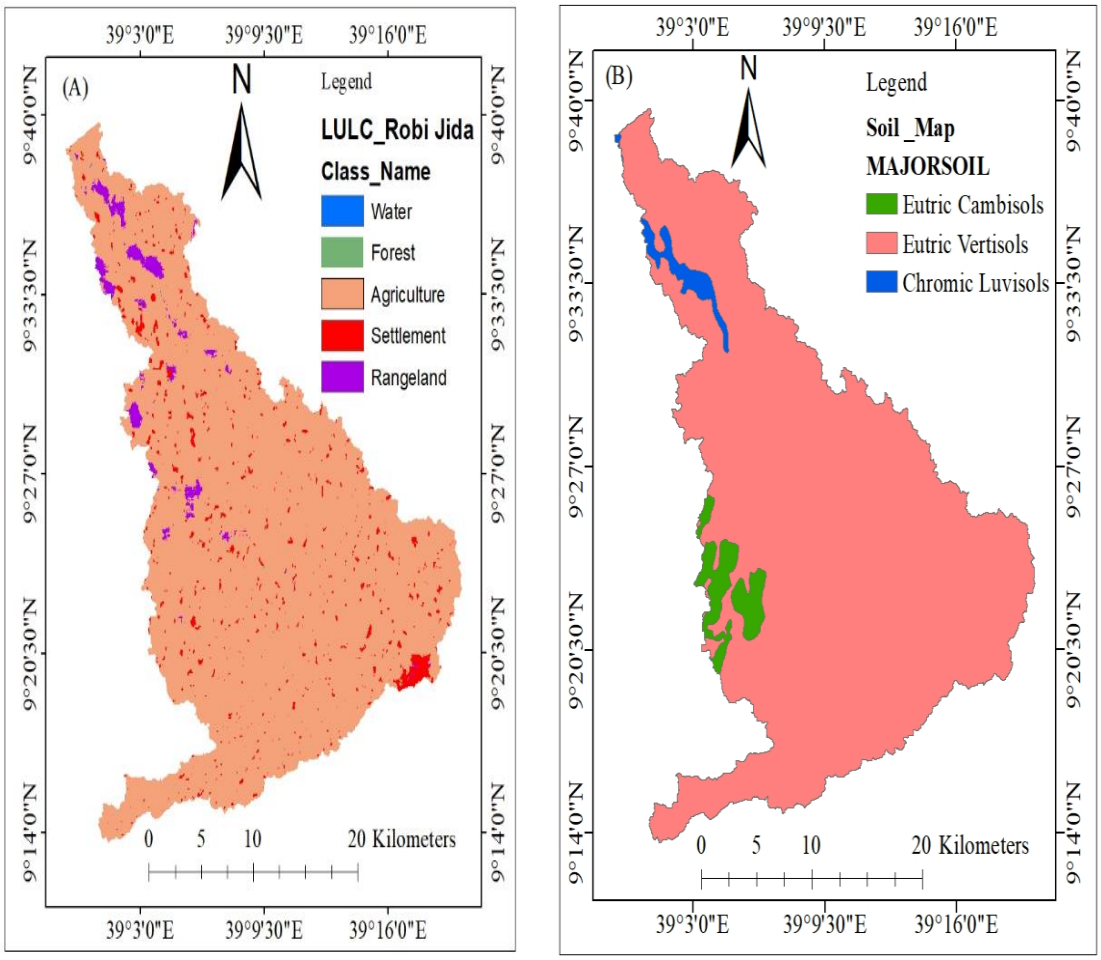

Figure 3-5: Land use/land cover map (A) and soil map (B) of the Robi Jida watershed.

Table 3-2: Land use/land covers, soil types and area coverage in Robi Jida watershed.

	No.	LULC/Soil	Area_(km^2)	Percent (%)
Major Land use/land cover	1.	Agriculture	723.45	94.85
	2.	Rangeland	14.99	1.97
	3.	Forest	0.12	0.02
	4.	Water	0.10	0.01
	5.	Settlement	0.61	3.16
Major soil	1.	Eutric Cambisols	25.45	3.34
	2.	Eutric Vertisols	725.35	95.10
	3.	Chromic Luvisols	11.95	1.57

3.2 Data Collection and Analysis

The SWAT model is highly data-intensive and requires specific information about the watershed to simulate stream flow and sediment yield, such as DEM, land use /land cover, soil, weather data, and other land management practices. These data were collected from different sources as shown in Table 3.3 below. Generally, the necessary data collected for this study can be classified as spatial and time-series data.

Table 3-3: Input data sources and their resolution.

Input data	Sources	Resolution	Period
Digital elevation model	Ministry of Water and Energy	30m*30m	
Land use/land cover data	Ministry of Water and Energy	30m*30m	2018
Soil data	Ministry of Water and Energy	90m*90m	
Metrological data	Ethiopian Meteorological Institute (EMI)	---------	1992-2021
Hydrological data			
✓ **Stream flow**	Ministry of Water and Energy	---------	1992-2018
✓ **Sediment data**	Ministry of Water and Energy	----------	1992-1996

3.2.1 Spatial Data

3.2.1.1 Digital Elevation Model (DEM)

DEM describes the elevation of any point in a given area at a specific spatial resolution as a digital file, and it is specifically made available in the form of a raster or regular grid of spot heights. DEM is the basic input of the Arc-SWAT hydrological model to delineate the watershed into several sub-watersheds or sub-basins and analyze the drainage pattern of the watershed, such as slope, stream length, width, etc. For this study, the Digital Elevation Model (DEM) of 30m x 30m resolution was obtained from the Ministry of Water and Energy (MoWE).

3.2.1.2 Land use/land cover and Soil data

Land use/land cover data are one of important factors that affect runoff, evapotranspiration, and surface erosion in the watershed. They are essential for the SWAT input for determining the watershed characteristics and are also used for stream flow and sediment yield modeling of the watershed. Land use/land cover and soil data are necessary to map a hydrological response unit (HRU). The soil map and its database were obtained from ministry of water and energy and has a 90 x 90 m resolution, and show (Appendix table 3 and 4) for the detailed property of the soil type code and their description. A reclassification of the land use and soil map was made to represent the land use, and soil according to the specific land use/land cover and soil types, and the respective crop parameters and user soil for the SWAT database as shown in the figure 3.6 below. A lookup table that identifies the SWAT land use and soil code for the different categories of land use/land cover and soil was prepared to relate the grid values to the SWAT land use/land cover and soil classes its special coverage and area coverage are shown in table 3.4 and 3.5 below.

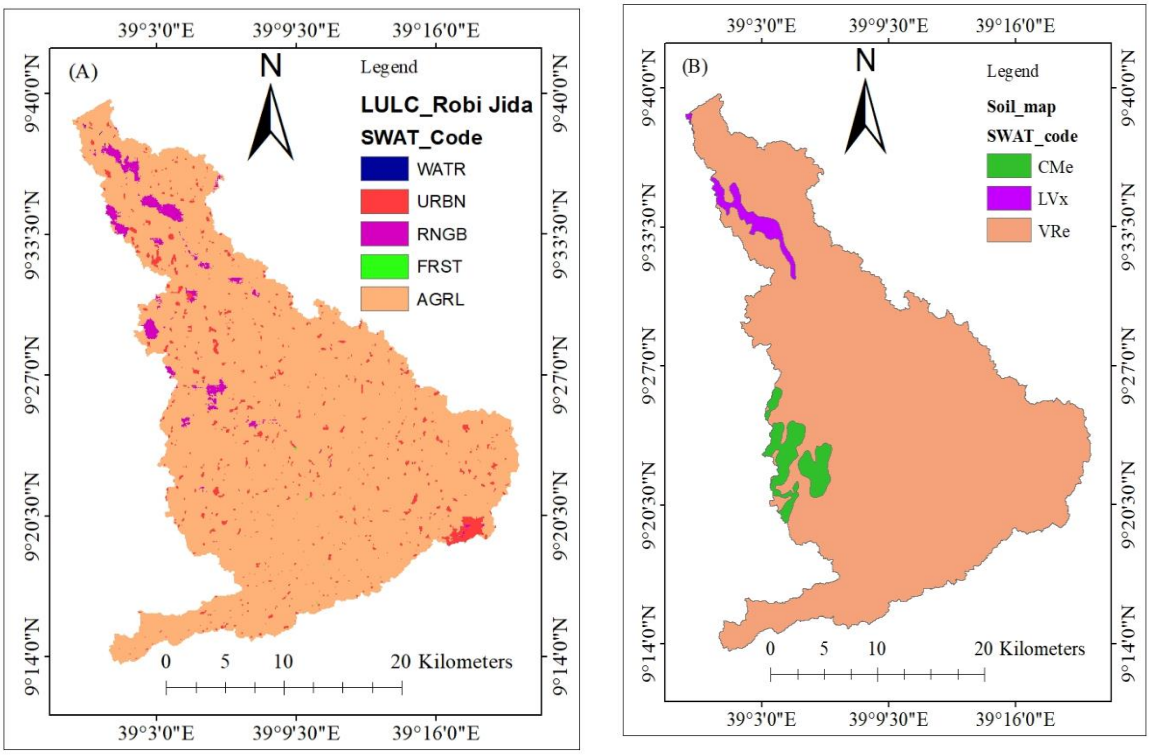

Figure 3-6: SWAT LULC and soil code in the Robi Jida watershed.

Table 3-4*:* Soil type and SWAT code in the Robi Jida watershed

No.	Major soil	SWAT_code	Area_(km^2)	Percent (%)
1	Eutric Cambisols	CMe	25.45	3.34
2	Eutric Vertisols	VRe	725.35	95.10
3	Chromic Luvisols	LVx	11.95	1.57

Table 3-5*:* Land use/land cover type and SWAT code in the Robi Jida watershed

No.	LULC Type	SWAT_code	Area (km^2)	Percent (%)
1	Agriculture	AGRL	723.45	94.85
2	Range-Brush	RNGB	24.10	3.16
3	Forest	FRST	0.12	0.02
4	Water	WATR	0.10	0.01
5	Settlement	URBN	24.10	3.16

3.2.2 Time Series

Time series data, such as metrological and hydrological data, were collected from the Ethiopian Meteorological Institute (EMI) and the Ministry of Water and Energy (MoWE), respectively.

3.2.2.1 Meteorological Data

Meteorological data are crucial in any hydrological analysis. These were daily data on precipitation, minimum and maximum temperature, solar radiation, wind speed, and relative humidity. All these meteorological data were collected for the Robi Jida Watershed from the Ethiopian Meteorological Institute in the time range from 1992 to 2021 for this study. The data distribution of six stations is selected for this study based on the Thiessen polygon as shown in Figure 3.7 results. The area coverage and mean annual of these selected stations is shown in table 3.6 below.

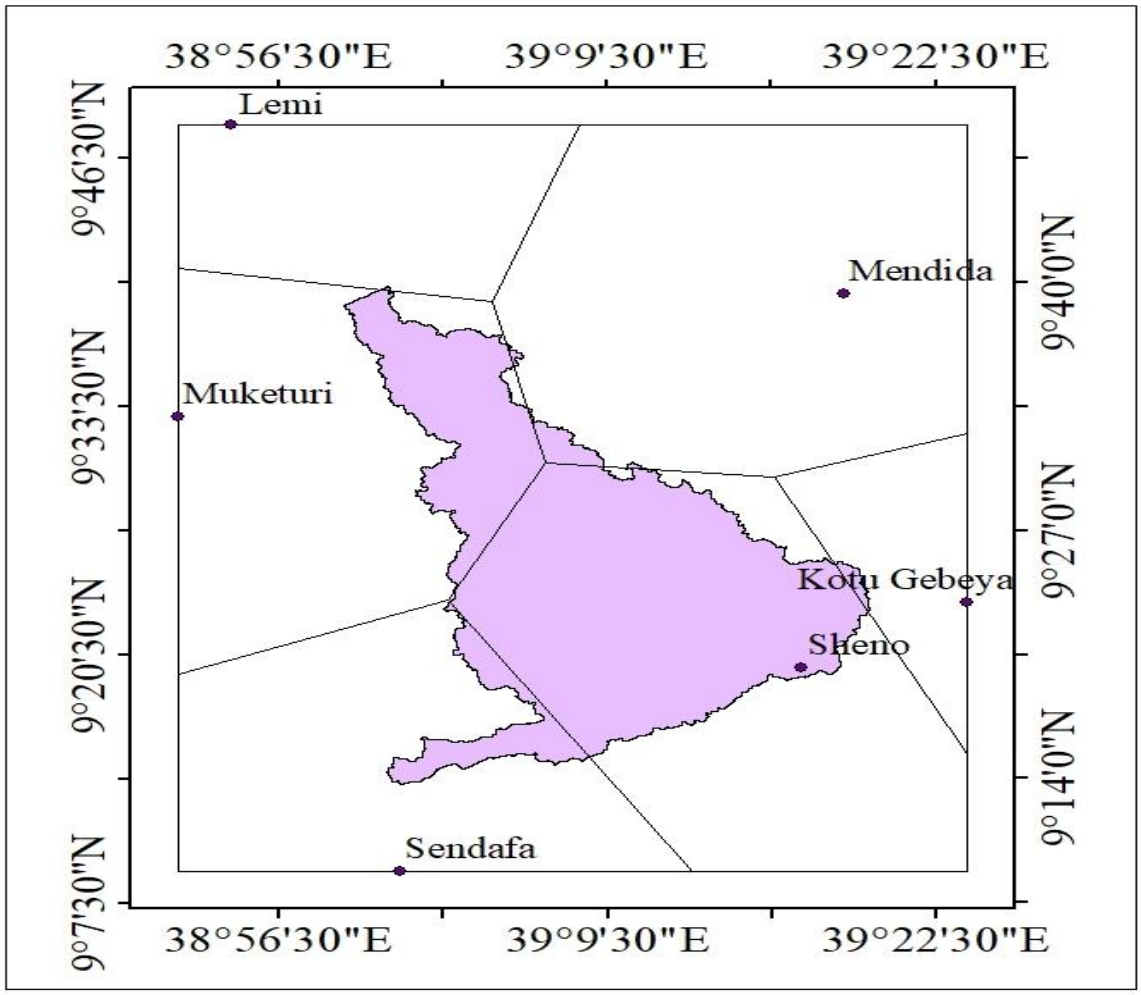

Figure 3-7: Thiessen polygon for selecting a contributing station.

Table 3-6: Area coverage of the selected station in the Robi Jida watershed.

Station name	Latitude (m)	Longitude (m)	Elevation (m)	Area coverage (km^2)	Mean Annual rainfall (mm)
Sendafa	502362.15	1011675.48	2558	56.14	1082.76
Sheno	531406.52	1031349.10	2870	517.54	975.10
Mendida	534467.04	1067407.15	2791	13.25	910.03
Muketuri	486282.08	1055551.49	2657	171.75	960.06
Lemi	490221.87	1083669.72	2663	0.12	1113.69
Kotu gebeya	543460.69	1037656.57	2954	3.94	991.08

3.2.2.2 Hydrological Data

a. Stream flow data

In-stream flow and sediment yield modeling, stream flow data are necessary to perform sensitivity analysis, calibration, and validation. In addition to this, the stream flow data helps to generate sediment data from the discharge-sediment rating curve. The stream flow data was collected from the Ministry of Water and Energy (MoWE) from 1992 to 2018 as shown in Figure 3.8 below.

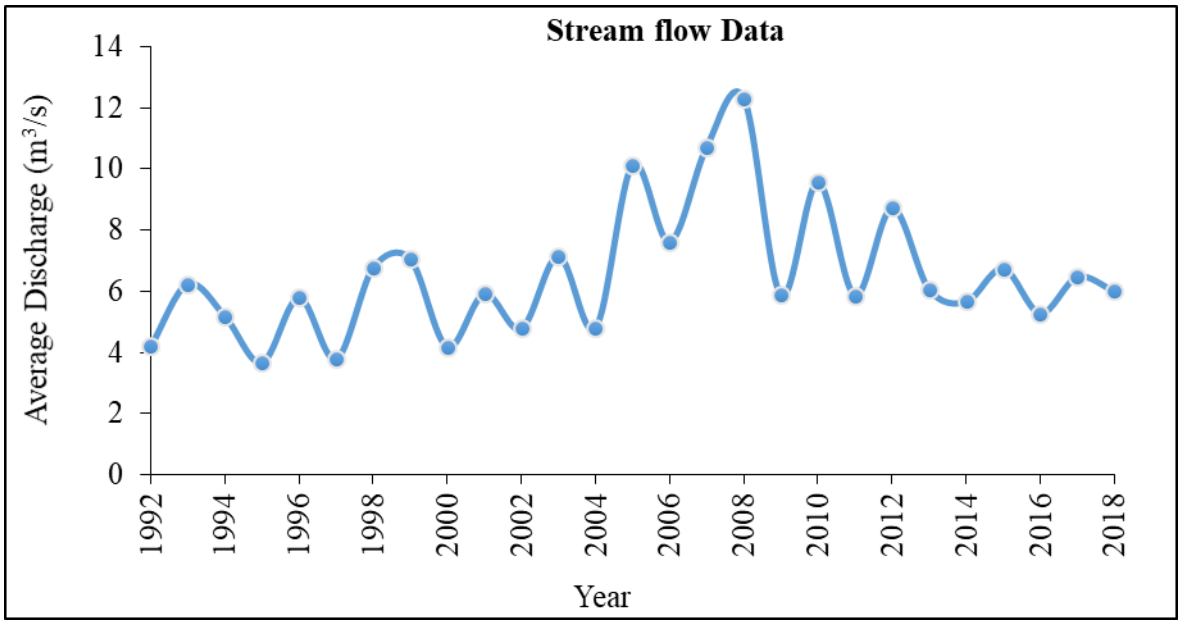

Figure 3-8: Yearly average flow data at Robi Jida river gage station from 1992-2018

b. Sediment data

Sediment concentration data for the Robi Jida River was taken by the Ministry of Water and Energy (MoWE) at the Robi Jida gauge station in a continuous time step from 1992 to 1996 (Appendixes table 5) by using stream flow and measured sediment data to generate sediment load data in a continuous time step, the relationship is known as the sediment rating curve. The analysis of sediment-rating curves depends on whether sediment transport is limited by the sediment transport capacity of the stream or the upstream supply of sediment (Pierre, 2010). Sediment concentration is changed into yield to make the rating curve relation in ton days^{-1} with the flow in cumecs (m^3s^{-1}) (Pierre, 2010; Subramanya, 1984) written as:

$$S = aQ^b \tag{3.1}$$

Where: S is the sediment load in tons per day, Q is the discharge in m^3/s, and a and b are the regression constants. Hence, the measured value that was collected from the MoWE

hydrology office was sediment concentration, so the first step was to convert this value into sediment load using the following formula:

$$S = 86.4 * Q * C \quad (3.2)$$

Where: S is sediment load (ton/day), Q is the stream flow (m^3/s), C is sediment concentration (kg/m^3) and 86.4 is the conversion factor. Therefore the relation between sediment load (S) and stream flow (Q) of Robi Jida watershed can be represents as in logarithmic plot (Figure 3.9).

After calculating the sediment load, the next step was to determine the relationship between the continuous (daily time step) measured flow in m^3/s and the measured sediment load (ton/day).

3.3 Filling Missing Records

Collected data contained missing records, so before using the data for detailed purposes, the missing data was filled in using different techniques. For this study, missing values in all stations were filled by the arithmetic mean and normal ratio methods, using normal ratio method when mean annual precipitation of each station is available and the magnitude differs from each considered precipitation stations by more than 10%. According to (Subramanya, 1984), the two formulas are described below.

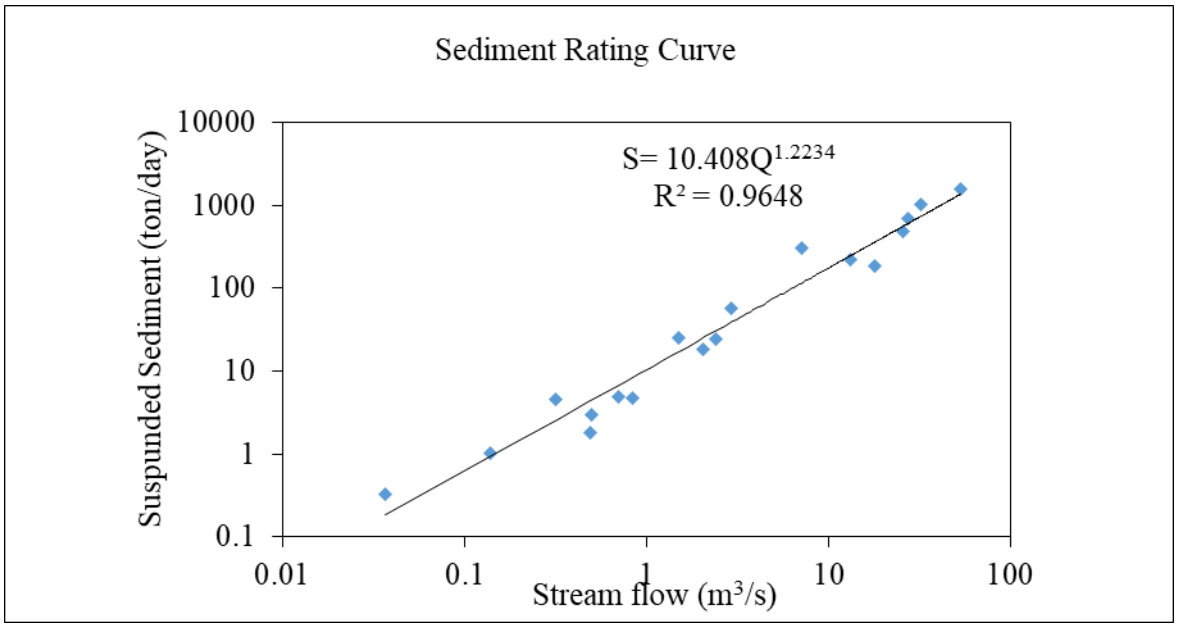

Figure 3-9: Sediment rating curve of Robi Jida River.

A. Arithmetic mean method

If the normal annual rainfalls at surrounding gauges are within 10% of the normal annual precipitation at the stations concerned, then the arithmetic procedure was adopted to estimate the missing data.

$$Px = \frac{P1+P2+P3+\cdots+Pn}{n} \quad (3.3)$$

Where: P_X – missed rainfall data, P_1, P_2, P_3... P_n - rainfall on non-missed years and n - Number of non-missed years.

B. Normal ratio method

This method is used if the normal annual precipitation of any surrounding gauges exceeds 10% of the gauge that is under consideration. The rainfall of the surrounding index stations was weighed by the ratio of normal annual rainfalls by using the following equation.

$$Px = \frac{\mathrm{Nx}}{\mathrm{n}}\left(\sum_{\mathrm{i}=1}^{\mathrm{n}} \frac{\mathrm{Pi}}{\mathrm{Ni}}\right) \quad (3.4)$$

Where: - P_X - missing data, N_X - the annual average precipitation at the gauge with the missing data, P_i - annual average values of neighboring stations, N_i - monthly rainfall data in the station for the same month of the missing station, n - the total number of gauges under consideration.

3.4 Checking Data Quality

The collected data can have errors sourced from an instrument, observers, and encoders (Subramanya, 1984). Therefore, the collected meteorological and hydrological data quality was checked using different statistical and hydrological software.

A. Consistency test

The consistency of the precipitation data was checked using double-mass curve analysis to use the data for further application (Adane et al., 2020). The inconsistency of meteorological recordings was checked using double mass curve analysis to prepare the data for further application. A double mass curve is a plot of accumulated rainfall data at the site of interest against the accumulated average at the surrounding stations (Subramanya, 1984). The consistency of metrological data for all stations was checked, which shows the data satisfies the consistency test, and the prepared double-mass curve for this study is shown in Figure 3.10 below.

B. Homogeneity test

The homogeneity test is an arithmetical test for detecting data changeability and checking whether a data series has been sourced from homogeneous or heterogeneous records. There are several methods available to check the data quality for homogeneity called absolute homogeneity and relative homogeneity. The representative meteorological station checking homogeneity of group stations is essential (Dhorde & Zarenistanak, 2013) . One of the methods to check homogeneity of the selected stations in the watershed is the non-dimensional rainfall records and plotted to compare the stations with each other. Non-dimensional values of the monthly precipitation of each station can be computed by:

$$Pi = \frac{Pi,av}{Pav} * 100 \quad (3.5)$$

Where Pi is the non-dimensional value of precipitation for the month in station i, Pi, av over years averaged monthly precipitation for station i, and Pav checking consistency and adjustment of rainfall stations are over year's averaged yearly precipitation of station i. The stations used for this study have a uni-modal rainfall pattern with the main rainfall season from Jun to September (Figure 3.11).

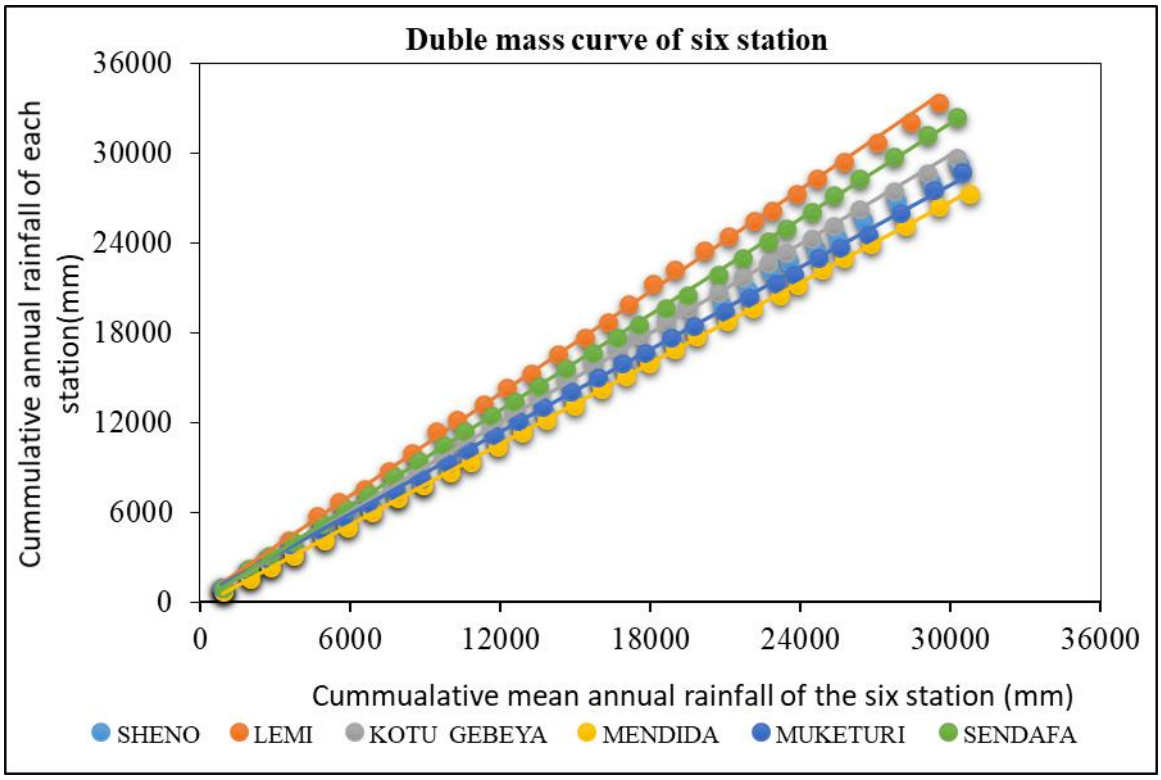

Figure 3-10: Consistency analysis of rainfall data using double Mass Curve.

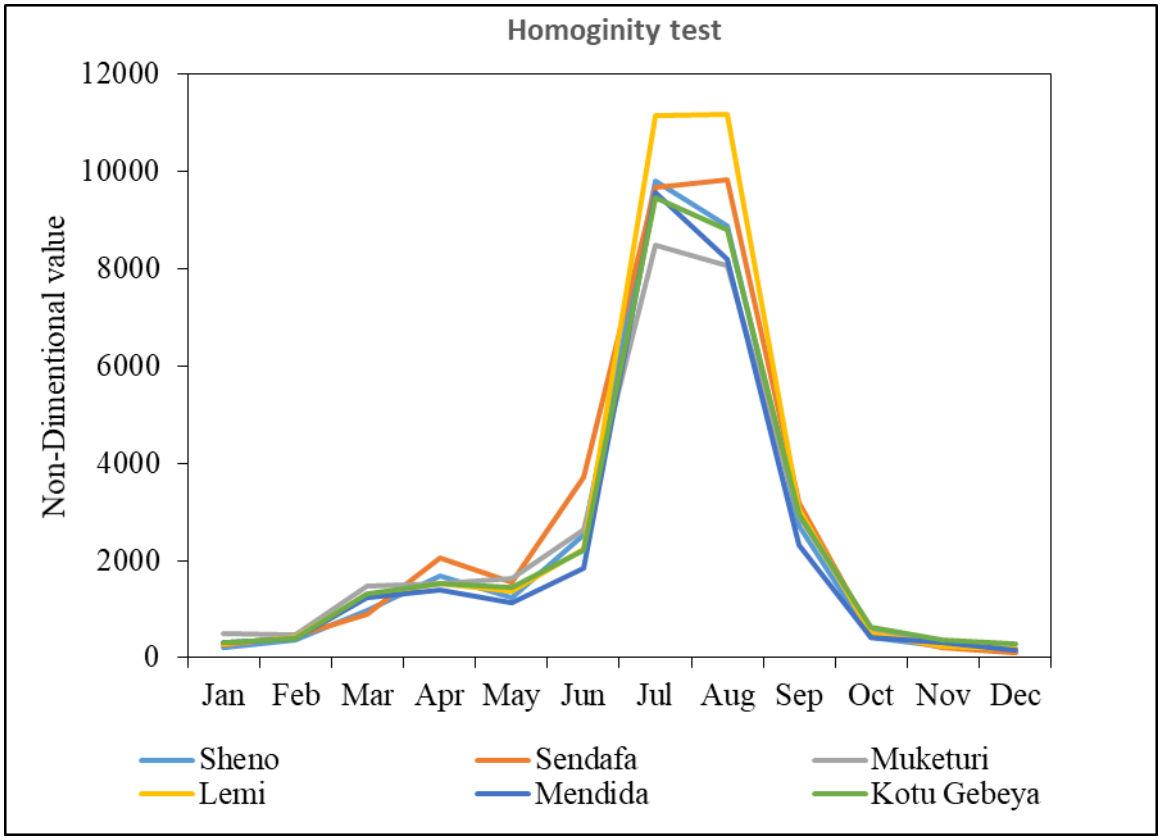

Figure 3-11: Non-dimensional plot of selected stations within & around the Robi Jida.

According to Raes et al. (2006), absolute homogeneity by using the Rainbow test predicts absolute consistency based on the cumulative deviation from the mean and clearly shows the probability of rejecting homogeneity as used by this formula:

$$S_k = \sum_{i=1}^{t}(X_i - \bar{X}) \quad k= 1... n \tag{3.6}$$

Where S_k is the cumulative deviation called a residual mass curve, Xi is the recorded time series data (i.e., metrological or hydrological data) X_1, X_2… X_n, and $\bar{X}$ is the mean. When the deviation crosses one of the horizontal lines, the homogeneity of the data set is rejected with probabilities of 90, 95, and 99%, respectively. Therefore, by using the Rainbow test, all rainfall and streamflow data were checked and satisfied the test for homogeneity. The homogeneity test of all station's rainfall and streamflow data was presented (Appendix Figure 1).

3.5 Description of SWAT Model

The Soil and Water Assessment Tool (SWAT) model was developed by the US Department of Agriculture's Agriculture Research Service (USDA-ARS). It is a physically based model,

and the SWAT uses HRUs to describe spatial heterogeneity in terms of land cover, soil type, and slope within a watershed**.** Its model components include weather, hydrology, erosion and sedimentation, plant growth, nutrients, pesticides, agricultural management, channel routing, pond and reservoir routing, and a conceptual, continuous-time model (Arnold & Fohrer, 2005; Neitsch et al., 2011). It can be used for both gauged and ungauged basins to estimate the runoff, sediment, and chemical yields (Arnold & Fohrer, 2005) with varying land use, soil, topography, and land management practices for long periods daily (Neitsch et al., 2011). The model allows the simulation of a high level of spatial detail by dividing the watershed into a large number of sub-watersheds.

3.5.1 Hydrological Modeling using SWAT

The model will divide the basin into sub-basins based on the size of the basin, the spatial detail of the available input data, and the amount of detail required. Further, the sub-basins will be divided into small portions called "hydrological response units" (HRU), characterized by uniformity of soil and land use (Setegn, et al., 2010). Hydrological processes are simulated in detail for each HRU and then aggregated for the sub-basin by a weighted average. The SWAT model accurately predict the movement of runoff, sediment, or nutrients, and pesticide simulation of the watershed is separated into two major divisions: the land phase and the routing phase of the hydrologic cycle. The land phase controls the amount of water, sediment, nutrients, and pesticides loaded into the main channel in each sub-watershed. In comparison, the routing phase is defined as the movement of water, sediments, etc. through the channel network of the watershed to the outlet (Neitsch et al., 2011).

A. Land phase of the hydrologic cycle

The land phase of the hydrologic processes by the SWAT model is based on the water balance equation (Neitsch et al., 2011), which is written as:

$$SW_t = SW_o + \sum_{i=1}^{t} \left(R_{day} - Q_{surf} - E_a - W_{see} - Q_{gw}\right) \quad (3.7)$$

Where SWt is the final soil water content; SWo is the initial soil water content (mm); t is time (days); R_{day} is the amount of precipitation on the day; Q_{surf} is the amount of surface runoff on the day; E_a is the amount of evapotranspiration; W_{seep} is the amount of water entering the vadose zone from the soil profile on the day; and Q_{gw} is the amount of returning to groundwater on the day.

B. Surface Runoff

Using daily or sub-daily rainfall amounts, SWAT simulates surface runoff volumes, peak Runoff rates and time of concentration for overland and channel flow for each sub-basin (Neitsch et al., 2011), by using the SCS curve number (SCS 1972) equation is:

$$Q_{surf} = \frac{\left(R_{day} - I_a\right)^2}{R_{day} - I_a + \mathrm{S}} \tag{3.8}$$

Where; Q_{surf} is the accumulated runoff or rainfall excess (mm), R_{day} is the rainfall depth for the day (mm), I_a is the initial abstractions which include surface storage, interception, and infiltration before runoff (mm), and S is the retention parameter (mm). The retention parameter varies spatially due to changes in soils, Land use, management, and slope and temporally due to changes in soil water content. The retention parameter is defined as;

$$\mathrm{S} = 25.4\left(\frac{1000}{\mathrm{CN}} - 10\right) \tag{3.9}$$

Where CN is the curve number for the day.

The initial abstraction, I_a is commonly approximated as 0.2S and the above equation becomes

$$Q_{surf} = \frac{\left(R_{day} - 0.2\mathrm{S}\right)^2}{R_{day} + 0.8\mathrm{S}} \qquad FOr\ R_{day} > I_a\ (= 0.2S) \tag{3.10}$$

C. Estimating potential evapotranspiration using SWAT

Potential evapotranspiration is the rate at which evapotranspiration would occur from a large area completely and uniformly covered with uniform vegetation that has access to unlimited supply of soil water. This rate is assumed to be unaffected by microclimatic processes such as advection or heat storage effects. The model offers three options for estimating potential evapotranspiration include; Hargreaves, Priestly-Taylor, and Penman-Monteith (Neitsch et al., 2011).

The SWAT model selects the methods of estimating potential evapotranspiration depending on the input meteorological data. The model uses the Hargreaves method of estimating evapotranspiration using meteorological data including the rainfall, and minimum and maximum temperature. In the case of Penman-Monteith, meteorological variables including rainfall, minimum, and maximum temperature, relative humidity, wind speed, and solar radiation were used, and for the case of Priestly-Taylor, all data used in Penman-Monteith

are used except wind data. In this study, the Penman-Monteith method for estimating evapotranspiration was used, because it incorporates all meteorological data.

3.5.2 Sediment Modeling in SWAT

The SWAT model calculates erosion and sediment yield from each HRU using the Modified Universal Soil Loss Equation(MUSLE) using the following equation(William, 1975).

$$\text{Sed} = 11.8 * \left(\text{Q}_{\text{surf}} * \text{q}_{\text{peak}} * \text{Area}_{\text{hru}}\right)^{0.56} * \text{K}_{\text{USLE}} * \text{C}_{\text{USLE}} * \text{P}_{\text{USLE}} * \text{LS}_{\text{USLE}} * \text{CFRG} \quad (3.11)$$

Where: S_{ed} is yield of sediment on a given day in ton/day; Q_{surf} is Volume of surface runoff (mm/ha); Q_{peak} is the Peak surface runoff rate (m^3/s); $Area_{HRU}$ is Hydrologic response unit area (ha); K_{USLE} is USLE soil erodibility factor; C_{USLE} is USLE topography cover factors; LS_{USLE} is USLE topography factors; P_{USLE} is USLE soil protection factors; and CFRG coarse fragment factor.

For channel networks, SWAT computes the sediment flow (Neitsch et al., 2011):

$$\text{Sed}_{\text{ch}} = \text{Sed}_{\text{chi}} - \text{Sed}_{\text{dep}} + \text{Sed}_{deg} \quad (3.12)$$

Where Sed_{ch} is the amount of suspended sediment in the reach; Sed_{deg} is the amount of sediment that reenters the reach segment; Sed_{dep} is the amount of sediment deposited in the reach segment; and Sed_{chi} is the amount of suspended sediment in the reach at the beginning of the time. Similarly, SWAT calculates the amount of sediment transported out of reach (Neitsch et al., 2011).

$$\text{Sed}_{\text{out}} = \text{Sed}_{\text{ch}} * \left(\frac{\text{V}_{out}}{\text{V}_{ch}}\right) \quad (3.13)$$

Where Sed_{out} is the amount of sediment transported out of the reach; Sed_{ch} is the amount of suspended sediment in the reach; V_{ch} is the volume of water in the reach segment, and V_{out} is the volume of outflow during the time step.

3.6 Data preparation for SWAT Model

Stream flow and sediment yield modeling at a watershed scale require different spatial and time-series data inputs. Thus, input data was obtained from different institutions, but the data was not arranged as the SWAT model requires. The time-series data like rainfall, maximum and minimum temperature, wind speed, solar radiation, and relative humidity data of different meteorological stations used for the study were arranged as the requirements of the model. Meteorological data and the names of the stations were prepared in text format using Notepad, and look-up tables were prepared for land use/ land cover, and soil to relate to the

grid values of land use /land cover classes, and soil. SWAT WGEN is used to fill the missing data using monthly statics (Schuol & Abbaspour, 2007). The SWAT weather generator database, which can obtained from https://swat.tamu.edu/software/, was utilized to develop weather generator for the Sheno meteorological station in this study. The weather generator data definition, the weather generator data file WGEN user, rainfall, temperature, relative humidity, solar radiation, and wind speed data were selected and added to the model, respectively. The output of the weather generators and the description of the parameters are shown (Appendix table 6). The spatial data inputs, including land use/land cover, and soil map, were prepared using Arc GIS 10.3.

3.7 SWAT Model Setup

The SWAT model setup is compatible with Arc GIS version 10.3, Arc-SWAT, 2012.10.3.19 was downloaded from the SWAT website https://swat .tamu.edu/software/arc swat/ and it's added to the ArcGIS window from toolbars of GIS. The model consists of steps from the SWAT project setup to the SWAT simulation.

3.7.1 Watershed Delineation

The first step in the SWAT model input is watershed delineation from the digital elevation model. The watershed delineation tool uses and expands the Arc GIS, and spatial analyst functions to perform watershed delineation (Neitsch et al., 2011) and the stream network was defined for the whole DEM by the model using the concept of flow direction and flow accumulation. The outlet of the Robi Jida watershed was added for reference, the monitoring point was added manually, and the definition of the watershed, sub-basin boundaries, and streams were set by selecting a threshold area. During this study, the 2500ha threshold area was taken. With this information, the watershed area was delineated as 762.74 $km^{2,}$ and 13 sub-watersheds are formed for the whole watershed as shown in Figure 3.12 and the area coverage of each sub-watershed is shown in Table 3.8 below.

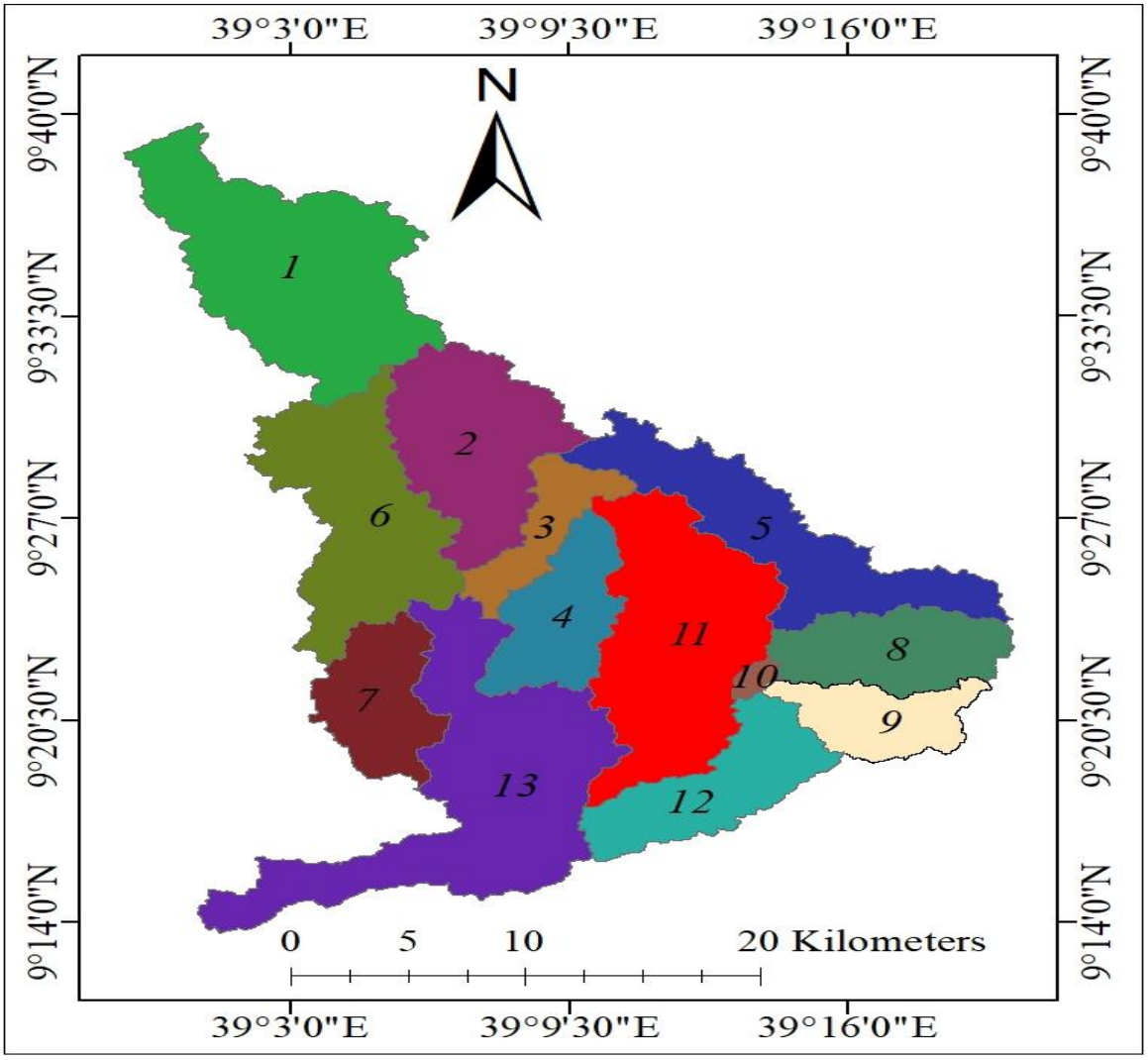

Figure 3-12: Number of sub-watersheds in the Robi Jida watershed.

Table 3-7: Area coverage of each sub-basin in the Robi Jida watershed.

Sub-basin	Area (km^2)	Percent (%)	Sub-basin	Area (km^2)	Percent (%)
1	109.15	14.31	8	40.94	5.37
2	68.11	8.93	9	28.97	3.80
3	23.17	3.04	10	3.05	0.40
4	38.70	5.07	11	98.35	12.89
5	68.41	8.97	12	45.53	5.97
6	78.76	10.33	13	122.14	16.01
7	37.46	4.91			

3.7.2 Hydrological Response Units (HRU) Analysis

The HRU analysis tool in Arc-SWAT helps to load LULC, soil layers and slope map to the project. HRU analysis in SWAT includes divisions of HRUs by slope classes in addition to Land use and soils. The multiple slope option (an option which considers different slope classes for HRU definition) were selected. The LULC, soil and slope map was reclassified in order to correspond with the parameters in the SWAT database. After reclassifying the land use, soil and slope in SWAT database, all these physical properties made to be overlaid for HRU distributions (Inchell et al., 2013).

The last step in the HRU analysis was the HRU definition. The HRU definition in this study was determined by assigning multiple HRU to each sub-watershed. In multiple HRU definition, a threshold level was used to eliminate minor land uses, soils or slope classes in each sub-basin. The multiple slope option which considers different slope classes for HRU definition was preferred over the single slope and the slope was classified into five (5) classes and therefore the ranges was 0-3%, 3-8%, 8-15%, 15-30%, and above 30%. Sub dividing the sub-watershed into areas having unique land use, soil and slope combinations makes it possible to study the differences in evapotranspiration and other hydrologic conditions for different land covers, soils and slopes (Arnold et al., 2012). HRUs was created by a 5%, 2%, and 2% threshold for slope, soil, and land use/land cover definition respectively.

3.7.3 Write input Tables

After HRU analysis, the weather data to be used in the watershed simulation was imported using the first command in the write input tables menu item on the Arc- SWAT toolbar. This tool aids in loading weather station locations into the current project and assigning weather data. The weather data definition is divided into six tabs containing weather generator data, rainfall, temperature, solar radiation, relative humidity, and wind speed data were selected and added to the model respectively.

3.7.4 Running SWAT Simulation

Once the weather variables are imported, the SWAT model run is set up to enter the simulation period. The SWAT model was simulated by warm-ups two years (1992 and 1993) as a warm-up period. The hydrological processes, including runoff and sediment output, were represented graphically by running the model for each process as well as performing a

SWAT check. The outputs were used to assess the model's performance using statistical tools for sensitivity analysis, calibration, and validation.

3.8 Model Sensitivity Analysis, Calibration, and Validation

3.8.1 Sensitivity Analysis

Sensitivity analysis refers to the identification of the most significant influencing factor in the model, and it is important to provide information on the basic steps of the research area and also helps to reduce number of parameters by identifying the non-sensitive (Abbaspour, 2012).

In this study, SWAT model sensitivity analysis was performed from January 1, 1994, to December 31, 2018, in which the first two years (1992 and 1993) were taken as for "model warm-ups'', and nineteen (19) stream flow and sediment parameter were tested. Table 3.8 and 3.9 shows that the sensitive parameters for stream flow and sediment are drawn by SWAT model within the SWAT-CUP SUFI-2 algorithm respectively.

3.8.2 Model Calibration

Calibration is a method of selecting the best model parameters to compare the simulated outputs and observed data. Model calibration is a critical step in catchment modeling studies that helps to reduce uncertainties in model predictions (Abbaspour et al., 2007).

Model users are often faced with difficult task of determining which parameters to calibrate so that the model response simulates the actual field conditions as closely as possible. In such cases, sensitivity analysis is helpful to identify and rank parameters that have a significant impact on specific model outputs of interest. Calibration of our model using the selected sensitive parameters means pushing our model to reality which helps to check the performance of the model by using two-thirds of our total data. Therefore in this study period 1994–2010 were used for calibration both stream flow and sediment yield.

Table 3-8: Stream flow sensitivity parameter initial range and sensitivity order.

No	Parameter name	Description	Initial range	t-stat	p-value
1.	r_cn2.mgt	SCS runoff curve number	-0.25 to 0.25	4.19	0.00
2.	v_esco.hru	Soil evaporation compensation factor	0 to 1	-3.26	0.01
3.	r_sol_awc(..).sol	Available water capacity of the soil layer	-0.25 to 0.25	3.00	0.01
4.	v_ch_k2.rte	Effective channel hydraulic conductivity	-0.01 to 500	-2.94	0.01
5.	v_rchrg_dp.gw	Deep aquifer percolation fraction	0 to 1	-2.84	0.02
6.	v_gw_revap.gw	Groundwater “revap” coefficient	0.02 to 0.2	2.48	0.03
7.	r_sol_k(..).sol	Saturated hydraulic conductivity	-0.25 to 0.25	-1.92	0.08
8.	a_gwqmn.gw	The threshold depth of water in the shallow aquifer required for return flow to occur	0 to 5000	-1.29	0.23
9.	a_gw_delay.gw	Groundwater delay	0 to 500	-1.21	0.26
10.	r_sol_alb(..).sol	Moist soil albedo	-0.25 to 0.25	-1.18	0.27
11.	v_alpha_bnk.rte	Base flow alfa factor for bank storage	0 to 1	-1.18	0.27
12.	a_epco.hru	Plant uptake compensation factor	0 to 1	-0.81	0.44
13.	v_surlag.bsn	Surface runoff lag time	0 to 10	0.70	0.50
14.	v_sol_bd(..).sol	Moist bulk density	0.9 to 2.5	0.56	0.58
15.	a_revapmn.gw	The threshold depth of water in the shallow aquifer for “revap” to occur	0 to 500	0.46	0.65
16.	v_ch_n2.rte	Manning coefficient for the channel	-0.01 to 0.3	0.42	0.69
17.	v_ov_n.hru	Manning's "n" value for overland flow	0.01 to 30	-0.37	0.72
18.	v_alpha_bf.gw	Base flow alfa factor	0 to 1	0.22	0.83
19.	r_sol_z(..).sol	Depth from soil surface to bottom of layer	-0.25 to 0.25	-0.13	0.90

Table 3-9: Sediment sensitivity parameter initial range and sensitivity order.

No	Parameter name	Description	Initial range	t-stat	p-value
1.	v_usle_k(..).sol	USLE soil erodibility (k) factor	0 to 0.65	-11.80	0.00
2.	v_slsubbsn.hru	Average slope length	10 to 150	-7.16	0.00
3.	r_cn2.mgt	SCS runoff curve number	-0.2 to 0.2	-7.05	0.00
4.	v_hru_slp.hru	Average slope steepness	0 to 1	-6.63	0.00
5.	v_usle_p.mgt	USLE support practice factor	0 to 1	-5.12	0.00
6.	v_usle_c{..}.plant.dat	Min value of USLE C factor applicable to the land cover/plant	0.001 to 0.5	-2.78	0.01
7.	v_adj_pkr.bsn	Peak rate adjustment factor for sediment routing in the sub-basin (tributary channels).	0 to 2	-2.07	0.04
8.	v_sol_awc (..).sol	Available water capacity of the soil layer.	0 to 1	1.92	0.06
9.	v_spcon.bsn	Linear parameter calculating the maximum amount of sediment that can be retrained during channel sediment routing.	0.0001to 0.01	-1.66	0.10
10.	v_ch_bnk_d50.rte	D50 median particle size diameter of channel bank sediment	0 to 10000	1.10	0.27
11.	v_lat_sed.hru	Sediment concentration in lateral flow and groundwater flow	0 to 5000	-0.82	0.41
12.	v_ch_cov2.rte	Channel cover factor	-0.001 to 1	-0.79	0.43
13.	v_biomix.mgt	Biological mixing efficiency	0 to 1	0.34	0.73
14.	v_ch_bnk_kd.rte	Erodibility of channel bank sediment by jet test	0.001 to 3.75	0.23	0.81
15.	v_sol_alb(..).sol	Moist soil albedo	0 to 0.25	-0.22	0.83
16.	v_rsdin.hru	Initial residue cover	0 to 10000	-0.18	0.85
17.	v_spexp.bsn	Exponent parameter for calculating sediment retained in channel sediment routing	1 to 1.5	-0.16	0.87
18.	v_sol_k(..).sol	Saturated hydraulic conductivity	0 to 2000	0.09	0.93
19.	v_ch_cov1.rte	Channel erodibility factor	0.01 to 0.6	-0.06	0.95

3.8.3 Model Validation

In order to utilize any predictive watershed model for estimating the effectiveness of future potential management practices the model must be first calibrated to measured data and should then be tested (without further parameter adjustment) against an independent set of measured data. This testing of model on an independent data set is commonly referred model verification (Abbaspour, 2012). Verification is described as the process of demonstrating that a given site specific model is capable of making sufficiently accurate simulations, also sufficiently accurate results can vary based on project goals (Arnold et al., 2012). It is used to test the calibrated parameters with an independent set of data without further changes to the parameters. In this study the validation was performed to compare the model outputs with an independent data set without making further change to parameters obtained during the calibration process. In addition, validation of the model was done using one-third of the data. The measured data of average monthly stream flow and sediment yield from 2011-2018 at the Robi Jida Gauging station was used for model verification.

3.9 Model Performance Evaluation

The accuracy, consistency, and adaptability performance of the model were evaluated (Goswami et al., 2005). An objective function estimate of the closeness of the simulated behavior of the model to observation is required to assess the performance of the model (Krause et al., 2005). The performance of the model was evaluated using efficiency criteria including, coefficient of determination (R^2), Nash-Sutcliff Efficiency (NSE), and percent of bias (PBIAS) to measure how well trends in the measured data were reproduced by simulated results over a specified period. The equation of the different model performance evaluation methods is shown below and the range of rating statistics are shown in table 3.10 below.

A. Coefficient of determination (R^2)

The coefficient of determination is a statistic that is widely used to determine the agreement between predicted and observed variables. Coefficient of determination (R^2) with a value of one indicates excellent agreement, and a value of zero reflects that there is no correlation between the observed and simulated values (Legates, 1999). The determination coefficient for the n-time step is determined by the equation below.

$$R^2 = \frac{\{\Sigma(Qsi-\bar{Q}s)*(Qoi-\bar{Q}o)\}^2}{\Sigma(Qsi-\bar{Q}s)^2*(Qoi-\bar{Q}o)^2} \quad (3.14)$$

Where R^2 Coefficient of determination, Q is a variable (discharge or sediment), o and s stand for observed and simulated, i is i^{th} measured or simulated data, and the bar stands for average.

B. Nash- Sutcliff efficiency (NSE)

Nash- Sutcliff efficiency **(**NSE) is normalized statistic that determines the relative magnitude of the residual variance compared to the measured data variance(Nash & Sutcliffe, 1970). NSE indicates how well the plot of observed versus simulated data fits the 1:1 line. It is computed by:

$$\mathrm{NSE} = 1 - \frac{\Sigma(\mathrm{Qoi}-\mathrm{Qsi})^2}{\Sigma(\mathrm{Qoi}-\bar{\mathrm{Q}}\mathrm{o})^2} \quad (3.15)$$

Where Q is a variable (discharge or sediment), o and s stand for observed and simulated, respectively, and the bar stands for average.

C. Percent of bias (PBIAS)

Percent of bias measures the average tendency of the simulated data to be larger or smaller than the observations, being the optimum value of zero. A positive value implies model underestimation bias, and a negative value indicates model overestimation bias (Gupta et al., 2005).

$$PBIAS = 100 * \frac{\sum_{i=1}^{n}(\mathrm{Qo}-\mathrm{Qs}),\mathrm{i}}{\sum_{i=1}^{n}(\mathrm{Qo},\mathrm{i})} \quad (3.16)$$

Where Q is a variable, o and s stand for observed and simulated respectively.

Table 3-10: General performance ratings statistics for a monthly time step.

Performance rating	R^2	NSE	PBIAS	
			Streamflow	Sediment
Very good	$0.75 < R^2 \leq 1.0$	$0.75 < NSE \leq 1.0$	$PBIAS < \pm 10$	$PBIAS < \pm 15$
Good	$0.65 < R^2 \leq 0.75$	$0.65 < NSE \leq 0.75$	$\pm 10 \leq PBIAS < \pm 15$	$\pm 15 \leq PBIAS < \pm 30$
Satisfactory	$0.5 < R^2 \leq 0.65$	$0.5 < NSE \leq 0.65$	$\pm 15 \leq PBIAS < \pm 25$	$\pm 30 \leq PBIAS < \pm 55$
Unsatisfactory	$R^2 \leq 0.5$	$NSE \leq 0.5$	$PBIAS \geq \pm 25$	$PBIAS \geq \pm 55$

*Sources (Moriasi et al., 2007).

3.10 Identification of Vulnerable Sub-Catchment

Identifying erosion-vulnerable sub-catchments for prioritization of watershed management is one of the objectives of this study. From the model simulation output, the main sediment source areas in the watershed were identified. Arc GIS, and SWAT viewer are very important tools that helps to identify which sub-watershed is highly affected by erosion and identify the most sediment-contributing areas in the watershed (Dibabaa & Ebsab, 2022; Setegn et al., 2009). Also, the SWAT model is applied to identify the spatially distributed soil erosion and sedimentation processes to assess the impact of Best Management Practices (BMPs) scenarios on sediment reductions in the watershed of erosion-prone area at the Hydrological Response Units (HRUs) level, which is useful for watershed management planning (Betrie et al., 2011). In this study, Arc GIS was used to identify the sensitive region for maximum sediment areas in the Robi Jida watershed for watershed management.

Based on the average annual sediment yield, soil erosion level in the Robi Jida was classified into four classes, negligible erosion class ($\leq$ 7.57 ton $ha^{-1}yr^{-1}$), acceptable erosion class (7.57 to $\leq$ 11.44 ton $ha^{-1}yr^{-1}$), moderately eroded class (11.44 to $\leq$ 18.18 ton $ha^{-1}yr^{-1}$), and severely eroded (> 18.18 ton $ha^{-1}yr^{-1}$) class categories.

3.11 Analysis of Best Management Practices (BMPs) Scenarios

Adequate Best Management practices (BMPs) were implemented in hotspot areas with significant damage to mitigate sediment movement and soil erosion in watersheds. For evaluating the effects of several best management scenarios on sediment reductions in the Robi Jida watershed, the SWAT model is helpful. At the Hydrological Response Units (HRUs) level, it showed the erosion-prone area, which is already helpful information for catchment management planning (Betrie et al., 2011). Different researchers in the upper blue Nile basin, were considered for the selection of BMPs (Asres and Awulachew 2010; Admas et al., 2022; Betrie et al., 2011; Lemma et al. 2019; Gashaw et al., 2022).

In this study, five Best management scenarios were chosen, all with independent impacts on flow and sediment characteristics. The five management methods were implemented in the critical sub-watershed with high sediment production. To investigate the effects of the alternative practices on the estimated sediment yield, these BMPs were modeled by varying the pertinent SWAT parameters.

Scenario 0: Baseline Scenario. This scenario, which involves the absence of BMPs, is meant to represent the scenario that existed when the simulation was initially performed. Without adjusting any modeling parameters, the simulation utilized the SWAT models calibrated data. When comparing the efficiency and reduction capacity of the chosen management solutions, the baseline scenario provides a point of reference.

Scenario II: Filter Strips (FS). Filter strips are vegetated areas or strips of land strategically placed along the edges of fields, water bodies, or drainage channels. Their primary purpose is to reduce soil erosion and filter pollutants from surface runoff before it enters water bodies. The FS acts as buffer zone, intercepting sediment, nutrients, and chemicals carried by runoff and typically planted with grasses, shrubs, or other vegetation (Waidler et al., 2011). The SWAT model allows the simulation of filter strips through the alteration of an optional scheduled management operations (.ops) file for every sub watershed where the practice is to be used. The model can simulate the width of filter strips from 1m to 10m based on local research experiences in Ethiopian watersheds (Asres and Awulachew 2010; Waidler et al., 2011; Lemma et al., 2019; Dibabaa and Ebsab ,2022; Gashaw et al., 2021). For evaluating the impacts of the filter strip scenario on sediment abstraction, the filter width of unit value (FILTERW = 1m and 5m) was considered for analysis of this study.

Scenario II: Vegetative contour strips (VS). Also known as vegetative filter strips or simply contour strips, are a type of land management practice used in agriculture and conservation to control erosion and manage water runoff. They involve the establishment of strips of vegetation, typically grasses or other suitable plants, along the contours of sloping land. The purpose of vegetative contour strips is to slow down and filter the flow of water across the land, reducing soil erosion and preventing sediment and pollutants from reaching nearby water bodies, such as streams or rivers. The strips act as buffers, intercepting runoff and allowing the vegetation to capture and absorb excess water and associated nutrients or chemicals (Dibabaa & Ebsab, 2022; Waidler et al., 2011).

Scenario III: **Stone/Soil bunds (SSB)**. In the highlands of Ethiopia, application of stone/soil bunds as a tactic to lessen erosion and sediment production regarded as a beneficial practice. By decreasing slopes and boosting watershed abstractions, the application of stone/soil bunds decreases overland flow and sediment loss (Addis et al., 2016). Reduced runoff, sheet scour, and slope length are goals of this approach. The impacts of creating stone/soil bunds

on steep slope is simulated by varying parameters such as the length of slope (SLSUBBSN), steepness of slope (HRU_SLP), soil conservation services (SCS) curve number (CN_2), and erosion control practice factor (USLE_P) for key sub-basins (Gashaw et al., 2021; Lemann et al., 2018).

***Scenario IV*: Contour.** Contour lines establish a water break that prevents the formation of gullies and rills during times of heavy precipitation. The CN_2 and corresponding USLE_P, a ratio that opposes soil loss from one support system with soil loss from up-and-down-cultivation, were adjusted in the SWAT model to reflect this conservation method.

***Scenario V*: Terracing.** By decreasing runoff and increasing infiltration, terracing acts as a barrier to runoff. As a result, siltation takes place and the erosion strength of overland flow is reduced. By using this method, more water is available for recharging aquifers in shallow depths. The terracing scenario was implemented through the adjustment of suitable elements such as the CN_2, USLE_P, and SLSUBBSN. The value of SLSUBBSN is altered based on slope classes. The soil class, gradient, and land use and land cover were used to determine the appropriate curve number and USLE_P (Leta et al., 2023).

3.12 General Framework of the Study

The general framework that shows input data, processes, and outputs to achieve the objective of the study was prepared in Figure 3.13. All the processes indicated in the chart were used to model stream flow and sediment yield generated from the Robi Jida watershed using the soil and water assessment (SWAT) model.

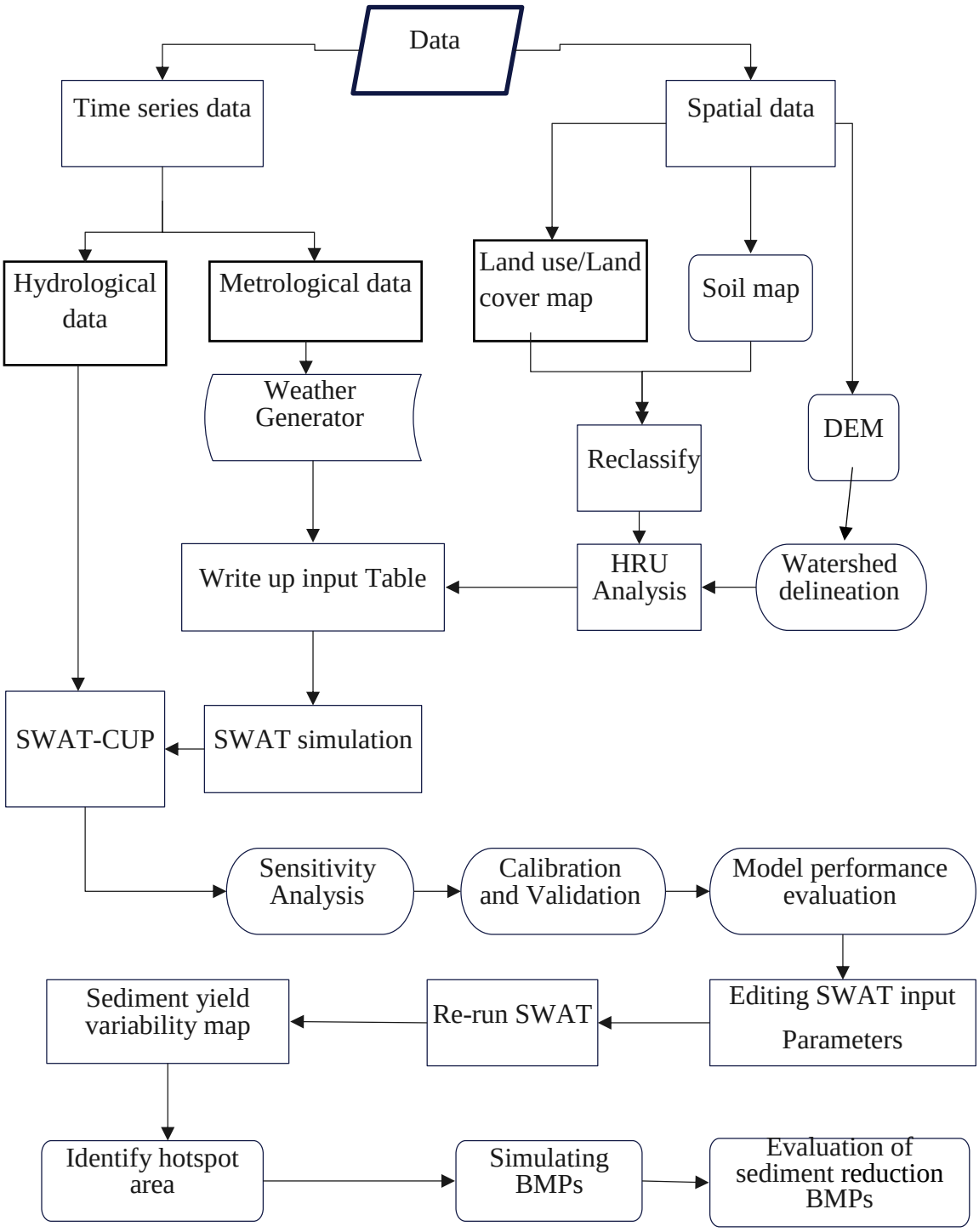

Figure 3-13: General framework to be used for the study.

4. RESULTS AND DISCUSSIONS

4.1 Stream Flow Modeling

4.1.1 Stream flow sensitivity analysis

According to the results obtained from the sensitivity analysis, the ranks of the parameters were assigned depending on the t-stat and p-value. Therefore, the parameters having a higher absolute value t-statistic indicate more sensitivity and a p-value closer to zero indicates more significance (Abbaspour, 2012). The identified sensitive parameters enable us to focus only on those parameters that affect most of the model output during calibration since the SWAT model has several parameters to deal with. Table 4.1 shows the sensitive parameters for stream flow drawn by the SWAT model within the SWAT-CUP SUFI-2 algorithm and also shows (Appendix Figure 2).

Table 4-1 Stream flow sensitive parameter, initial rang, and ranks in Robi Jida watershed.

No	Parameter with operation	Global rang		Verification technique		t-stat	p-value	Rank	Relative sensitivity
		min	max	min	max				
1	r_cn_2.mgt	35	98	-0.25	0.25	4.19	0.00	1	Higher
2	v_esco.hru	0	1	0	1	-3.26	0.01	2	Higher
3	r_sol_awc(..).sol	0	1	-0.25	0.25	3.00	0.01	3	Higher
4	v_ch_k_2.rte	-0.01	500	-0.01	500	-2.94	0.01	4	Higher
5	v_rchrg_dp.gw	0	1	0	1	-2.84	0.02	5	Higher
6	v_gw_revap.gw	0.02	0.2	0.02	0.2	2.48	0.03	6	Higher
7	r_sol_k(..).sol	0	2000	-0.25	0.25	-1.92	0.08	7	Medium
8	a_gwqmn.gw	0	5000	0	5000	-1.29	0.23	8	Medium
9	a_gw_delay.gw	0	500	0	500	-1.21	0.26	9	Medium
10	r_sol_alb(..).sol	0	0.25	-0.25	0.25	-1.18	0.27	10	Medium
11	v_alpha_bnk.rte	0	1	0	1	-1.18	0.27	11	Medium

* r_ is the existing parameter value multiplied by (1+ given value); v_ is the existing parameter value to be replaced by a given value, and a_ is a given value added to the existing parameter value (Abbaspour, 2012).

Nineteen hydrological parameters were tested for their sensitivity in streamflow simulation. The analysis revealed that six parameters exhibited greater sensitivity based on t-statistics and p-values. The most sensitive parameters identified were the SCS runoff curve number (CN_2), soil evaporation compensation factor (ESCO), soil available water content (SOL_AWC), effective channel hydraulic conductivity (CH_K_2), deep aquifer percolation fraction (RCHRG_DP), and groundwater "revap" coefficient (GW_REVAP). These parameters were determined the most influential for streamflow in the Robi Jida watershed. The sensitivity of these parameters aligns well with previous studies conducted in the upper Blue Nile Basin (Addis et al., 2016; Asres & Awulachew, 2010; Lemma et al., 2019; Setegn, 2008; Sitotaw et al., 2021). Additionally, Worku, (2017) supported these findings in the Beressa watershed, where he modeled the runoff-sediment response to land use and land cover changes using integrated GIS and SWAT models.

4.1.2 Stream flow calibration

After the sensitive parameters were selected, the calibration process focuses on determining the gap between simulated and observed values by adjusting the sensitive flow parameters in the recommended range. The more influential eleven (11) stream flow parameters, ranging from high to medium sensitivity, were used and adjusted further by varying iteratively in their allowable range until satisfactory agreement between measured and simulated stream flow was obtained, as shown (Table 4.2). The minimum and maximum range of parameters in the first calibration were taken from the range used in the sensitivity analysis, and fitted values were obtained from the final calibration.

Dibabaa & Ebsab (2022) conducted research on the SWAT model, focusing on hotspot area identification and the evaluation of optimal management scenarios in the Toba watershed, located in the upper Blue Nile Basin. They used initial parameter values for CN_2 parameter ranged from (-0.25 to 0.25). Similarly, Asres and Awulachew, (2010) investigated SWAT-based runoff and sediment yield modeling in the Gumera watershed, also in upper Blue Nile Basin. Their study employed initial parameter values for various parameters, specifically: CN_2 (-0.25 to 0.25), GWQMN (0 to 5000), ESCO (0 to 1), SOL_AWC (-0.25 to 0.25), RCHRG_DP (0 to 1), and SOL_K (-0.25 to 0.25). Notably, the fitted value for SOL_AWC was 0.2, which aligns with findings of this study. Furthermore, Setegn, et al., (2010) explored the application of the SWAT model and conducted a prediction uncertainty analysis in the Lake Tana Basin. Their research indicated that the lower and upper bounds for parameters

such as the SCS runoff curve number (CN_2), soil evaporation compensation factor (ESCO), soil available water content (SOL_AWC), and the threshold depth of water in the shallow aquifer necessary for return flow (GWQMN) were similar to those in this study. The fitted values for ESCO and SOL_AWC were also similar.

Table 4-2: Stream flow sensitive parameters, initial range and fitted value.

No	Parameter name with operation	Global rang		Verification techniques		Fitted value
		min	max	min	max	
1.	r_CN_2.mgt	35	98	-0.25	0.25	-0.0307
2.	v_ESCO.hru	0	1	0	1	0.6063
3.	r_SOL_AWC(..).sol	0	1	-0.25	0.25	0.1669
4.	v_CH_K_2.rte	-0.01	500	-0.01	500	307.44
5.	v_RCHRG_DP.gw	0	1	0	1	0.002
6.	v_GW_REVAP.gw	0.02	0.2	0.02	0.2	0.1458
7.	r_SOL_K(..).sol	0	2000	-0.25	0.25	-0.0294
8.	a_GWQMN.gw	0	5000	0	5000	3751.47
9.	a_GW_DELAY.gw	0	500	0	500	284.64
10.	r_SOL_ALB(..).sol	0	0.25	-0.25	0.25	0.1372
11.	v_ALPHA_BNK.rte	0	1	0	1	0.1991

The streamflow hydrograph and scatter plot of observed versus simulated streamflow during the calibration period are shown in Figures 4.1 and 4.2 below. As we have seen in Figure 4.1, the observed and simulated streamflow hydrographs during the calibration period at some season underestimated and at some seasons overestimated because the observed data in august (2005, 2007, 2008 and 2010) was very higher as we have seen in page 24 of the flow data, but the rainfall recorded at this period/season is small. The slope of scatter plot from Figure 4.2 between observed and simulated streamflow was 0.80, which indicates the correlation between observed and simulated is very good and also the other performance evaluation parameters are shown in Table 4.3 below and also shows the calibrated output (Appendix Figure 3).

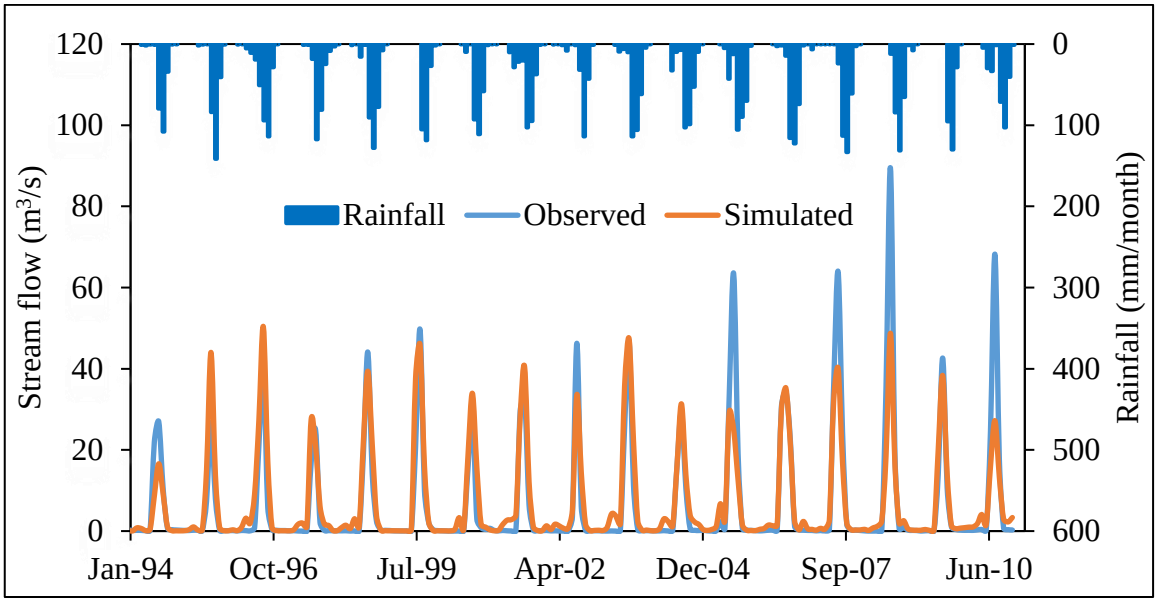

Figure 4-1: Observed and simulated flow with rainfall during the calibration period

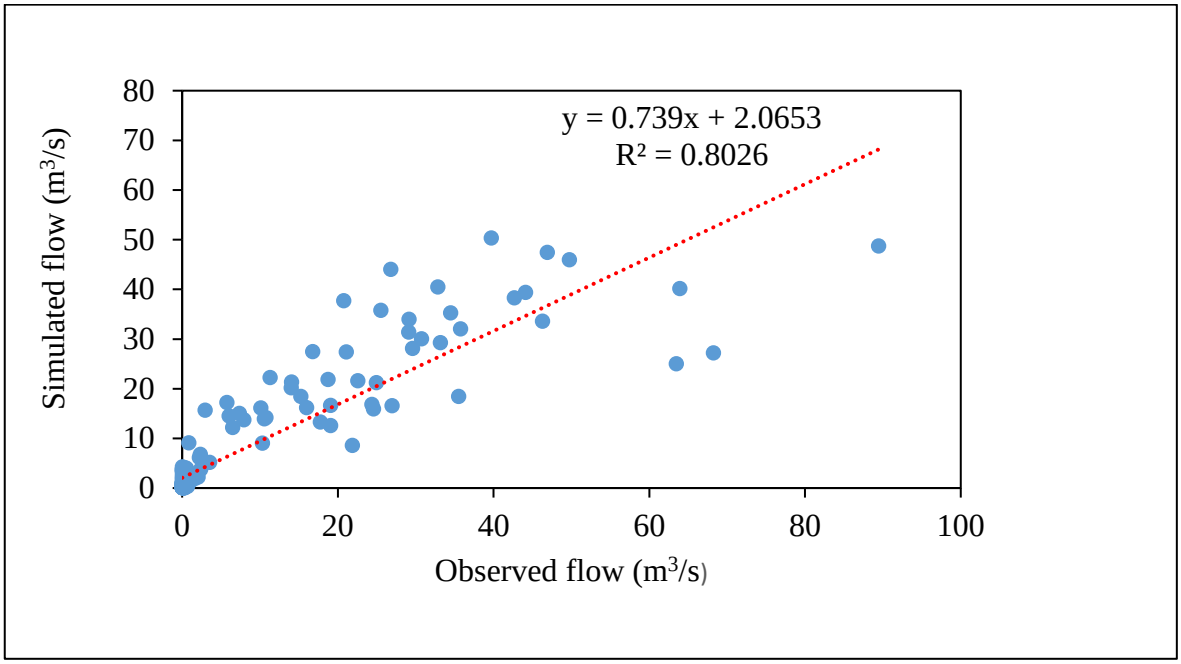

Figure 4-2: Scatter plot of observed versus simulated flow during the calibration period.

4.1.3 Stream flow validation

After calibration, the model calibrated parameters was validated by using an independent set of measured flow data wasn't used during model calibration. Flow validation was carried out from January 1, 2011, to December 31, 2018, without further adjustment of parameters of the stream flows. Accordingly, a good match between monthly measured and simulated

flows in the validation period shown (Figure 4.3) was demonstrated by the correlation coefficient (R^2) of 0.77, Nash-Sutcliffe simulation efficiency (ENS) of 0.77, and percent of bias (PBIAS) -4.7 as shown (figure 4.4) below and also shows validation output (Appendix Figure 4).

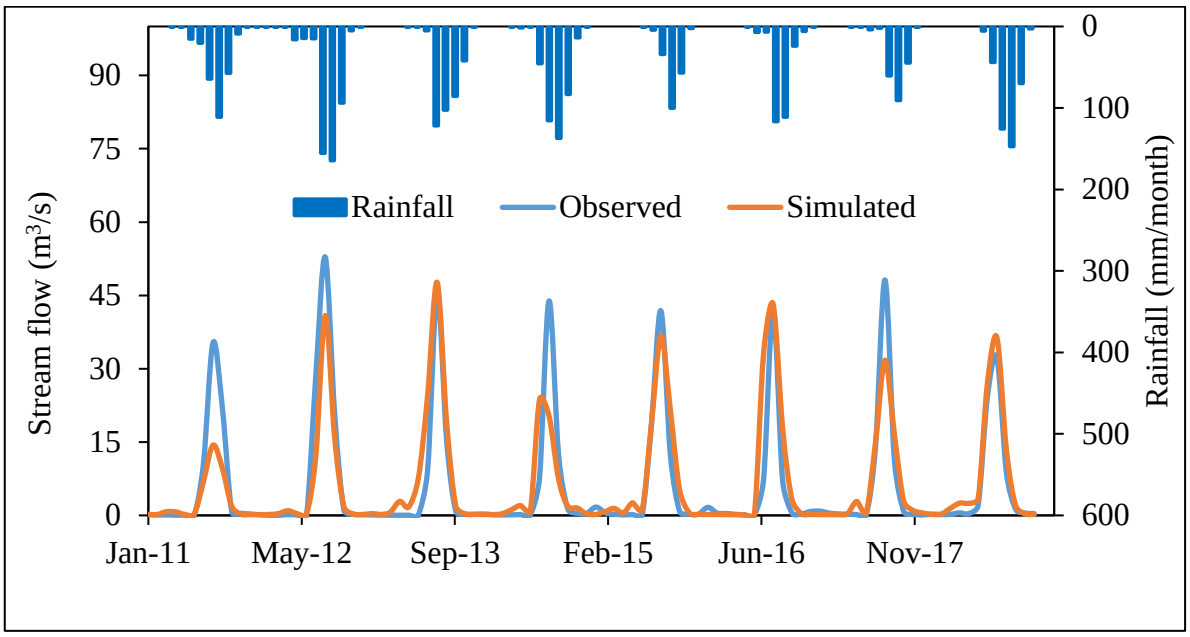

Figure 4-3: Observed and simulated flow with rainfall during the validation period

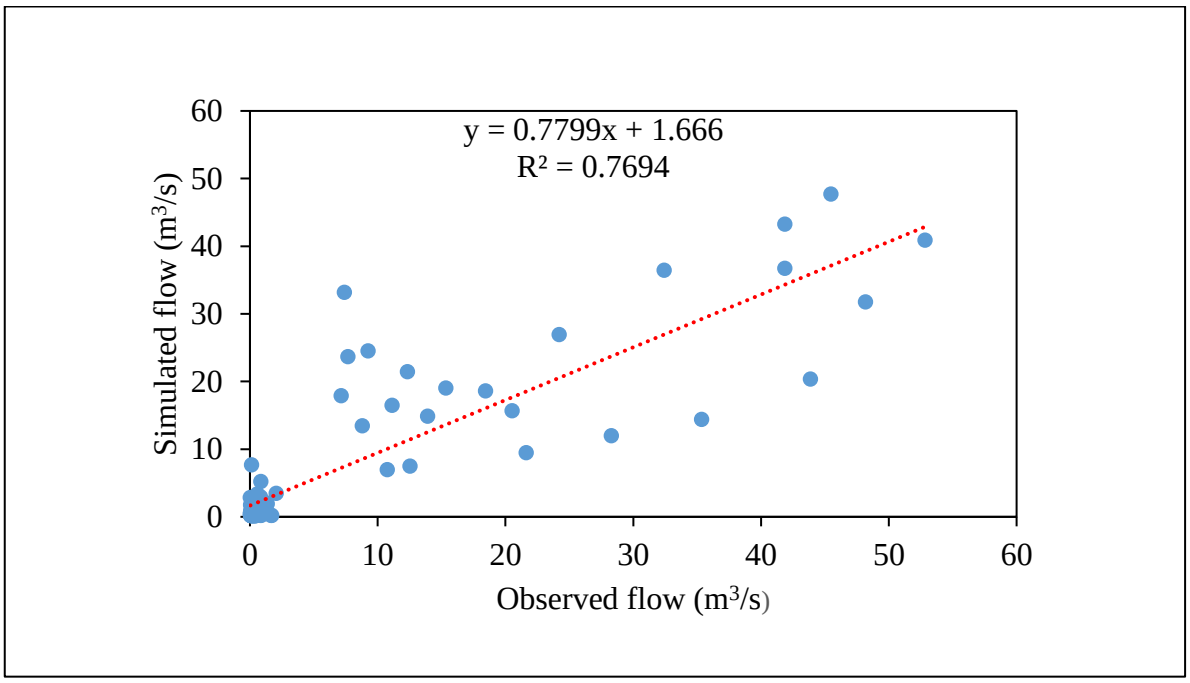

Figure 4-4: Scatter plot of observed versus simulated flow during the validation period.

As we have seen in the above observed and simulated streamflow hydrographs during the validation period, some seasons were underestimated and at some seasons overestimated because the observed data in July (2013, 2014, and 2016) was very small flow, but the rainfall recorded at this period/season is higher, and the simulated data is also higher.

Table 4-3: Mean monthly simulated and observed flow calibration and validation results.

Simulation period	Average flow (m^3/s)		Model performance evaluation parameters		
	Simulated	Observed	R^2	NSE	PBIAS
Calibration(1994-2010)	7.01	6.69	0.80	0.80	-4.8
Validation (2011-2018)	6.52	6.23	0.77	0.77	-4.7

The above result, which is summarized (Table 4.3) as the mean monthly simulated stream flow and observed stream flow during calibration and validation, indicates good correlation, as confirmed by the visual comparison of the hydrograph and model evaluation statistics. According to Moriasi *et al.* (2007), the model evaluation statistics for monthly stream flow calibration and validation for this study, as obtained from the SWAT model, demonstrated very good performance.

Generally in this study, as we have seen in the above figures, the observed and simulated streamflow hydrographs during calibration and validation period at some seasons were the model has very good performance for small flow, but its performance is week for high flow. The divergence of observed stream flow and simulated stream flow may be the problem of input data, model calibration parameters, and the model prediction errors or uncertainty may occur due to the quality of the observed stream flow data used for model calibration and validation. Generally, the estimated results of stream flows indicate that the SWAT model is a good predictor of stream flow in the Robi Jida watershed.

4.2 Water Balances

The main water balance components are: Total amount of precipitation falling on the sub basin, actual evapotranspiration from the sub basin, water that percolates past the root zone, and the net amount of water that leaves the sub basin and contributes to streamflow in the reach that is water yield. The water yield includes groundwater contribution to streamflow,

surface runoff contribution to streamflow in the main channel, lateral flow contribution to streamflow, and transmission losses. Therefore water yield calculated by the equation:

WYLD = SURQ + LATQ + GWQ – TLOSS

The mean annual water balance simulated before and after calibration in the Robi Jida watershed are shown (Table 4.4) below. There was a distinct difference between the water balance before and after calibration. For instance, surface runoff before calibration is higher than after calibration by 61.39mm (16.5%), indicating more accurate representation of hydrological processes., while the actual evapotranspiration before calibration is less than after calibration by 52.97mm (18.4%),suggesting that the model now better captures the effects of vegetation and soil moisture on water loss through evapotranspiration. This reflects a healthier water cycle and potentially improved land management practices. Particularly a wide variation of the hydrological model component was seen on groundwater contribution to the stream flow (GW_Q) before calibration is higher than after calibration by 184.30mm (65%). This reduction indicates that the initial model may have overestimated groundwater contributions, suggesting a need for further investigation into aquifer characteristics and recharge rates. The amount of water in the soil profile (SW) before calibration is less than after calibration by 134.27mm (10.3%), know the model is more accurately simulating the water retention capacity of the soil, aligning better with observed conditions. Net amount of water that leaves the sub basin (WYLD) after calibration is less than before calibration 260.44mm (38.6%). This change emphasizes a shift in the hydrological dynamics, indicating that a greater portion of precipitation is retained in the system rather than being lost as runoff.

The main objective of calibration is to ensure simulation results are close to measurement. In this respect, the SWAT model should be re-run using the optimal parameters and water balance component were identified for the output files (Bo et al., 2020). After calibration, average surface runoff, actual evapotranspiration, streamflow water yield, and percolation from the soil layer account for 310.81mm (31.8%), 340.74mm (35%), 413.66mm (42.5%), and 319.64mm (32.8%) of the average annual precipitation of the water budget respectively (Appendix Table 8).

Generally, after calibration of stream flow of the SWAT model has led to more realistic representation of hydrological processes in the Robi Jida watershed, particularly in terms of surface runoff and evapotranspiration, while revealing important insights into groundwater dynamics and soil characteristics. These findings emphasize the necessity for ongoing

monitoring and management to address the hydrological challenges within the Robi Jida watershed.

Table 4-4: Hydrological model component before and after calibration.

No	Hydrological component	Before calibration	After calibration
1	Precipitation	973.69	973.69
2	Potential evapotranspiration	622.73	622.73
3	Actual evapotranspiration	287.77	340.74
4	Soil water content	1297.89	1432.16
5	Percolation	311.46	319.64
6	Surface runoff	372.20	310.81
7	Groundwater	283.51	99.21
8	Water yield	674.10	413.66
9	Lateral flow contribution	2.78	3.01

* All units in mm

4.3 Sediment Yield Modeling

4.3.1 Sediment yield sensitivity analysis

During the sensitivity analysis of sediment, nineteen (19) parameters were checked for sensitivity; from these, nine (9) parameters were selected for calibration based on the value of t-stat (larger absolute t-values are more sensitive) and p-vale (a value close to zero is more significant). The remaining parameter values do not cause significant changes in the model output. The selected sediment sensitivity parameters are shown (table 4.5) below and the output summary results are also shown (Appendix Figure 5).

USLE soil erodibility (K) factor (USLE_K), average slope length (SLSUBBSN), SCS runoff curve number (CN_2), average slope steepness (HRU_SLP), USLE support practice factor (USLE_P), minimum value of USLE_C factor applicable to the land cover/plant (USLE_C), and peak rate adjustment factor for sediment routing in the sub-basin (tributary channels) (ADJ_PKR) have a P-value less than 5% and are more sensitive parameters (Abbaspour, 2012) in the Robi Jida watershed. These susceptible parameters for sediment agree well with previous studies conducted in the upper Blue Nile Basin (Asres & Awulachew, 2010; Assfaw, 2019; Kefay et al., 2022; Lemma et al., 2019).

Table 4-5: Sensitive parameters of sediment yield in the Robi Jida watershed.

No	Parameter name with operation	Global range		Verification techniques		t-stat	p-value	Rank	Relative sensitivity
		min	max	min	max				
1	v_usle_k(..).sol	0	0.65	0	0.65	-11.8	0.00	1	Higher
2	v_slsubbsn.hru	10	150	10	150	-7.16	0.00	2	Higher
3	r_cn2.mgt	35	98	-0.2	0.2	-7.05	0.00	3	Higher
4	v_hru_slp.hru	0	1	0	1	-6.63	0.00	4	Higher
5	v_usle_p.mgt	0	1	0	1	-5.12	0.00	5	Higher
6	v_usle_c{..}.plant.dat	0.001	0.5	0.001	0.5	-2.78	0.01	6	Higher
7	v_adj_pkr.bsn	0	2	0	2	-2.07	0.04	7	Higher
8	v_sol_awc (..).sol	0	1	0	1	1.92	0.06	8	Medium
9	v_spcon.bsn	0.0001	0.01	0.0001	0.01	-1.66	0.10	9	Medium

4.3.2 Sediment yield calibration

After the sensitive parameters are selected, calibration process focuses on knowing the gap between the simulated and observed values by adjusting the sensitive sediment parameters in the recommended range. Nine (9) more influential sediment parameters from high to medium sensitive were used and were adjusted further varying iteratively in their allowable range until satisfactory agreement between measured and simulated sediment yield was obtained are shown (table 4.6). The minimum and maximum range of parameters in the first calibration was taken from the range used in the sensitivity analysis and fitted values were obtained from the final calibration. Similar to streamflow calibration, sediment calibration was conducted using sediment yield data from 1994 to 2010 by taking two years as a warmup period.

Table 4-6: Sediment yield sensitivity parameter, initial range, and fitted value.

No	Parameter name with operation	Global range		Verification techniques		Fitted value
		min	max	min	max	
1	v_usle_k(..).sol	0	0.65	0	0.65	0.5115
2	v_slsubbsn.hru	10	150	10	150	99.5555
3	r_cn2.mgt	35	98	-0.2	0.2	-0.1943
4	v_hru_slp.hru	0	1	0	1	0.0242
5	v_usle_p.mgt	0	1	0	1	0.2582
6	v_usle_c{..}.plant.dat	0.001	0.5	0.001	0.5	0.4446
7	v_adj_pkr.bsn	0	2	0	2	1.0289
8	v_sol_awc (..).sol	0	1	0	1	0.5354
9	v_spcon.bsn	0.0001	0.01	0.0001	0.01	0.0064

* r_ is the existing parameter value multiplied by (1+ given value); v_ is the existing parameter value to be replaced by a given value, and a_ is a given value added to the existing parameter value.

The sediment yield hydrograph and scatter plot of observed versus simulated sediment yield during the calibration period are shown (figures 4.5 and 4.6) below also shows the calibration output (Appendix Figure 6).

From the figure 4.5 and finger 4.6, shows that the observed and simulated sediment yield hydrograph during calibration period, at some season's underestimation and at some seasons slight overestimation. The divergence of observed sediment and simulated sediment yield results may be occurs due to input data, model calibration parameters, and model structure problems. But according to the general performance rating proposed by (Moriasi et al., 2007), the sediment yield performance statistics value obtained during calibration period, the SWAT model performed reasonably with R^2 of 0.70, NSE of 0.70, and PBIAS of 1.1 indicated a good model performance.

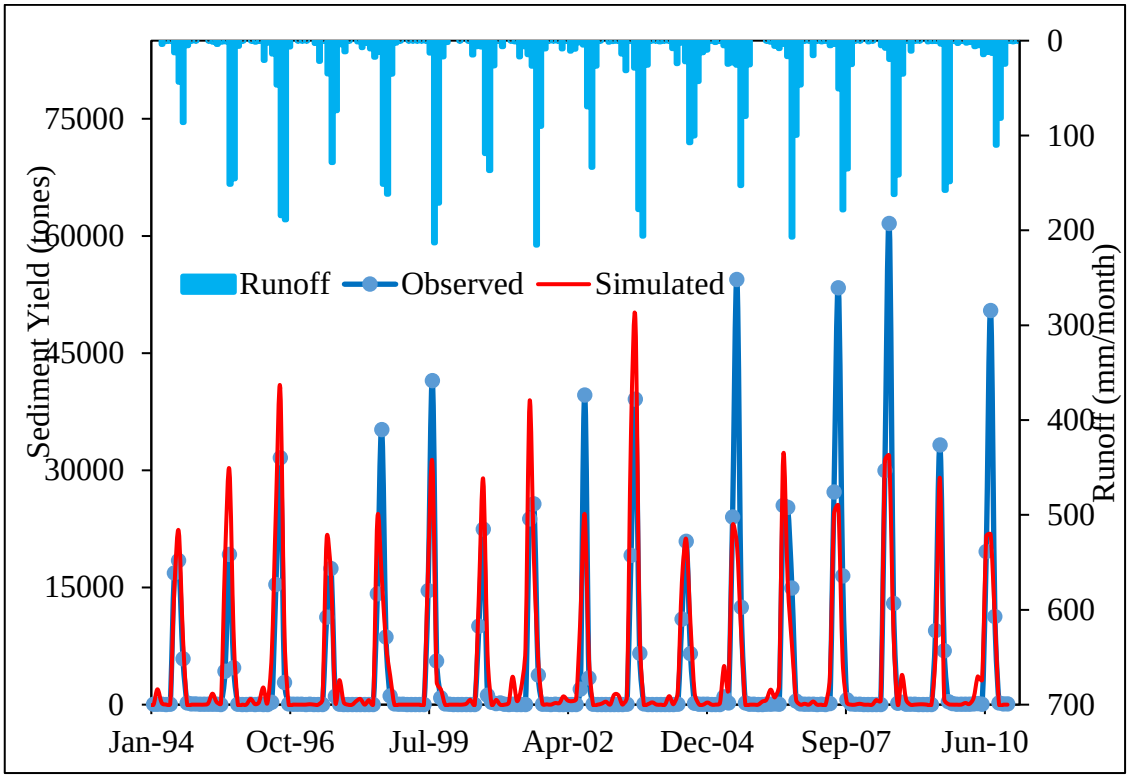

Figure 4-5: Observed and simulated sediment with runoff during the calibration period.

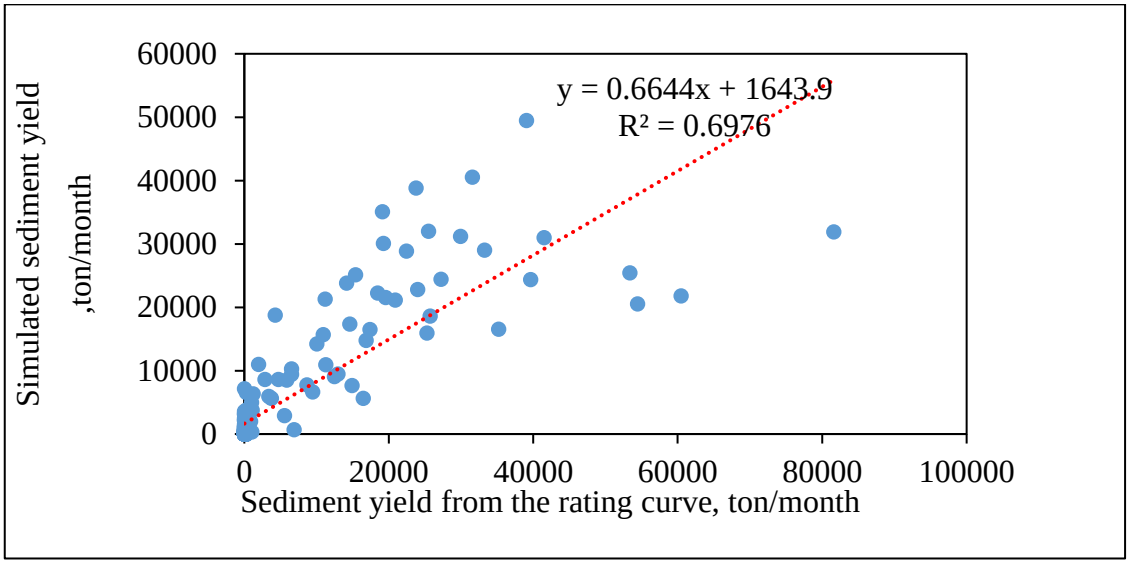

Figure 4-6: Scatter plot of observed vs simulated sediment during the calibration period.

4.3.3 Sediment yield validation

Like flow validation, the validation of sediment yield was conducted using the sediment yield data from 2011 to 2018.

The sediment yield hydrograph and scatter plot of observed versus simulated sediment yield during the validation period are shown in Figures 4.7 and 4.8 below. As shown in the figure 4.7 that the observed and simulated sediment yield hydrograph during the validation period aligns in a good, but in some seasons have seen divergence. The slope of the scatter plot Figure 4.8 between observed and simulated sediment yield was 0.72, which indicates the correlation between observed and simulated sediment yield is acceptable. Summarized monthly sediment yield SWAT model performance statistics values during the calibration and validation period are tabulated in Table 4.7 and also shows the validation output (Appendix Figure 7).

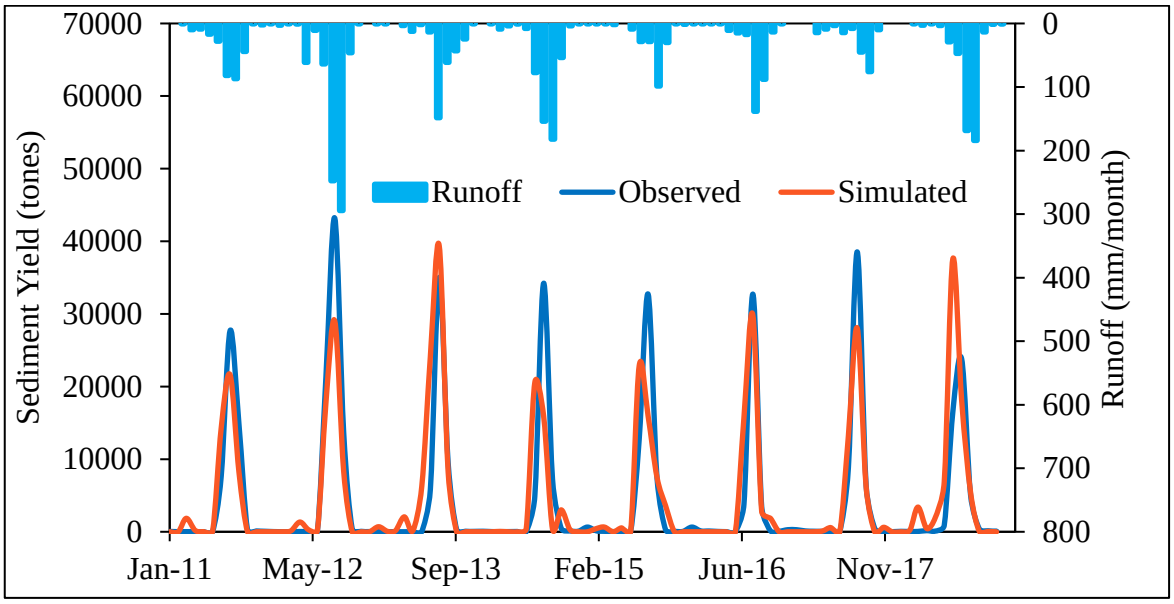

Figure 4-7: Observed and simulated sediment with runoff during the validation period

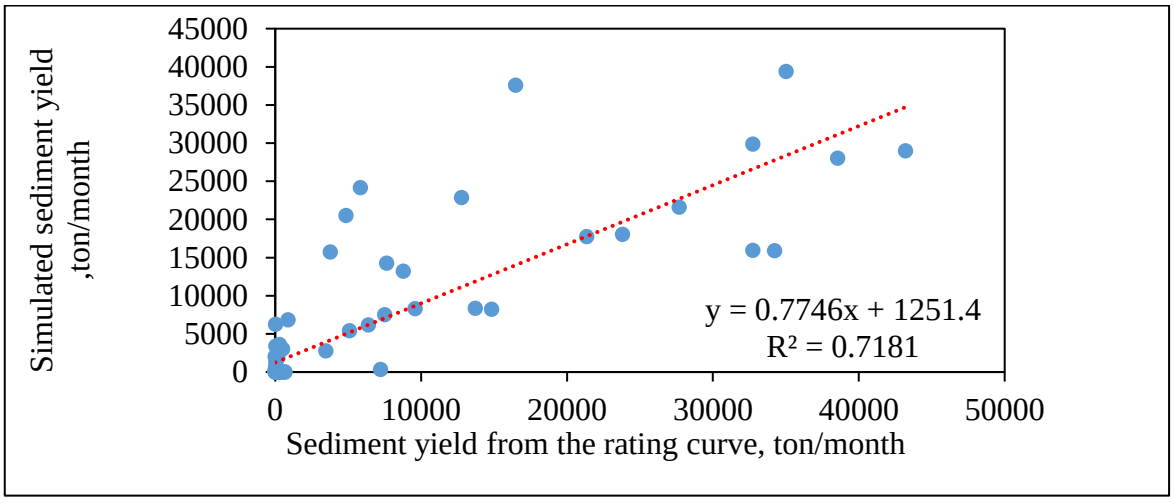

Figure 4-8: Scatter plot of observed vs simulated sediment during the validation period.

Table 4-7: Monthly sediment yield calibration and validation results.

Simulation period	Average sediment yield (ton/year)		Model performance evaluation parameters		
	Simulated	Observed	R^2	NSE	PBIAS
Calibration(1994-2010)	5009.19	4918.38	0.70	0.70	1.1
Validation (2011-2018)	4685.39	4433.44	0.72	0.71	-5.7

4.4 Annual Sediment yield of Robi Jida Watershed

After calibration and validation of sediment yield, the average annual sediment yield transported from the Robi Jida watershed was estimated. The result showed that the average annual sediment yield from the total catchment area of 76274 hectares with a mean annual sediment yield of 6.42ton/ha/year in the baseline scenario. Similar research was conducted by researchers in different watersheds in which the average annual sediment yield from the watershed was similar to this study. Nadew *et al* (2019) conducted research entitled runoff sediment yield modeling and development of management intervention scenarios, a case study of Guder watershed, Blue Nile Basin, Ethiopia and they obtained an average annual sediment yield of 7.5 ton $ha^{-1}yr^{-1}$ and also (Nadew, 2018) conducted research entitled stream flow and sediment yield modeling in the case study of Beles watershed, Upper Blue Nile Basin, Ethiopia and they obtained an average annual sediment yield of 4.81ton $ha^{-1}yr^{-1}$. In addition, Ayele and Gebremariam (2020) and Aga *et al* (2018) obtained an average annual sediment yield of 9.99 and 5.85 ton $ha^{-1}yr^{-1}$ from Rift valley regions, Ethiopia respectively.

In general, the model simulation result after calibration and validation at the Robi Jida gauge station for sediment yield shows a good relation and the result estimation is more near to the observed data. Therefore, the SWAT model is good for the estimation of sediment yield in the Robi Jida watershed. The SWAT model accurately predicted the sediment yield from the rating curve in different watershed sizes of the Upper Blue Nile basin (Adem et al., 2016; Ayele et al., 2017; Betrie et al., 2011; Gashaw et al., 2021; Lemann et al., 2016; Setegn et al., 2010). This study also confirmed the satisfactory performance of the SWAT model in stream flow and sediment yield in the Robi Jida watershed between 1992 and 2018.

4.5 Temporal Variability of Sediment Yield in the Robi Jida

Temporal variability of sediment yield is the sediment generated on a time base annually or mean annually. As the mean annual sediment yield graph estimated by the SWAT model (Figure 4.9) shows, the sediment yield increased during the year of the high rainfall and runoff and the maximum average annual rainfall was recorded as 1458 mm in year 2012, correspondingly the maximum average annual runoff was 438mm, and average annual sediment yield 16.5ton/ha/year in year 2012. In this study the highest sediment yield 27.5ton/ha/year occurs in 1996.

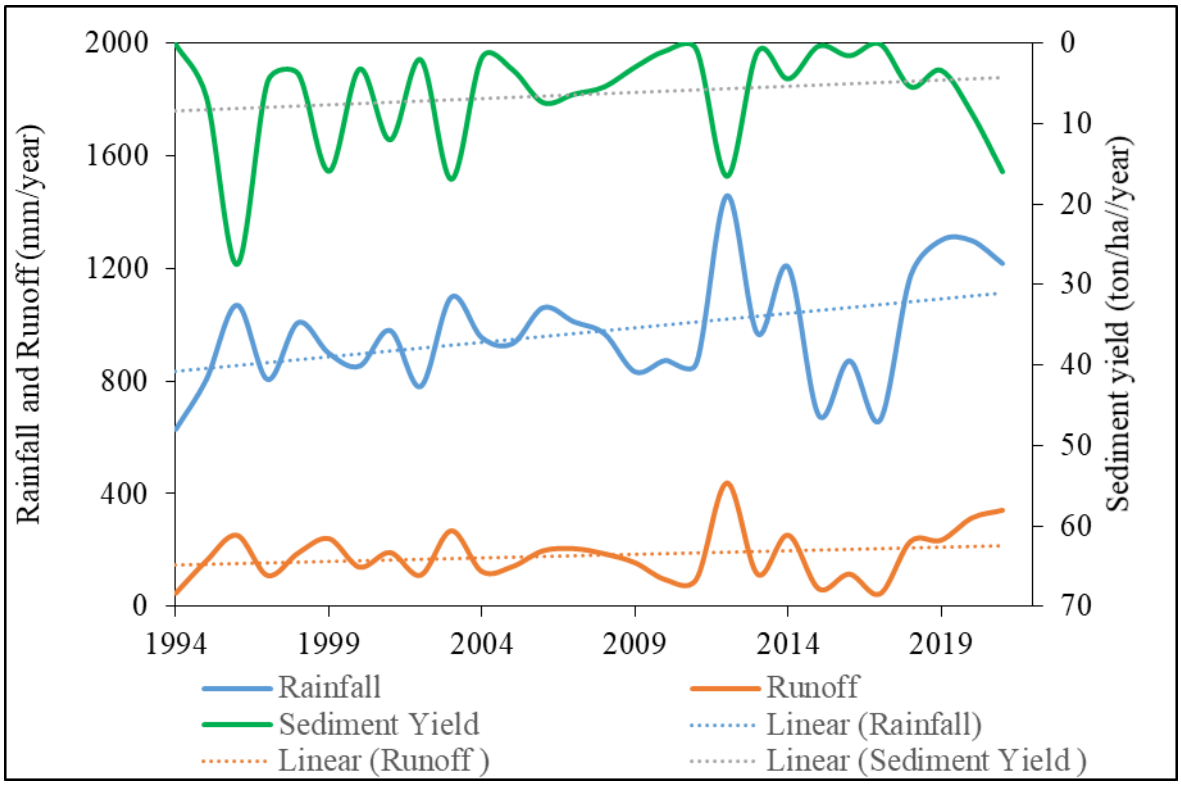

Figure 4-9: Sediment yield variability in the Robi Jida watershed.

4.6 Spatial Distribution of Sediment Yield and Identify Hotspot Area in the Robi Jida

The spatial distribution of sediment yield in the Robi Jida watershed is illustrated (Figure 4.11). This figure highlights the sediment potential of each sub-watershed and identifies erosion hotspot areas at the sub-watershed level through spatial visualization. Researchers determined these erosion hotspots by comparing the mean annual sediment yield derived from model simulation results. In the sub-watersheds, the mean annual sediment yield ranges from 3.95 ton/ha/year to 21.25 ton/ha/year. The SWAT model simulation classified the

sediment yield of sub-catchments into four levels of erosion vulnerability: severe, moderate, acceptable, and negligible, as detailed (Table 4.8) below. According to Asres & Awulachew (2010), the yields below 10ton/ha/year are classified as lower risk, while yields of 11–15 ton/ha/year and 16–22 ton/ha/year fall into the moderate and severe categories, respectively.

The variability in sediment yield is significantly influenced by land use, soil type, and terrain slope. Notably, severe to moderate erosion and sediment yield occur primarily in cultivated (agricultural) areas. High sediment yield in these regions results from land degradation due to intensive cropland use without adequate management, deforestation practices (such as forest burning and the expansion of cultivated lands), cultivation on steep slopes and marginal lands, insufficient resources (financial and technical), poorly designed roads and drainage systems, and a lack of awareness regarding erosion issues and preventive measures. Overall, land use/land cover, soil type, and slope are the main factors contributing to erosion in the affected sub-watersheds.

To assess the spatial variability of sediment yield, researchers calculated the sediment yield-area ratio for each sub-catchment. This analysis clearly demonstrates the extent of soil erosion in the area and aids in ranking the levels of erosion vulnerability.

Table 4-8: Sediment yield classes and area coverage in the Robi Jida watershed.

Classes	Average sediment yield (ton/ha/year)	Area coverage(km^2)	Area coverage (%)
Negligible erosion	<7.57	187.91	24.64
Acceptable erosion	7.57 -11.44	74.50	9.77
Moderately eroded	11.44 -18.18	310.08	40.65
Severely eroded	>18.18	190.25	24.94

Table 4.8 indicates that 65.59% of the watershed area is classified as critical, while 34.41% falls into the negligible and acceptable sediment yield categories. Within this watershed, four sub-watersheds exhibit acceptable levels of soil loss, suggesting that implementing Best Management Practices (BMPs) is less urgent. In contrast, nine sub-watersheds fall into moderate and severe categories, indicated a need for immediate sediment management interventions to reduce soil loss, enhance agricultural productivity, and minimize

sedimentation. The critical sub watersheds generate an average sediment yield of 17.85 ton/ha/year, compared to 14.98 ton/ha/year for the entire catchment.

The map further reveals the spatial distribution of sediment yields among the 13 sub watersheds. Specifically, two sub-watersheds (2 and 13) are severely eroded, while seven (3, 4, 5, 7, 8, 10, 11, and 13) are moderately eroded. The remaining four sub watersheds are categorized as having acceptable or negligible erosion levels. Additionally, the average annual sediment yield in ton/ha/year for each sub-watershed is summarized in Table 4.9 below.

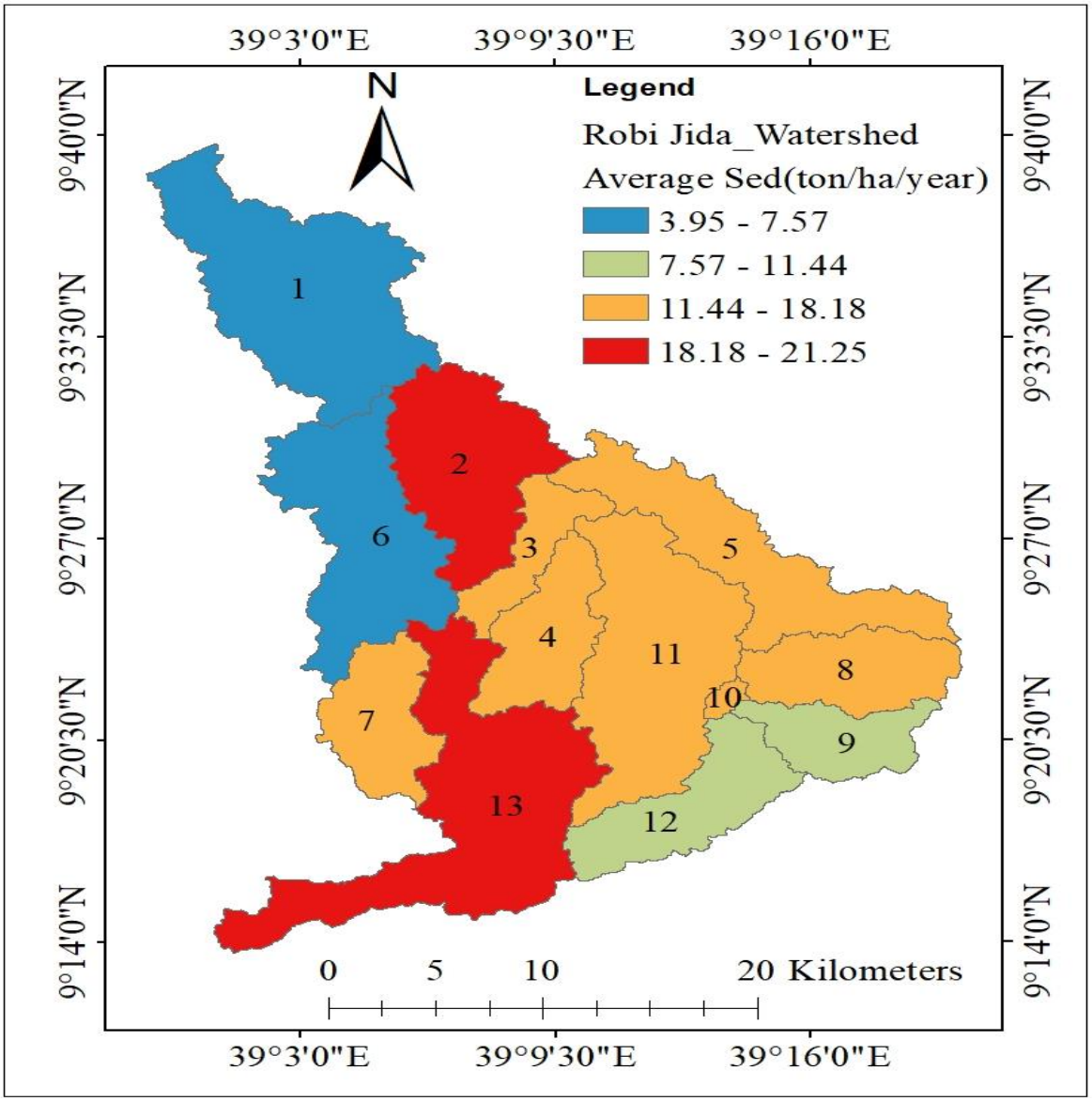

Figure 4-11: Spatial variability map of sediment yield in the Robi Jida watershed.

Table 4-9: Average annual sediment yield in each sub-watershed (ton $ha^{-1}yr^{-1}$).

Sub Watershed	Average Sed (ton/ha/year)	Sub Watershed	Average Sed (ton/ha/year)
1	3.95	8	14.65
2	21.25	9	11.15
3	18.18	10	17.17
4	16.47	11	18.18
5	17.16	12	11.44
6	7.57	13	19.80
7	17.78		

The sediment yield map at the Woreda level, shown in Figure 4.10, illustrates the spatial variability of erosion in the Robi Jida watershed. The severely eroded areas include Kembibit (25.35%), Wuchalena Jido (24.85%), Berehna Aleltu (45.83%), and Abichuna Gne'a (3.97%). In terms of moderate erosion, Kembibit, Wuchalena Jido, Berehna Aleltu, and Abichuna Gne'a account for 92.25%, 1.52%, 6.22%, and 0.012%, respectively. Table 4.10 provides detailed information on the area coverage of the various soil erosion categories within the Robi Jida watershed (km^2).

Table 4-10: Area coverage of each soil erosion category in the Woreda level (km^2).

Categories	Kembibit	Wuchalena Jido	Berehna Aleltu	Abichuna Gne'a	Hagere Mariamna	Debirna Wayu & Ensaro
Negligible erosion	5.55	159.54	NA	NA	NA	22.82
Acceptable erosion	29.63	NA	42.48	NA	2.39	NA
Moderately eroded	286.1	4.71	19.28	0.036	NA	NA
Severely eroded	48.22	47.27	87.20	7.56	NA	NA

*NA - Not available soil erosion category.

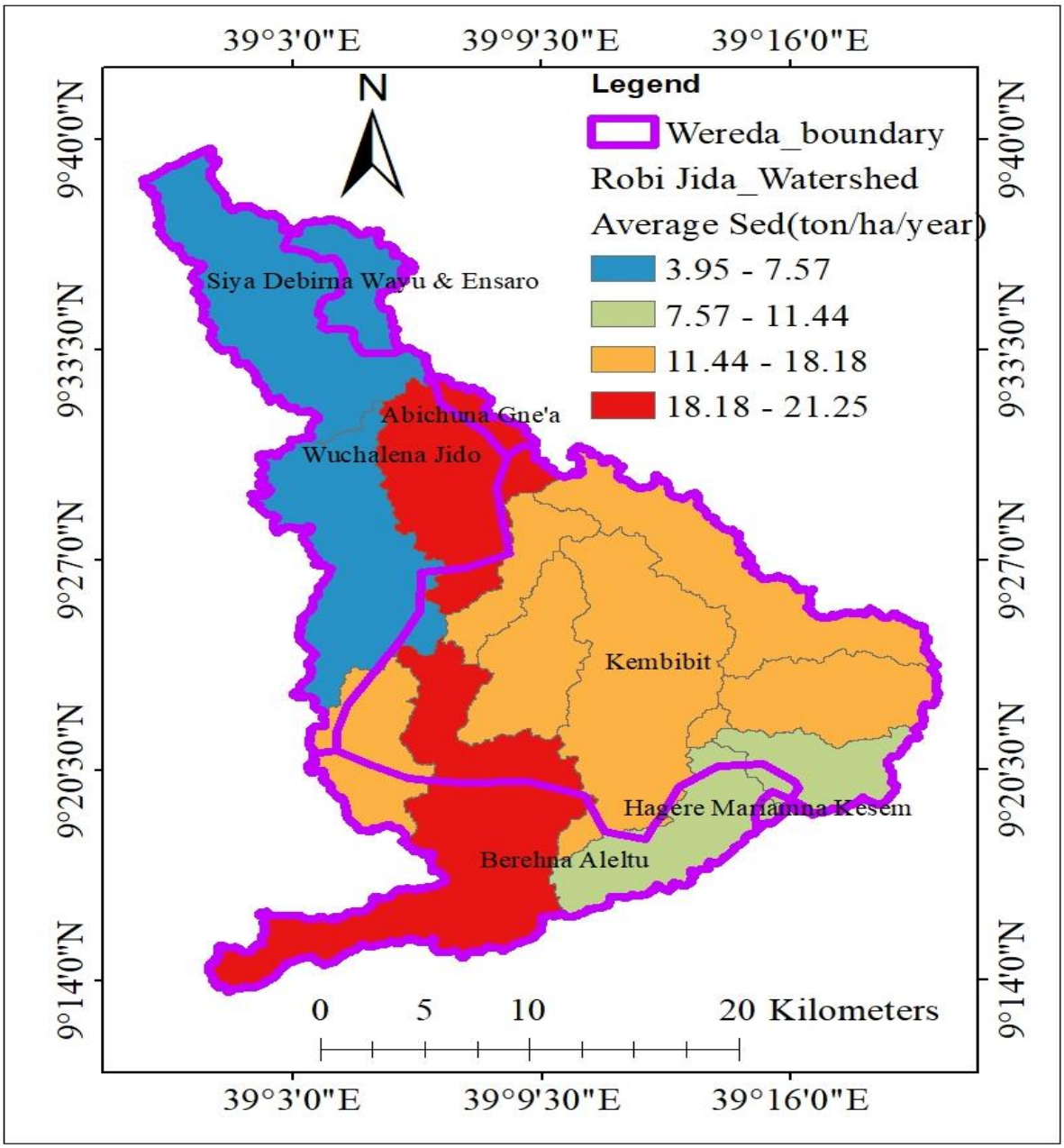

Figure 4-10: Sediment yield map in Woreda level of Robi Jida watershed.

4.7 Analysis and Evaluation of Best Management Practices

***Scenario 0: Baseline scenario*.** The baseline scenario represents the current conditions without any best management practices (BMPs) and serves as the starting point for the scenario simulations. This scenario provides a reference for comparing the effectiveness of the developed sediment reduction strategies. In this simulation, the SWAT model used default and calibrated values without any modifications to the model parameters.

Scenario I: Applying Filter Strips (FS). As shown in Table 4.11, implementing 1meter and 5meter filter strips led to a reduction in the average annual sediment yield for critical sub watershed (sub_2, sub_3, sub_4, sub_5, sub_7, sub_8, sub_10, sub_11, and sub_13) sediment yield decreased from 17.85 ton/ha/year to 14.43 ton/ha/year and 11.60 ton/ha/year, achieving the average reductions of 19.15% and 35.01%, respectively.

The sediment reduction capacity of 19.15% in Scenario I, which applies a 1meter wide filter strip, aligns with findings from previous studies in the upper Blue Nile Basin and other regions. For instance, implementing 1meter filter strip in the Gumara watershed (Gashaw et al., 2021), Ribb watershed (Admas et al., 2022), Azuari watershed (Mequanient & Kebede, 2023), and Nashe watershed (Leta et al., 2023) resulted in sediment yield reductions of 13.7%, 28%, 35.61%, and 34.88%, respectively. Similarly, in the Akaki watershed of the upper Awash Basin (Zeberie, 2020), Awata watershed in the Dawa Basin (Kefay et al., 2022),and Dawe watershed of the Wabi Shebelle river basin (Roba et al., 2021) , reductions of 75.6%, 17.48%, and 15.7% were observed, respectively. Additionally, sediment reduction capacity of Scenario I using 5meter filter width in the Gumara watershed was reported to be 61% (Asres & Awulachew, 2010).

Table 4-11: Reduction of sediment yield due to filter strips.

BMPs	Parameter	Default value	Simulated value	Mean annual sed. yield (ton/ha/year)	Reduction (%)	Critical sub watershed
BS				17.85		
FS	FILTERW	0	1	14.43	19.15	2,3,4,5,7,8,10,11 ,and 13 slopes >8%
FS	FILTERW	0	5	11.60	35.01	

Figure 4.11 below illustrates the mean annual sediment yield estimates for the baseline scenario and for the 1meter and 5meter filter strip BMPs at the critical sub-watershed scale.

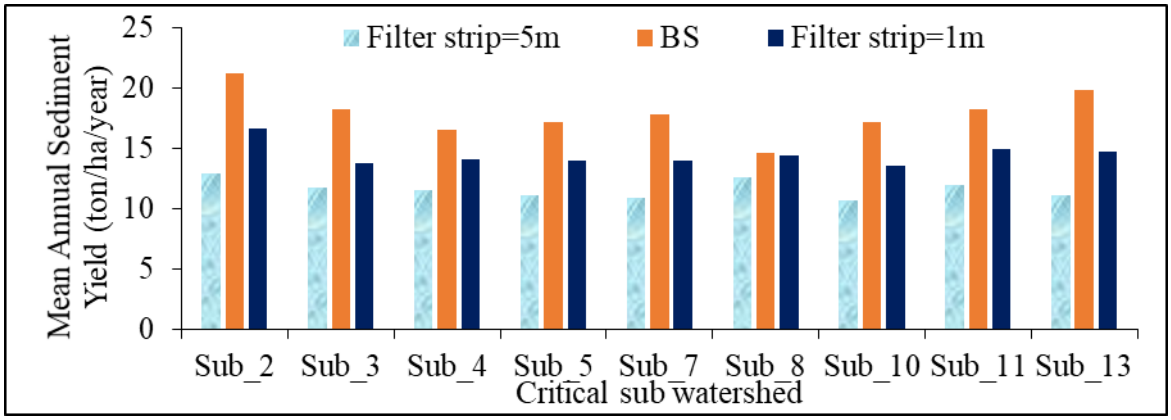

Figure 4-11: Reduction of sediment yield due to Filter strip, compared to the base case.

Scenario II: Applying Vegetative contour strips (VS). Vegetative contour strips are widely used in agricultural settings, particularly in areas with sloping terrain or highly erodible soils. These strip are often implemented alongside other erosion control practices, such as terracing, conservation tillage, and cover cropping, to enhance their effectiveness in reducing soil erosion and protecting water quality.

As shown in Table 4.12 below, the application of vegetative contour strips significantly reduced the average annual sediment yield for the critical sub-basins (sub_2, sub_3, sub_4, sub_5, sub_7, sub_8, sub_10, sub_11, and sub_13), decreasing from 17.85 ton/ha/year to 9.44 ton/ha/year. This represents an average reduction capacity of 47.13%.

Table 4-12: Reduction of sediment yield due to vegetative contour strips.

BMPs	Parameter	Default value	Simulated value	Mean annual sed. yield (ton/ha/year)	Reduction (%)	Critical sub watershed
BS				17.85		
VS	FILTERW	0	1	9.44	47.13	2,3,4,5,7,8, 10,11, and 13 slopes > 8%
	USLE_P	0.26	0.34			
	SLSUBBSN	99.56	0.5*C			
	HRU_SLP	0.024	0.75*C			

* “C” calibrated value of sediment parameter after re-running the SWAT model.

The sediment reduction capacity (47.13%) of Scenario II is also aligned with the findings of previous studies. For example, the implementation of vegetative contour strips in the Lake

Tana basin (Lemma et al., 2019) has reduced sediment yield by 51%. The mean annual sediment yield estimated at the baseline situation and the vegetative contour strips BMPs at the critical sub-watershed scale are presented in Figure 4.12 below.

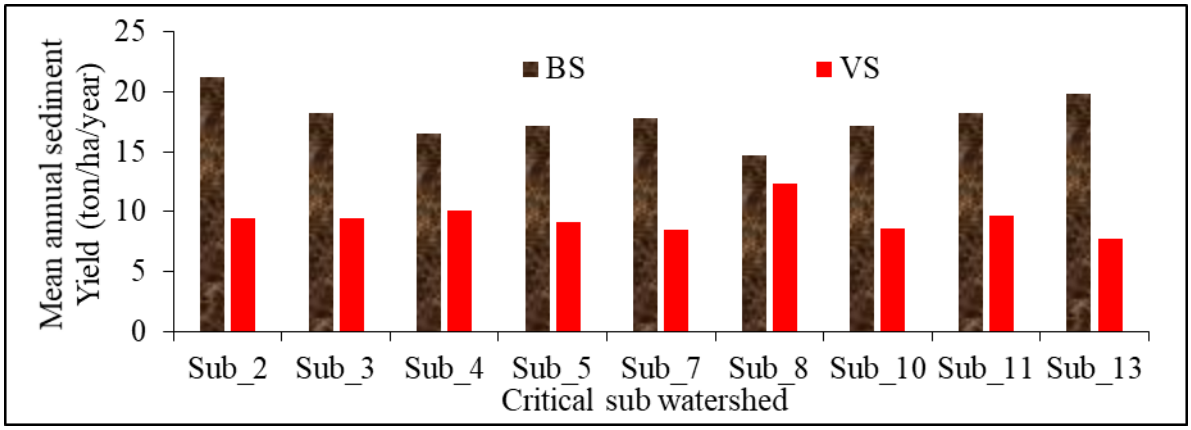

Figure 4-12: Reduction of sediment yield due to Counter strip, compared to base case.

Scenario III: Applying soil/stone bund (SB). It is an important tool in soil and water conservation, helping to prevent erosion, retain soil moisture, and promote sustainable land management practices in agricultural areas. As shown in Table 4.13 below, the application of soil/stone bund reduced the average annual sediment yield for critical sub-basins (i.e. sub _2, sub_3, sub_4, sub_5, sub_7, sub_8, sub_10, sub_11 and sub_13) from 17.85 ton/ha/ year to 7.66 ton/ha/year, with an average of 57.09% reduction capacity.

Table 4-13: Reduction of sediment yield due to soil/ stone bund.

BMPs	Parameter	Default value	Simulated value	Mean annual sed. yield (ton/ha/year)	Reduction (%)	Critical sub watershed
BS				17.85		
SB	CN_2	68	60	7.66	57.09	2,3,4,5,7,8, 10,11& 13 slopes >8%
	SLSUBBSN	99.56	0.5*C			
	HRU_SLP	0.024	0.75*C			

* “C” calibrated value of sediment parameter after re-running the SWAT model.

The sediment reduction capacity of 57.09% in Scenario III, which involves the application of soil/stone bunds, aligns from the previous studies. For instance, the implementation of soil/stone bunds in the Gumara watershed (Gashaw et al., 2021), Ribb watershed (Admas et

al., 2022), Lake Tana basin (Lemma et al., 2019), and Nashe watershed (Leta et al., 2023) resulted in sediment yield reductions 30.5%, 76%, 51%, and 57.98%, respectively. Similarly, the Akaki watershed in the upper Awash basin (Zeberie, 2020), Dawe watershed of the Wabi Shebelle river basin (Roba et al., 2021) achieved a sediment yield reduction of 69.6%, and 21.3% respectively. Figure 4.13 below presents the mean annual sediment yield estimates for the baseline scenario and the soil/stone bund BMPs at the critical sub-watershed scale.

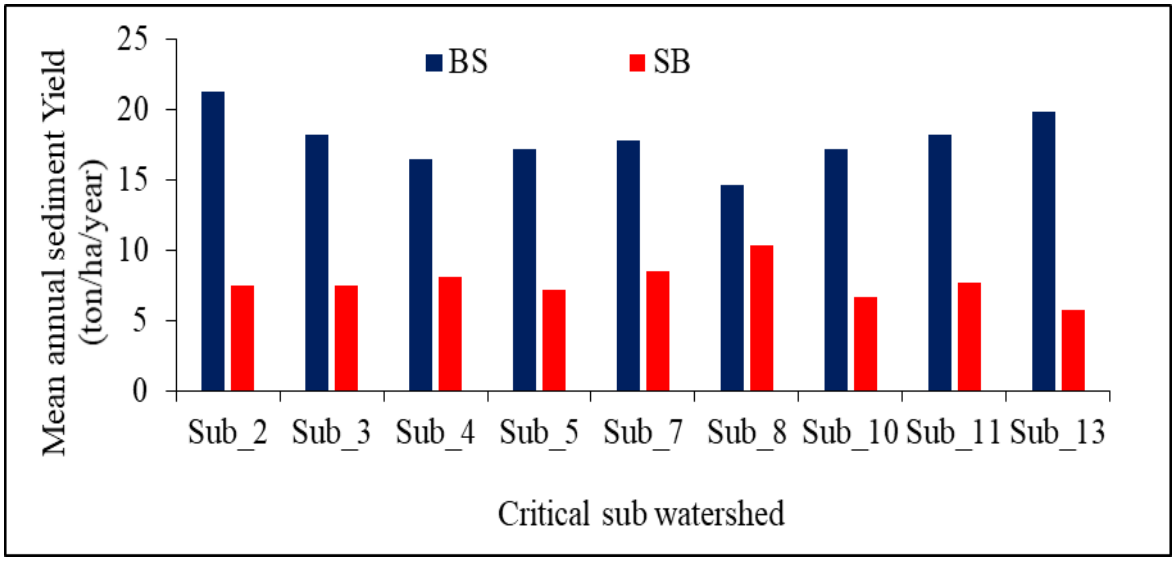

Figure 4-13: Reduction of sediment yield due to soil bund, compared to the base case.

Scenario IV*: *Applying Terracing. This study evaluated terracing sediment management practices in the critical sub-watershed by adjusting the operation the SWAT model terrace parameters of curve number (TERR_CN_2), slope length (TERR_SL), and crop practice (TERR_P). This management practice was evaluated only on agricultural land, all soil types, and slopes greater than 8%. As shown in Table 4.14 below, the application of terracing reduced the average annual sediment yield for critical sub-basins (i.e. sub _2, sub_3, sub_4, sub_5, sub_7, sub_8, sub_10, sub_11, and sub_13) from 17.85ton/ha/year to 4.76 ton/ha/year, with an average of 73.37% reduction capacity.

Table 4-14: Reduction of sediment yield due to Terracing.

BMPs	Parameter	Default value	Simulated value	Mean annual sed. yield (ton/ha/year)	Reduction (%)	Critical sub watershed
BS				17.85		
Terrace	TERR_P	0.5	0.2	4.76	73.37	2,3,4,5,7,8,10,11, and 13 slopes > 8%
	TERR_CN_2	60	76			
	TERR_SL	20	25			

The sediment reduction capacity (73.37%) of Scenario IV is also aligned with the previous studies upper Blue Nile basin or any other basin. For example, the implementation of Terracing in Nesha watershed (Leta et al., 2023), Azuari watershed (Mequanient & Kebede, 2023) in upper Blue Nile basin has reduced sediment yield by 54.77%,and 20.44% respectively. Similarly Akaki watershed, upper Awash basin (Zeberie, 2020) and Awata watershed, Dawa basin (Kefay et al., 2022) has reduced sediment yield by 68.8% ,and 47.05% respectively. The mean annual sediment yield estimated at the baseline situation and the terracing BMPs at the critical sub-watershed scale are presented in Figure 4.14 below.

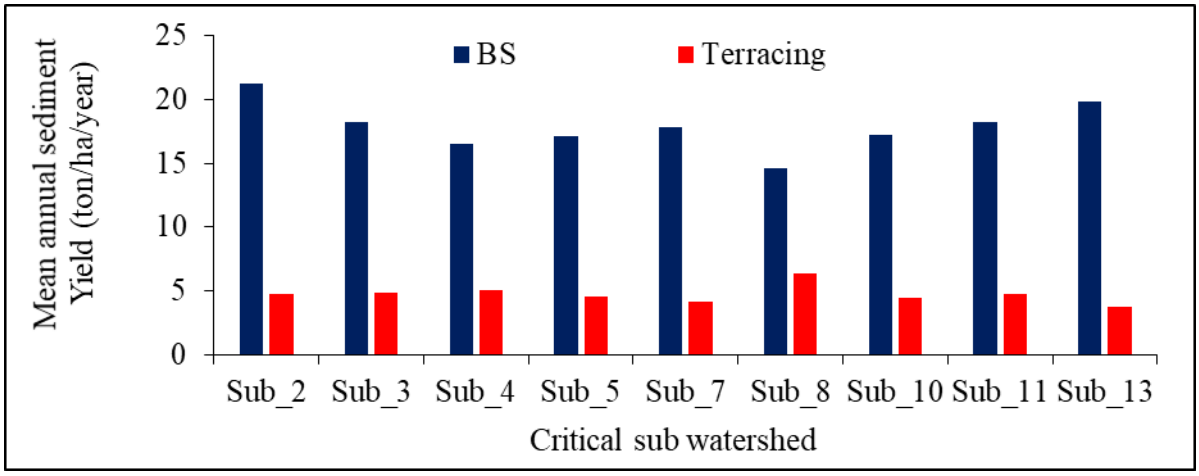

Figure 4-14: Reduction of sediment yield due to Terracing, compared to base case.

Scenario V: Applying Contouring. In this study, contour farming was assessed in the SWAT model operations by adjusting the contouring parameters of curve number (CONT_CN_2) and crop practices (CONT_P). This sediment management option was implemented in the critical sub-watershed, where, in the agricultural area, all soil types and the land slopes

greater than 8%. As shown in Table 4.15, the application of contouring reduced the average annual sediment yield for critical sub-basins (i.e. sub _2, sub_3, sub_4, sub_5, sub_7, sub_8, sub_10, sub_11, and sub_13) from 17.85 ton/ha/ year to 8.42 ton/ha/year, with an average of 52.81% reduction capacity.

The sediment reduction capacity (52.8%) of Scenario V is also aligned with the findings of previous studies upper Blue Nile basin or any other basin. For example, the implementation of contouring in the Nesha watershed (Leta et al., 2023), Azuari watershed (Mequanient & Kebede, 2023) in the upper Blue Nile basin has reduced sediment yield by 39.55%, and 43.6% respectively. Similarly, the Awata watershed, Dawa basin (Kefay et al., 2022) has reduced sediment yield by 33.43%. The mean annual sediment yield estimated at the baseline situation and the contouring BMPs at the critical sub-watershed scale are presented in Figure 4.15 below.

Table 4-15: Reduction of sediment yield due to Contouring.

BMPs	Parameter	Default value	Simulated value	Mean annual sed. yield (ton/ha/year)	Reduction (%)	Critical sub watershed
BS				17.85		
Contour	CONT_P CONT_CN_2	0.5 60	0.2 75	8.42	52.81	2,3,4,5,7,8,10,11, and 13 slopes >8%

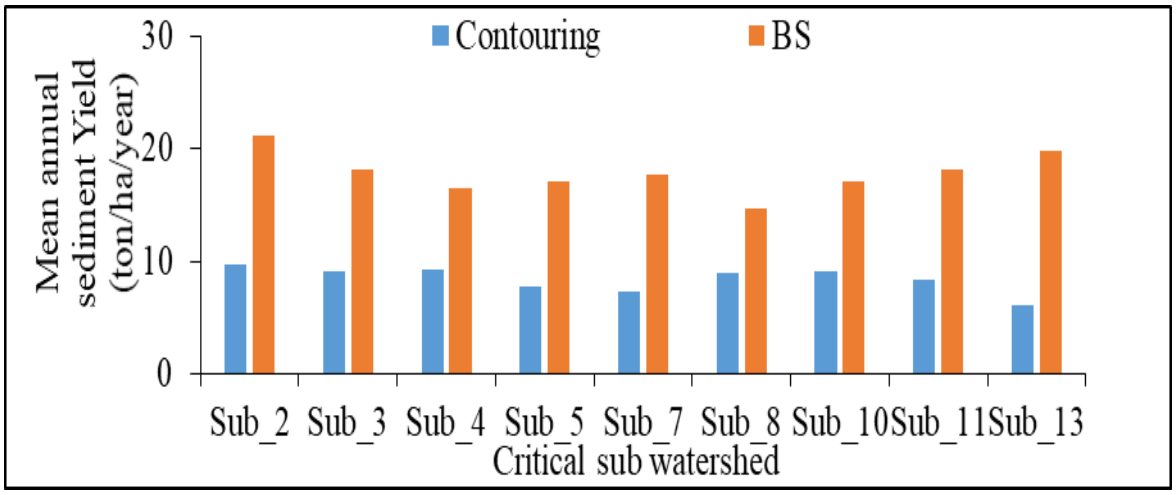

Figure 4-15: Reduction of sediment yield due to Contouring, compared to base case.

Generally from those the above different BMPs, we can observe that **Terracing Scenario** results is the highest reduction sediment yield, and the second is the soil/stone bund scenario. Therefore Terracing and soil/stone bund practices effectively minimize sediment loads and contribute to better soil and water conservation in the Robi Jida watershed. Mean annual sediment yield estimated at the baseline situation and five considered BMPs at the critical sub watershed are illustrated in figure 4.16 and table 4.16 below.

Table 4-16: Average annual change in sediment yield associated with applying BMPs.

Mean annual sediment yield								Reduction in sediment yield (%)					
Critical sub basin	BS	FS=1m	FS=5m	SB	VS	Terrace	Counter	FS=1m	FS= 5M	SSB	VS	Terrace	Counter
2	21.2	16.6	12.9	7.4	9.4	4.8	9.8	21.7	39.1	65.0	55.5	77.4	54.0
3	18.2	13.7	11.7	7.5	9.5	4.9	9.2	24.5	35.4	58.8	47.8	73.2	49.6
4	16.5	14.1	11.5	8.0	10.0	5.1	9.3	14.6	30.1	51.2	39.1	69.1	43.4
5	17.2	13.9	11.1	7.1	9.1	4.6	7.7	18.8	35.3	58.4	46.8	73.4	55.3
7	17.8	13.9	10.9	8.5	8.5	4.2	7.3	21.7	38.9	52.3	52.3	76.6	59.0
8	14.6	14.4	12.6	10.3	12.3	6.3	9.0	1.4	14.1	29.6	15.9	56.8	38.8
10	17.2	13.5	10.6	6.6	8.6	4.4	9.2	21.4	38.1	61.4	49.8	74.2	46.6
11	18.2	15.0	12.0	7.7	9.7	4.8	8.4	17.7	34.2	57.7	46.7	73.7	53.8
13	19.8	14.7	11.1	5.7	7.7	3.8	6.0	25.9	44.1	71.1	60.9	81.1	69.5
Avg	***17.8***	***14.4***	***11.6***	***7.7***	***9.4***	***4.8***	***8.4***	***19.1***	***35.0***	***57.1***	***47.1***	***73.4***	***52.8***

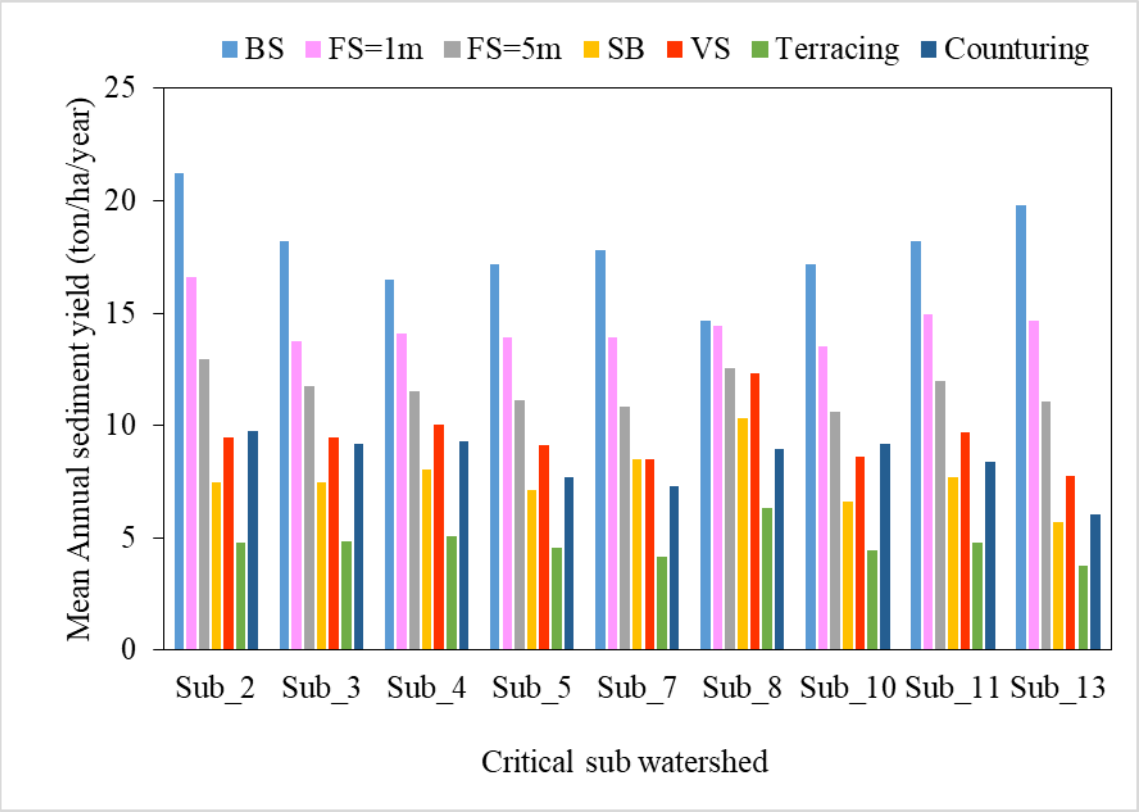

Figure 4-16: Reduction of sediment yield due to BMPs, as compared to base case.

5. CONCLUSION AND RECOMMENDATION

5.1 Conclusions

Soil erosion and sedimentation studies are necessary to support the agricultural sector through watershed planning and management to feed people without any food scarcity. Skills and techniques are required to extend the scarce data for the developmental application. The main aim of this study was to model stream flow and sediment yield of the Robi Jida watershed in the Upper Blue Nile Basin, Ethiopia, and look at the spatial variability of sediment yield evaluation, sediment reduction scenario, and selecting the best scenario using the SWAT model.

Historical records of meteorological, hydrological, and suspended sediment concentration data were used for the hydrological modeling. Sediment yield data was generated from the discharge-sediment rating curve equation using the suspended sediment concentration data. Spatially, a 30*30m digital elevation model (DEM), a land use and land cover map, and soil data were used as inputs for the hydrological model. The physical-based soil and water assessment tool (SWAT) was used to model the streamflow and sediment yield in a monthly time step. The entire watershed was subdivided into 13 sub-basins that were spatially linked by stream networks. Overlaying slope, land use, and soils were performed to generate 124 HRUs from intersections. The period between 1994 and 2010 was used for calibration, and the period from 2011 to 2018 was used for validation.

The stream flow sensitivity analysis of the SWAT model showed that SCS runoff curve number (CN_2), soil evaporation compensation factor (ESCO), soil available water content (SOL_AWC), and effective channel hydraulic conductivity (CH_K2), deep aquifer percolation fraction (RCHRG_DP),and Groundwater “revap” coefficient (GW_REVAP) were more sensitive. In addition, the sediment yield sensitivity analysis of the SWAT model shows USLE soil erodibility (K) factor (USLE_K), Average slope length (SLSUBBSN), SCS runoff curve number (CN_2), average slope steepness (HRU_SLP), USLE support practice factor (USLE_P), min value of USLE C factor applicable to the land cover/plant (USLE_C), and peak rate adjustment factor for sediment routing in the sub-basin (tributary channels) (ADJ_PKR) were more sensitive.

The modeling result showed that the SWAT model well predicted streamflow and sediment yield and performance of the model was evaluated using calibration and validation statistics.

A good relation between measured and simulated monthly stream flow and sediment in the gauging station was demonstrated by a coefficient of determination (R^2) of 0.80 and 0.77, Nash-Sutcliffe efficiency (NSE) of 0.80 and 0.77, and a percent of bias (PBIAS) of -4.8 and -4.7 during calibration and validation periods, respectively. Similarly, the model predicted the sediment yield with R^2 of 0.7 and 0.72, NSE of 0.7 and 0.71, and PBIAS of 1.1 and -5.7 for calibration and validation, respectively.

The vulnerable sub-catchments were identified from the results of the model sub-catchments 2, 3, 4, 5,7,8,10,11, and 13, which have high sediment generation compared to the other catchments. Based on the calibrated spatial results, about 24.94% of the Robi Jida watershed was severely eroded, 40.65% was moderately eroded, 9.77% was acceptable erosion, and 24.64% was negligible erosion area. The severely eroded area of the Robi Jida watershed covers Kembibit (25.35%), Wuchalena Jido (24.85%), Berehna Aleltu (45.83%), and Abichuna Gne'a (3.97%). The moderately eroded area covers Kembibit Woreda, Wuchalena Jido, Berehna Aleltu, and Abichuna Gne'a covers 92.25%, 1.52%, 6.22%, and 0.012% respectively. The average annual sediment yield of the Robi Jida watershed was estimated at 6.42 ton/ ha/year.

At the watershed scale, applying the different management scenarios, filter stripe 1m and 5 m, vegetative contour strip, soil/stone bund, terracing, and contouring resulted in a 19.15%, 35.01%, 47.13%, 57.09%, 73.37and 52.81% decrease in the average annual sediment yield, respectively. The highest reduction in sediment yield was achieved through the application of soil/stone bund and terracing scenarios.

5.2 Recommendations

According to the findings of this study, the following recommendations were provided:

In this study, sediment yield was estimated by identifying areas prone to sedimentation and developing management practices for the critical sub-watersheds based on current watershed conditions. It is recommended that future research focus on estimating sediment yield in the context of climate change and changes in land use/ land cover.

The spatial variability of sediment yield and the identification of erosion-vulnerable sub-catchments of the Robi Jida watershed are mapped at the Woreda level. Each Woreda should first carry out the recommended soil and water conservation practices for the severely and moderately eroded sub-watersheds to minimize soil fertility decline.

The study involved modeling filter strips 1m and 5m, soil/stone bund, vegetative counter strip, contouring, and terracing with scenarios are used to prevent erosion and sedimentation in the Robi Jida watershed. Further studies could consider these or other structural or non-structural conservation practices that could be implemented in the land management options for the effectiveness of erosion and sediment reduction and the economic feasibility of assessing optimized and economical erosion and sediment reduction options.

Finally, the study could help different stakeholders plan and implement erosion and sediment yield reduction options in the study watershed. The analyzed and identified management scenario was indicated as effective for erosion and sediment reduction. So policymakers will better equipped to make educated decisions on appropriate land use activities and effective management techniques, according to the study's findings.

6. REFERENCES

Abbaspour, K. C. (2012). Calibration and Uncertainty Programs. *Science And Technology*, 106. http://swat.tamu.edu/media/114860/usermanual_swatcup.pdf

Abbaspour, K. C., Yang, J., Maximov, I., Siber, R., Bogner, K., Mieleitner, J., Zobrist, J., & Srinivasan, R. (2007). Modelling hydrology and water quality in the pre-alpine/alpine Thur watershed using SWAT. *Journal of Hydrology*, *333*(2–4), 413–430. https://doi.org/10.1016/j.jhydrol.2006.09.014

Abebaw, W. A. (2019). Review on Impacts of Land Degradation on Agricultural Production in Ethiopia. *Journal of Resources Development and Management*, *57*(2003), 21–29. https://doi.org/10.7176/jrdm/57-03

Abebe, B. K., Zimale, F. A., Gelaye, K. K., Gashaw, T., Dagnaw, E. G., & Adem, A. A. (2022). Application of Hydrological and Sediment Modeling with Limited Data in the Abbay (Upper Blue Nile) Basin, Ethiopia. *Hydrology*, *9*(10), 1–21. https://doi.org/10.3390/hydrology9100167

Adane, G. B., Hirpa, B. A., Song, C., & Lee, W. K. (2020). Rainfall characterization and trend analysis of wet spell length across varied landscapes of the upper awash river basin, ethiopia. *Sustainability (Switzerland)*, *12*(21), 1–14. https://doi.org/10.3390/su12219221

Addis, H. K., Abera, A., & Abebaw, L. (2020). Economic benefits of soil and water conservation measures at the sub-catchment scale in the northern Highlands of Ethiopia. *Progress in Physical Geography*, *44*(2), 251–266. https://doi.org/10.1177/0309133319878118

Addis, H. K., Strohmeier, S., Ziadat, F., Melaku, N. D., & Klik, A. (2016). *Modeling streamflow and sediment using SWAT in Ethiopian Highlands*. *9*(5), 51–66. https://doi.org/10.3965/j.ijabe.20160905.2483

Adem et al., 2016. (2016). Climate Change Impact on Sediment Yield in the Upper Gilgel Abay Catchment, Blue Nile Basin, Ethiopia. In *Landscape Dynamics, Soils and Hydrological Processes in Varied Climates* (pp. 615–644).

Admas, B. F., Gashaw, T., Adem, A. A., Worqlul, A. W., Dile, Y. T., & Molla, E. (2022a). Identification of soil erosion hot-spot areas for prioritization of conservation measures using the SWAT model in Ribb watershed, Ethiopia. *Resources, Environment and Sustainability*, *8*(April), 100059. https://doi.org/10.1016/j.resenv.2022.100059

Admas, B. F., Gashaw, T., Adem, A. A., Worqlul, A. W., Dile, Y. T., & Molla, E. (2022b).

Identification of soil erosion hot-spot areas for prioritization of conservation measures using the SWAT model in Ribb watershed, Ethiopia. *Resources, Environment and Sustainability*, *8*(April), 100059. https://doi.org/10.1016/j.resenv.2022.100059

Admas, M., Melesse, A. M., Abate, B., & Tegegne, G. (2022). Soil Erosion, Sediment Yield, and Runoff Modeling of the Megech Watershed Using the GeoWEPP Model. *Hydrology*, *9*(12). https://doi.org/10.3390/hydrology9120208

Aga, A. O., Chane, B., & Melesse, A. M. (2018). Soil erosion modelling and risk assessment in data Scarce Rift Valley Lake Regions, Ethiopia. *Water (Switzerland)*, *10*(11). https://doi.org/10.3390/w10111684

Ali, Y. S. A., Crosato, A., Mohamed, Y. A., Abdalla, S. H., & Wright, N. G. (2014). Sediment balances in the Blue Nile River Basin. *International Journal of Sediment Research*, *29*(3), 316–328. https://doi.org/10.1016/S1001-6279(14)60047-0

Amaru Ayele, M., & Gebremariam, B. (2020). Evaluation of Spatial and Temporal Variability of Sediment Yield on Bilate Watershed, Rift Valley Lake Basin, Ethiopia. *Journal of Water Resources and Ocean Science*, *9*(1), 5. https://doi.org/10.11648/j.wros.20200901.12

Andualem Gessese and Yonas M. dualem Gessese, & van Engelen, V. W. P. (2008). Prediction of Sediment Inflow to legedadi Reservoir Using SWAT Watershed and CCHE1D Sediment Transport Models. *Nile Basin Water Engineering Scientific Magazine*, *1*, 65–74.

Arnold, J. G., & Fohrer, N. (2005). SWAT2000: Current capabilities and research opportunities in applied watershed modelling. *Hydrological Processes*, *19*(3), 563–572. https://doi.org/10.1002/hyp.5611

Arnold, J. G., Kiniry, J. R., Srinivasan, R., Williams, J. R., Haney, E. B., & Neitsch, S. L. (2012). *Soil & Water Assessment Tool*.

Asmamaw, L. B., & Mohammed, A. A. (2019). Identification of soil erosion hotspot areas for sustainable land management in the Gerado catchment, North-eastern Ethiopia. *Remote Sensing Applications: Society and Environment*, *13*(February 2018), 306–317. https://doi.org/10.1016/j.rsase.2018.11.010

Asres, M. T., & Awulachew, S. B. (2010). SWAT based runoff and sediment yield modeling: A case study of the Gumera watershed in the Blue Nile basin. *Ecohydrology and Hydrobiology*, *10*(2–4), 191–199. https://doi.org/10.2478/v10104-011-0020-9

Asselman, N. E. M. (2000). Fitting and interpretation of sediment rating curves. *Journal of*

Hydrology, *234*(3–4), 228–248. https://doi.org/10.1016/S0022-1694(00)00253-5

Assfaw, A. T. (2019). Calibration, Validation and Performance Evaluation of Swat Model for Sediment Yield Modelling in Megech Reservoir Catchment, Ethiopia. *Journal of Environmental Geography*, *12*(3–4), 21–31. https://doi.org/10.2478/jengeo-2019-0009

Awulachew, S.B., Mccartney, M., Steenhuis, T.S., Ahmed, A. A. (2008). *A Review of Hydrology,Sediment and Water Resource Use in the Blue Nile Basin. International Water Management Institute* (Issue January).

Ayalew, L. T., & Bharti, R. (2020). Modelling sediment yield of Rib watershed , Northwest Ethiopia Modelling sediment yield of Rib watershed , Northwest Ethiopia. *ISH Journal of Hydraulic Engineering*, *00*(00), 1–12. https://doi.org/10.1080/09715010.2020.1797544

Ayele, G. T., Teshale, E. Z., Yu, B., Rutherfurd, I. D., & Jeong, J. (2017). Streamflow and sediment yield prediction for watershed prioritization in the upper Blue Nile river basin, Ethiopia. *Water (Switzerland)*, *9*(10). https://doi.org/10.3390/w9100782

B, N. (2018). Stream Flow and Sediment Yield Modeling: A Case Study of Beles Watershed, Upper Blue Nile Basin. *Irrigation & Drainage Systems Engineering*, *07*(03). https://doi.org/10.4172/2168-9768.1000216

Badege Bishaw. (2014). *Deforestation and Land Degradation in the Ethiopian Highlands : A Strategy for Physical Recovery Author (s): Badege Bishaw Source : Northeast African Studies , New Series , Vol . 8 , No . 1 , Special Issue : Natural Resource Management , Human Developme*. *8*(1).

Barbier, E. B. (2000). The economic linkages between rural poverty and land degradation: Some evidence from Africa. *Agriculture, Ecosystems and Environment*, *82*(1–3), 355–370. https://doi.org/10.1016/S0167-8809(00)00237-1

Berhanu, B., Melesse, A. M., & Seleshi, Y. (2013). GIS-based hydrological zones and soil geo-database of Ethiopia. *Catena*, *104*(January 2018), 21–31. https://doi.org/10.1016/j.catena.2012.12.007

Berihun, M. L., Tsunekawa, A., Haregeweyn, N., Dile, Y. T., Tsubo, M., Fenta, A. A., Meshesha, D. T., Ebabu, K., Sultan, D., & Srinivasan, R. (2020). Evaluating runoff and sediment responses to soil and water conservation practices by employing alternative modeling approaches. *Science of the Total Environment*, *747*, 141118. https://doi.org/10.1016/j.scitotenv.2020.141118

Betrie, G. D., Mohamed, Y. A., Van Griensven, A., & Srinivasan, R. (2011). Sediment

management modelling in the Blue Nile Basin using SWAT model. *Hydrology and Earth System Sciences*, *15*(3), 807–818. https://doi.org/10.5194/hess-15-807-2011

Bo, H., Dong, X., Li, Z., Reta, G., Li, L., & Wei, C. (2020). Analysis of water balance components and parameter uncertainties based on swat model with cmads data and sufi-2 algorithm in huangbaihe river Catchment, China. *Nature Environment and Pollution Technology*, *19*(2), 637–650. https://doi.org/10.46488/NEPT.2020.V19I02.018

Chakraparni, G. J. (2005). *Factors controlling varations in river sediment load*. *88*(4), 569–575.

Cigizoglu, H. K. (2004). Estimation and forecasting of daily suspended sediment data by multi-layer perceptrons. *Advances in Water Resources*, *27*(2), 185–195. https://doi.org/10.1016/j.advwatres.2003.10.003

Cigizoglu, H. K. (2008). Artificial neural networks in water resources. *NATO Security through Science Series C: Environmental Security*, 115–148. https://doi.org/10.1007/978-1-4020-6575-0_8

Clark, M. P., Slater, A. G., Rupp, D. E., Woods, R. A., Vrugt, J. A., Gupta, H. V., Wagener, T., & Hay, L. E. (2008). Framework for Understanding Structural Errors (FUSE): A modular framework to diagnose differences between hydrological models. *Water Resources Research*, *44*(12), 1–14. https://doi.org/10.1029/2007wr006735

Cooper, M. (2010). Advanced Bash-Scripting Guide An in-depth exploration of the art of shell scripting Table of Contents. *Okt 2005 Abrufbar Uber Httpwww Tldp OrgLDPabsabsguide Pdf Zugriff 1112 2005*, *2274*(November 2008), 2267–2274. https://doi.org/10.1002/hyp

Cunderlik, J. (2003). *Hydrologic model selection for the CFCAS project: assessment of water resources risk and vulnerability to changing climatic conditions. Department of Civil and Environmental Engineering,*. The University of Western Ontario.

Dhorde, A. G., & Zarenistanak, M. (2013). Three-way approach to test data homogeneity : An analysis of temperature and precipitation series over southwestern Islamic Republic of Iran. *J. Ind. Geophys. Union*, *17*(3), 233–242.

Dibaba, W. T., Demissie, T. A., & Miegel, K. (2021). Evaluation of Best Management Practices in Highland Ethiopia, Finchaa Catchment. *Land*, *10*(650). https://doi.org/10.3390/land10060650

Dibabaa, W. T., & Ebsab, D. G. (2022). Identifying Erosion Hot Spot Areas and Evaluation of Best Management Practices in the Toba Watershed, Ethiopia. *Water Conservation*

and Management, *6*(1), 30–38. https://doi.org/10.26480/wcm.01.2022.30.38

Easton, Z. M., Fuka, D. R., White, E. D., Collick, A. S., Biruk Ashagre, B., McCartney, M., Awulachew, S. B., Ahmed, A. A., & Steenhuis, T. S. (2010). A multi basin SWAT model analysis of runoff and sedimentation in the Blue Nile, Ethiopia. *Hydrology and Earth System Sciences*, *14*(10), 1827–1841. https://doi.org/10.5194/hess-14-1827-2010

García-Orenes, F., Roldán, A., Mataix-Solera, J., Cerdà, A., Campoy, M., Arcenegui, V., & Caravaca, F. (2012). Soil structural stability and erosion rates influenced by agricultural management practices in a semi-arid Mediterranean agro-ecosystem. *Soil Use and Management*, *28*(4), 571–579. https://doi.org/10.1111/j.1475-2743.2012.00451.x

Gashaw, T., Dile, Y. T., Worqlul, A. W., Bantider, A., Zeleke, G., Bewket, W., & Alamirew, T. (2021). Evaluating the Effectiveness of Best Management Practices On Soil Erosion Reduction Using the SWAT Model: for the Case of Gumara Watershed, Abbay (Upper Blue Nile) Basin. *Environmental Management*, *68*(2), 240–261. https://doi.org/10.1007/s00267-021-01492-9

Gashaw, T., Tulu, T., Argaw, M., & Worqlul, A. W. (2019). Modeling the impacts of land use–land cover changes on soil erosion and sediment yield in the Andassa watershed, upper Blue Nile basin, Ethiopia. *Environmental Earth Sciences*, *78*(24). https://doi.org/10.1007/s12665-019-8726-x

Gebrekristos, S. T. (2015). *Understanding catchment processes and hydrological modelling in the Abay/Upper Blue Nile basin, Ethiopia*.

Gorfu, D., & Ahmed, E. (2011). *Dereje Gorfu and Eshetu Ahmed Senior Researchers, Ethiopian Institute of Research*.

Goswami, M., O'Connor, K. M., Bhattarai, K. P., & Shamseldin, A. Y. (2005). Assessing the performance of eight real-time updating models and procedures for the Brosna River. *Hydrology and Earth System Sciences*, *9*(4), 394–411. https://doi.org/10.5194/hess-9-394-2005

Gupta, H. V, Beven, K. J., & Wagener, T. (2005). Model Calibration and Uncertainty Estimation. *Encyclopedia of Hydrological Sciences*, 1–17. https://doi.org/10.1002/0470848944.hsa138

Haile, G. W., & Fetene, M. (2012). Assessment of soil erosion hazard in kilie catchment, East Shoa, Ethiopia. *Land Degradation and Development*, *23*(3), 293–306. https://doi.org/10.1002/ldr.1082

Haregeweyn, N., Poesen, J., Nyssen, J., De Wit, J., Haile, M., Govers, G., & Deckers, S.

(2006). Reservoirs in Tigray (Northern Ethiopia): Characteristics and sediment deposition problems. *Land Degradation and Development*, *17*(2), 211–230. https://doi.org/10.1002/ldr.698

Haregeweyn, N., Tsunekawa, A., Nyssen, J., Poesen, J., Tsubo, M., Tsegaye Meshesha, D., Schütt, B., Adgo, E., & Tegegne, F. (2015). Soil erosion and conservation in Ethiopia: A review. *Progress in Physical Geography*, *39*(6), 750–774. https://doi.org/10.1177/0309133315598725

Ilci, V., Ozulu, I. M., Alkan, R. M., Erol, S., Uysal, M., Kalkan, Y., Bilgi, S., & Seker, D. Z. (2019). Determination of Reservoir Sedimentation With Bathymetric Survey: a Case Study of Obruk Dam Lake. *Fresenius Environmental Bulletin*, *28*(3), 2305–2313.

Inchell, M. W., Rinivasan, R. S., & Uzio, M. D. I. L. (2013). *A RC SWAT I NTERFACE F OR SWAT2012 U SER ' S G UIDE*.

Kassie, M., Pender, J., Yesuf, M., Kohlin, G., Bluffstone, R., & Mulugeta, E. (2008). Estimating returns to soil conservation adoption in the northern Ethiopian highlands. *Agricultural Economics*, *38*(2), 213–232. https://doi.org/10.1111/j.1574-0862.2008.00295.x

Kefay, T., Abdisa, T., & Tumsa, B. C. (2022). Prioritization of Susceptible Watershed to Sediment Yield and Evaluation of Best Management Practice: A Case Study of Awata River, Southern Ethiopia. *Applied and Environmental Soil Science*, *2022*. https://doi.org/10.1155/2022/1460945

Kenderessy, P., & Lieskovský, J. (2014). Impact of the soil erosion on soil properties along a slope catena-case study Horný Ohaj Vineyards, Slovakia. *Carpathian Journal of Earth and Environmental Sciences*, *9*(2), 143–152.

Kiage, L. M. (2013). Perspectives on the assumed causes of land degradation in the rangelands of Sub-Saharan Africa. *Progress in Physical Geography*, *37*(5), 664–684. https://doi.org/10.1177/0309133313492543

Kidane Bahir, D., & Alemu, B. (2015). The Effect of Upstream Land Use Practices on Soil Erosion and Sedimentation in the Upper Blue Nile Basin, Ethiopia Integrated waterhsed management practices View project Remote Sensing and GIS-Based Soil Loss Estimation Using RUSLE in Bahir Dar Zuria Dist. *Researchgate.Net*, *4*(April 2018), 55–68. https://www.researchgate.net/profile/Binyam-Alemu/publication/324845331_The_Effect_of_Upstream_Land_Use_Practices_on_Soil_Erosion_and_Sedimentation_in_the_Upper_Blue_Nile_Basin_Ethiopia/links/5ae7

9275aca2725dabb33f77/The-Effect-of-Upstream-Land-Use-Practi

Kothyari, U. C., & Jain, S. K. (1997). Estimation de l'exportation de sédiments par utilisation d'un SIG. *Hydrological Sciences Journal*, *42*(6), 833–843. https://doi.org/10.1080/02626669709492082

Krause, P., Boyle, D. P., & Bäse, F. (2005). Comparison of different efficiency criteria for hydrological model assessment. *Advances in Geosciences*, *5*, 89–97. https://doi.org/10.5194/adgeo-5-89-2005

Lal and Stewart, 1990. (1990). *Advances in soil science: Soil Degradation* (11th ed.). springer-verlag.

Lal, R. (1995). Erosion-Crop Productivity Relationships for Soils of Africa. *Soil Sci. Soc. Am. J.*, *59*, 661–667.

Legates, G. (1999). *Evaluating the use of "goodness-of- fit" measures in hydrologic and hydroclimatic model validation. Wa- ter Resources Research. 35*(1), 1–9.

Lemann, T., Roth, V., Zeleke, G., Subhatu, A., Kassawmar, T., & Hurni, H. (2018). Spatial and temporal variability in hydrological responses of the upper Blue Nile basin, Ethiopia. *Water (Switzerland)*, *11*(1). https://doi.org/10.3390/w11010021

Lemann, T., Zeleke, G., Amsler, C., Giovanoli, L., Suter, H., & Roth, V. (2016). Modelling the effect of soil and water conservation on discharge and sediment yield in the upper Blue Nile basin , Ethiopia. *Applied Geography*, *73*, 89–101. https://doi.org/10.1016/j.apgeog.2016.06.008

Lemma, H., Frankl, A., Griensven, A., Poesen, J., Adgo, E., & Nyssen, J. (2019). Identifying erosion hotspots in Lake Tana Basin from a multisite Soil and Water Assessment Tool validation: Opportunity for land managers. *Land Degradation & Development*, *30*(12), 1449–1467. https://doi.org/10.1002/ldr.3332

Leta, M. K., Waseem, M., Rehman, K., & Tränckner, J. (2023). Sediment yield estimation and evaluating the best management practices in Nashe watershed, Blue Nile Basin, Ethiopia. *Environmental Monitoring and Assessment*, *195*(6). https://doi.org/10.1007/s10661-023-11337-z

López-Ballesteros, A., Senent-Aparicio, J., Srinivasan, R., & Pérez-Sánchez, J. (2019). Assessing the impact of best management practices in a highly anthropogenic and ungauged watershed using the SWAT model: A case study in the El beal watershed (Southeast Spain). *Agronomy*, *9*(10), 1–15. https://doi.org/10.3390/agronomy9100576

Mahata, S., & Sharma, V. N. (2021). The global problem of land degradation: A review.

National Geographical Journal of India, *67*(2), 216–231. https://doi.org/10.48008/ngji.1773

Mazzucato, V., & Niemeijer, D. (2000). Rethinking soil and water conservation in a changing society: a case study in Burkina Faso. *Rethinking Soil and Water Conservation in a Changing Society: A Case Study in Burkina Faso.*, 380-pp.

Mengistu, D., Bewket, W., & Lal, R. (2015). Sustainable Intensification to Advance Food Security and Enhance Climate Resilience in Africa. *Sustainable Intensification to Advance Food Security and Enhance Climate Resilience in Africa*. https://doi.org/10.1007/978-3-319-09360-4

Mequanient, M. B., & Kebede, H. H. (2023). Simulation of sediment yield and evaluation of best management practices in Azuari watershed, Upper Blue Nile Basin. *H2Open Journal*, *6*(3), 493–506. https://doi.org/10.2166/h2oj.2023.159

Moges, M. A., Zemale, F. A., Alemu, M. L., Ayele, G. K., & Dagnew, D. C. (2015). Sediment concentration rating curves for a monsoonal climate: upper Blue Nile Basin. *SOIL Discussions*, *2*(2), 1419–1448. https://doi.org/10.5194/soild-2-1419-2015

Moges, M. M. (2021). Sedimentation in Small Irrigation Dams: A threat for food security. *Academia Letters*, *April 2021*, 1–5. https://doi.org/10.20935/al653

Moges, M. M., Abay, D., & Engidayehu, H. (2018). Investigating reservoir sedimentation and its implications to watershed sediment yield: The case of two small dams in data-scarce upper Blue Nile Basin, Ethiopia. *Lakes and Reservoirs: Research and Management*, *23*(3), 217–229. https://doi.org/10.1111/lre.12234

Moriasi, D. N., Arnold, J. G., Liew, M. W. Van, Bingner, R. L., Harmel, R. D., & Veith, T. L. (2007). *MODEL EVALUATION GUIDELINES FOR SYSTEMATIC QUANTIFICATION OF ACCURACY IN WATERSHED SIMULATIONS*. *50*(3), 885–900.

Nadew', B., Chaniyalew, E., & Tsegaye, T. (2019). Runoff Sediment Yield Modeling and Development of Management Intervention Scenarios, Case Study of Guder Watershed, Blue Nile Basin, Ethiopia. *Hydrology: Current Research*, *9*(4), 0–16. https://doi.org/10.4172/2157-7587.1000306

Nash, J. E., & Sutcliffe, J. V. (1970). River Flow Forecasting Through Conceptual Models - Part I - A Discussion of Principles. *Journal of Hydrology*, *10*(1970), 282–290.

Neitsch, S. ., Arnold, J. ., Kiniry, J. ., & Williams, J. . (2011). Soil & Water Assessment Tool Theoretical Documentation Version 2009. *Texas Water Resources Institute*, 1–647.

https://doi.org/10.1016/j.scitotenv.2015.11.063

Pechlivanidis, I. G., Jackson, B. M., Mcintyre, N. R., & Wheater, H. S. (2011). Catchment scale hydrological modelling: A review of model types, calibration approaches and uncertainty analysis methods in the context of recent developments in technology and applications. In *Global Nest Journal* (Vol. 13, Issue 3, pp. 193–214). https://doi.org/10.30955/gnj.000778

pierre y. julien. (2010). *Erosion and sedimentation* (Colorado State University (ed.); second). Cambridge University Press,.

Pimentel, D., Harvey, C., Resosudarmo, P., Sinclair, K., Kurz, D., McNair, M., Crist, S., Shpritz, L., Fitton, L., Saffouri, R., & Blair, R. (1995). Environmental and Economic Costs of Soil Erosion and Conservation Benefits. *Science*, *267*(5201), 1117–1123. https://doi.org/10.1126/science.267.5201.1117

Raes, D., Willems, P., & Gbaguidi, F. (2006). RAINBOW–A software package for hydrometeorological frequency analysis and testing the homogeneity of historical data sets. *Proceedings of the 4th International Workshop on 'Sustainable Management of Marginal Drylands (SUMAMAD), February*, 27–31.

Remesan, R., Shamim, M. A., Han, D., & Mathew, J. (2009). Runoff prediction using an integrated hybrid modelling scheme. *Journal of Hydrology*, *372*(1–4), 48–60. https://doi.org/10.1016/j.jhydrol.2009.03.034

Roba, N. T., Kassa, A. K., Geleta, D. Y., & Harka, A. E. (2021). Streamflow and sediment yield estimation, and area prioritization for better conservation planning in the Dawe River watershed of the Wabi Shebelle River Basin, Ethiopia. *Heliyon*, *7*(12), e08509. https://doi.org/10.1016/j.heliyon.2021.e08509

Saha, S., Gayen, A., Pourghasemi, H. R., & Tiefenbacher, J. P. (2019). Identification of soil erosion-susceptible areas using fuzzy logic and analytical hierarchy process modeling in an agricultural watershed of Burdwan district, India. *Environmental Earth Sciences*, *78*(23), 1–18. https://doi.org/10.1007/s12665-019-8658-5

Schuol, J., & Abbaspour, K. C. (2007). Using monthly weather statistics to generate daily data in a SWAT model application to West Africa. *Ecological Modelling*, *201*(3–4), 301–311. https://doi.org/10.1016/j.ecolmodel.2006.09.028

Setegn, S. G. (2008). *Hydrological and Sediment Yield Modelling in Lake Tana Basin, Blue Nile Ethiopia* (Issue June).

Setegn, S. G., Dargahi, B., Srinivasan, R., & Melesse, A. M. (2010). Modeling of sediment

yield from anjeni-gauged watershed, Ethiopia using swat model1. *Journal of the American Water Resources Association*, *46*(3), 514–526. https://doi.org/10.1111/j.1752-1688.2010.00431.x

Setegn, S. G., Srinivasan, R., Dargahi, B., & Melesse, A. M. (2009). *Spatial delineation of soil erosion vulnerability in the Lake Tana Basin , Ethiopia*. *3750*(October), 3738–3750. https://doi.org/10.1002/hyp

Setegn, S. G., Srinivasan, R., Melesse, A. M., & Dargahi, B. (2010). *SWAT model application and prediction uncertainty analysis in the Lake Tana Basin , Ethiopia*. *367*(September 2009), 357–367. https://doi.org/10.1002/hyp

Sitotaw, G., Geremew, T., Gebre, S., & Gebreyohannes, A. (2021). Hydrological modeling in the Upper Blue Nile basin using soil and water analysis tool (SWAT). *Modeling Earth Systems and Environment*, *0123456789*. https://doi.org/10.1007/s40808-021-01085-9

Sonneveld, B. G., Keyzer, M. A., & Albersen, P. J. (2001). A Non-Parametric Analysis of Qualitative and Quantitative Data for Erosion Modeling: A Case Study for Ethiopia. *Sustaining the Global Farm*, *February*, 979–993.

Stoorvogel, J. J., & Smaling, E. M. A. (1990). Assessment of soil nutrient depletion in Sub-Saharan Africa: 1983-2000. Vol. 2: Nutrient balances per crop and per land use systems. *The Winand Staring Centre, Wageningen (The Netherlands), Report 28*, 585.

Subramanya, D. K. (1984). *Engineering hydrology*. https://doi.org/10.1201/9780429094811-13

Surfleet, C. G., Tullos, D., Chang, H., & Jung, I. W. (2012). Selection of hydrologic modeling approaches for climate change assessment: A comparison of model scale and structures. *Journal of Hydrology*, *464–465*, 233–248. https://doi.org/10.1016/j.jhydrol.2012.07.012

Syvitski, J. P., Morehead, M. D., Bahr, D. B., & Mulder, T. (2000). Estimating fluvial sediment transport : The rating parameters parameters (a and b) are defined by a power law relating discharge values of a river mathematical concentration is inversely proportional to the long-term. *Water Resources*, *36*(9), 2747–2760.

Taddese, G. (2001). Land degradation: A challenge to Ethiopia. *Environmental Management*, *27*(6), 815–824. https://doi.org/10.1007/s002670010190

Tamene, L., Park, S. J., Dikau, R., & Vlek, P. L. G. (2006). Analysis of factors determining sediment yield variability in the highlands of northern Ethiopia. *Geomorphology*, *76*(1–

2), 76–91. https://doi.org/10.1016/j.geomorph.2005.10.007

Tamene, L., & Vlek, P. L. G. (2007). Assessing the potential of changing land use for reducing soil erosion and sediment yield of catchments: A case study in the highlands of northern Ethiopia. *Soil Use and Management*, *23*(1), 82–91. https://doi.org/10.1111/j.1475-2743.2006.00066.x

Taye, M., Simane, B., Selsssie, Y. G., Zaitchik, B., & Setegn, S. (2018). Analysis of the spatial variability of soil texture in a tropical highland: The case of the Jema Watershed, Northwestern Highlands of Ethiopia. *International Journal of Environmental Research and Public Health*, *15*(9), 1–10. https://doi.org/10.3390/ijerph15091903

Tesfu. (2015). Modeling Runoff and Sediment Yield of Kesem Dam Watershed , Awash Basin , Ethiopia. *Msc Thesis, Arba Minch University*.

Tully, K., Sullivan, C., Weil, R., & Sanchez, P. (2015). The State of soil degradation in sub-Saharan Africa: Baselines, trajectories, and solutions. *Sustainability (Switzerland)*, *7*(6), 6523–6552. https://doi.org/10.3390/su7066523

Tundu, C., Tumbare, M. J., & Onema, J. M. K. (2018). Sedimentation and its impacts/effects on river system and reservoir water quality: Case study of Mazowe catchment, Zimbabwe. *Proceedings of the International Association of Hydrological Sciences*, *377*, 57–66. https://doi.org/10.5194/piahs-377-57-2018

Verstraeten, G., Poesen, J., Verstraeten, G., & Poesen, J. (2000). *Progress in Physical Geography assessment of sediment yield Estimating trap efficiency of small reservoirs and ponds : methods and sediment yield*. https://doi.org/10.1177/030913330002400204

Waidler, D., White, M., Steglich, E., Wang, S., Williams, J., Jones, C. a, & Srinivasan, R. (2011). *Conservation Practice Modeling Guide for SWAT and APEX*. *399*, 78. http://swat.tamu.edu/media/57882/conservation-practice-modeling-guide.pdf

Walling, D. E., & Collins, A. L. (2016). Fine Sediment Transport and Management. *River Science: Research and Management for the 21st Century*, 37–60. https://doi.org/10.1002/9781118643525.ch3

Warrick, J. A. (2015). Trend analyses with river sediment rating curves. *Hydrological Processes*, *29*(6), 936–949. https://doi.org/10.1002/hyp.10198

William. (1975). Present and prospective technology for predicting sediment yields and sources. *Using a Scour and Deposition Model to Determine Sediment Yield*, 208.

Womber, Z. R., Zimale, F. A., Kebedew, M. G., Asers, B. W., Deluca, N. M., Guzman, C. D., Tilahun, S. A., & Zaitchik, B. F. (2021). Estimation of Suspended Sediment

Concentration from Remote Sensing and in Situ Measurement over Lake Tana, Ethiopia. *Advances in Civil Engineering*, *2021*. https://doi.org/10.1155/2021/9948780

Worku, T. (2017). Modeling runoff – sediment response to land use / land cover changes using integrated GIS and SWAT model in the Beressa watershed. *Environmental Earth Sciences*, 1–14. https://doi.org/10.1007/s12665-017-6883-3

Xu, C. yu, Tunemar, L., Chen, Y. D., & Singh, V. P. (2006). Evaluation of seasonal and spatial variations of lumped water balance model sensitivity to precipitation data errors. *Journal of Hydrology*, *324*(1–4), 80–93. https://doi.org/10.1016/j.jhydrol.2005.09.019

Yesuf, H. M., Assen, M., Alamirew, T., & Melesse, A. M. (2015). Modeling of sediment yield in Maybar gauged watershed using SWAT, northeast Ethiopia. *Catena*, *127*, 191–205. https://doi.org/10.1016/j.catena.2014.12.032

Zeberie, W. (2020). Assessment of sediment yield and conservation practices in Akaki watershed , Upper Awash Basin. *World News of Natural Sciences*, *28*(November 2019), 103–120.

7. APPENDICES

Table 7-1: Mean annual point rainfall of selected stations.

Year	Sheno	Sendafa	Muke Turi	Mendida	Lemi	Kotu Gebeya
1992	2.52	2.62	2.71	1.94	2.66	2.12
1993	2.61	3.57	3.16	2.36	2.77	2.61
1994	1.62	2.35	2.27	2.12	2.59	2.38
1995	2.15	2.53	2.52	2.20	3.31	2.37
1996	2.97	3.41	2.63	2.71	4.37	3.26
1997	2.20	2.77	2.27	2.45	2.71	2.65
1998	2.81	2.65	2.49	2.69	2.23	3.06
1999	2.49	3.07	2.30	2.60	3.35	2.84
2000	2.33	2.93	2.31	2.33	3.35	2.93
2001	2.68	2.87	2.73	2.43	3.87	2.82
2002	2.12	2.60	2.27	1.87	2.27	2.27
2003	3.02	2.85	2.96	2.81	2.86	2.89
2004	2.62	2.37	2.52	2.53	2.97	2.87
2005	2.57	2.95	2.49	2.27	2.51	2.70
2006	2.92	3.17	2.83	2.77	3.55	3.14
2007	2.80	3.03	2.60	2.94	3.05	3.00
2008	2.65	2.63	2.66	2.33	2.85	2.67
2009	2.36	2.40	1.86	2.37	3.28	2.35
2010	2.32	2.97	2.78	2.61	3.70	2.39
2011	2.41	2.55	2.13	2.42	2.68	2.57
2012	4.22	3.68	2.66	2.76	3.47	2.86
2013	2.67	3.14	2.58	2.32	2.72	2.66
2014	3.46	3.06	2.45	2.37	2.80	2.61
2015	1.87	2.36	1.80	1.75	1.88	1.92
2016	2.29	2.89	2.91	2.86	2.99	2.55
2017	1.80	3.04	1.87	2.19	2.72	2.45
2018	3.36	3.10	2.45	2.47	3.14	2.91
2019	3.48	4.04	3.99	3.42	3.57	3.30

2020	3.42	3.95	4.23	3.44	3.73	3.29
2021	3.33	3.38	3.39	2.39	3.52	2.96

Table 7-2: Annual rainfall of selected station.

Year	Sheno	Sendafa	Muke Turi	Mendida	Lemi	Kotu Gebeya
1992	921.77	958.20	991.97	709.22	972.74	775.67
1993	953.51	1303.46	1152.41	861.48	1011.04	952.12
1994	592.44	858.17	830.35	773.51	944.22	869.93
1995	786.27	924.92	921.59	804.31	1209.93	865.73
1996	1088.44	1248.00	964.27	991.83	1601.16	1193.25
1997	801.60	1009.58	829.59	894.83	989.82	967.24
1998	1025.47	966.38	909.78	982.69	814.69	1117.34
1999	910.52	1120.76	840.05	949.15	1222.97	1037.19
2000	854.52	1072.21	846.63	853.66	1224.55	1071.79
2001	977.24	1046.82	994.95	887.51	1411.40	1030.10
2002	772.75	947.65	828.53	682.07	827.69	826.77
2003	1101.48	1041.17	1082.19	1026.04	1042.32	1056.11
2004	960.27	867.00	922.19	926.17	1086.50	1051.63
2005	938.57	1077.82	909.08	830.33	914.94	985.19
2006	1066.21	1156.96	1031.19	1012.17	1296.43	1144.39
2007	1021.77	1105.44	950.26	1071.41	1112.73	1096.61
2008	968.19	964.02	974.73	854.10	1041.39	978.99
2009	861.92	876.48	679.99	866.25	1197.34	856.38
2010	848.51	1083.46	1015.48	951.77	1350.80	873.74
2011	879.33	931.75	776.07	884.80	976.43	938.92
2012	1546.30	1346.08	974.24	1009.64	1271.81	1045.15
2013	973.58	1146.26	942.38	845.70	992.55	970.80
2014	1261.63	1115.93	892.53	863.35	1021.72	953.04
2015	682.07	862.86	658.29	640.49	687.83	699.33
2016	837.18	1057.22	1066.79	1048.30	1094.51	932.87
2017	657.82	1111.06	682.18	797.87	992.41	892.93

2018	1225.08	1131.43	892.90	901.64	1144.45	1060.63
2019	1271.89	1474.11	1455.77	1249.32	1304.48	1204.60
2020	1252.52	1444.70	1549.85	1260.15	1365.55	1202.88
2021	1214.29	1233.06	1235.63	871.30	1286.33	1081.10

Table 7-3: Description of soil parameters.

N layer	Number of layers in soil profile
Hyd Grp	Soil hydrologic group
Sol_Zmax	Maximum rooting depth of profile
Sol_Z	Depth to bottom of the soil layer (mm)
Sol_BD	Moist bulk density of the soil layer (Mg/m3)
Sol_AWC	Available water capacity of the the soil layer (mmH2O/mm soil)
Sol_K	Saturated hydraulic conductivity of the soil layer (mm/hr)
Sol_CBN	Organic carbon content of the soil layer (%)
Clay	Clay content of the soil layer (%)
Silt	Silt content of the soil layer (%)
Sand	Sand content of the soil layer (%)
Rock	Rock content of the soil layer (%)
Sol_ALB	Moist soil albedo
USLE_K	USLE equation soil erodibility (K) factor
Sol_EC	Electrical conductivity

Table 7-4: Robi Jida watershed soil code and there characteristics.

Soil code	N layer	Hyd Grp	Sol_Zmax	Sol_Z	Sol_BD	Sol_AWC	Sol_K	Sol_CBN	Clay	Silt	Sand	Rock	Sol_ALB	USLE_K	Sol_EC
Cme	1	D	1400	250	1.3	0.12	2.44	4.2	47.1	28.3	24.6	0.03	0.11	0.15	0.09
Cme	2	D	1400	700	1.33	0.13	1.75	2.3	47	30.7	22.3	0	0.24	0.15	0.07
Cme	3	D	1400	1400	1.3	0.12	0.84	1.27	53.9	26.2	19.9	0	0.36	0.15	0.07
VRe	1	D	1450	200	1.19	0.07	1.77	3.59	68	24.6	7.32	0	0.14	0.18	0.11
VRe	2	D	1450	650	1.11	0.07	1.27	1.84	74.6	18.6	6.53	0.23	0.29	0.17	0.11
VRe	3	D	1450	1450	1.1	0.09	0.98	1.14	73.1	18.3	8.59	0	0.38	0.15	0.16
LVx	1	D	1600	250	1.22	0.11	2.64	3.77	56.9	32.6	10.5	0	0.13	0.18	0.09
LVx	2	D	1600	650	1.17	0.1	1.34	1.74	65.7	25.6	8.74	0	0.3	0.17	0.06
LVx	3	D	1600	1600	1.13	0.1	0.98	0.46	68.4	22.4	9.26	0	0.5	0.16	0.06

Table 7-5: Measured sediment concentration data of Robi Jida River.

River / Stream	Station / Near	Basin	Date & Time of	Time Taken (s)	Flow (m^3/s)	Sediment Conc.m
Robi Jida	Mukature	Abbay	7-Nov-92	10	0.316	160.33
Robi Jida	Mukature	Abbay	7-Nov-92	8	0.316	170.91
Robi Jida	Mukature	Abbay	7-Nov-92	9	0.316	163.11
Robi Jida	Mukature	Abbay	25-Sep-92	13	2.933	202.50
Robi Jida	Mukature	Abbay	25-Sep-92	12	2.933	209.50
Robi Jida	Mukature	Abbay	25-Sep-92	14	2.933	268.75
Robi Jida	Mukature	Abbay	16-Aug-94	30	32.589	375.19
Robi Jida	Mukature	Abbay	16-Aug-94	25	32.589	349.66
Robi Jida	Mukature	Abbay	16-Aug-94	32	32.589	345.00
Robi Jida	Mukature	Abbay	19-Jul-95	48	13.348	210.30
Robi Jida	Mukature	Abbay	19-Jul-95	48	13.348	186.90
Robi Jida	Mukature	Abbay	19-Jul-95	42	13.348	171.00
Robi Jida	Mukature	Abbay	30-Jul-95	1.75	7.161	1097.20
Robi Jida	Mukature	Abbay	30-Jul-95	2.05	7.161	520.70
Robi Jida	Mukature	Abbay	30-Jul-95	1.35	7.161	479.00
Robi Jida	Mukature	Abbay	9-Aug-95	1.95	25.677	196.30
Robi Jida	Mukature	Abbay	9-Aug-95	2.55	25.677	241.20
Robi Jida	Mukature	Abbay	9-Aug-95	1.85	25.677	214.50
Robi Jida	Mukature	Abbay	10-Aug-95	43	53.366	353.30
Robi Jida	Mukature	Abbay	10-Aug-95	48	53.366	328.70
Robi Jida	Mukature	Abbay	10-Aug-95	48	53.366	349.80
Robi Jida	Mukature	Abbay	24-Aug-95	58	18.022	119.31
Robi Jida	Mukature	Abbay	24-Aug-95	66	18.022	113.81
Robi Jida	Mukature	Abbay	24-Aug-95	68	18.022	119.66
Robi Jida	Mukature	Abbay	21-Aug-95	48	27.343	319.35
Robi Jida	Mukature	Abbay	21-Aug-95	44	27.343	264.59
Robi Jida	Mukature	Abbay	21-Aug-95	49	27.343	295.00
Robi Jida	Mukature	Abbay	28-Jan-95	14	0.037	106.89

Robi Jida	Mukature	Abbay	28-Jan-95	15	0.037	93.93
Robi Jida	Mukature	Abbay	28-Jan-95	16	0.037	106.04
Robi Jida	Mukature	Abbay	29-Apr-95	27	0.489	36.39
Robi Jida	Mukature	Abbay	29-Apr-95	24	0.489	50.67
Robi Jida	Mukature	Abbay	29-Apr-95	26	0.489	42.93
Robi Jida	Mukature	Abbay	22-Sep-95	18	2.041	104.80
Robi Jida	Mukature	Abbay	22-Sep-95	18	2.041	103.10
Robi Jida	Mukature	Abbay	22-Sep-95	20	2.041	107.30
Robi Jida	Mukature	Abbay	20-Sep-95	10	2.429	107.40
Robi Jida	Mukature	Abbay	20-Sep-95	14	2.429	119.80
Robi Jida	Mukature	Abbay	20-Sep-95	16	2.429	123.20
Robi Jida	Mukature	Abbay	1-Oct-95	16	0.836	72.00
Robi Jida	Mukature	Abbay	1-Oct-95	17	0.836	55.00
Robi Jida	Mukature	Abbay	1-Oct-95	12	0.836	72.40
Robi Jida	Mukature	Abbay	2-Oct-95	13	0.706	100.30
Robi Jida	Mukature	Abbay	2-Oct-95	12	0.706	88.00
Robi Jida	Mukature	Abbay	2-Oct-95	10	0.706	52.70
Robi Jida	Mukature	Abbay	17-Aug-96	17	1.510	160.00
Robi Jida	Mukature	Abbay	17-Aug-96	13	1.510	99.70
Robi Jida	Mukature	Abbay	17-Aug-96	15	1.510	229.00
Robi Jida	Mukature	Abbay	20-Dec-96	33	0.138	94.00
Robi Jida	Mukature	Abbay	20-Dec-96	33	0.138	61.10
Robi Jida	Mukature	Abbay	20-Dec-96	35	0.138	98.90
Robi Jida	Mukature	Abbay	14-Jun-96	18	0.499	78.98
Robi Jida	Mukature	Abbay	14-Jun-96	15	0.499	69.89
Robi Jida	Mukature	Abbay	14-Jun-96	17	0.499	55.96

Figure 7-1: Homogeneity test of rainfall and stream flow data using Rainbow test.

A. Sheno rainfall

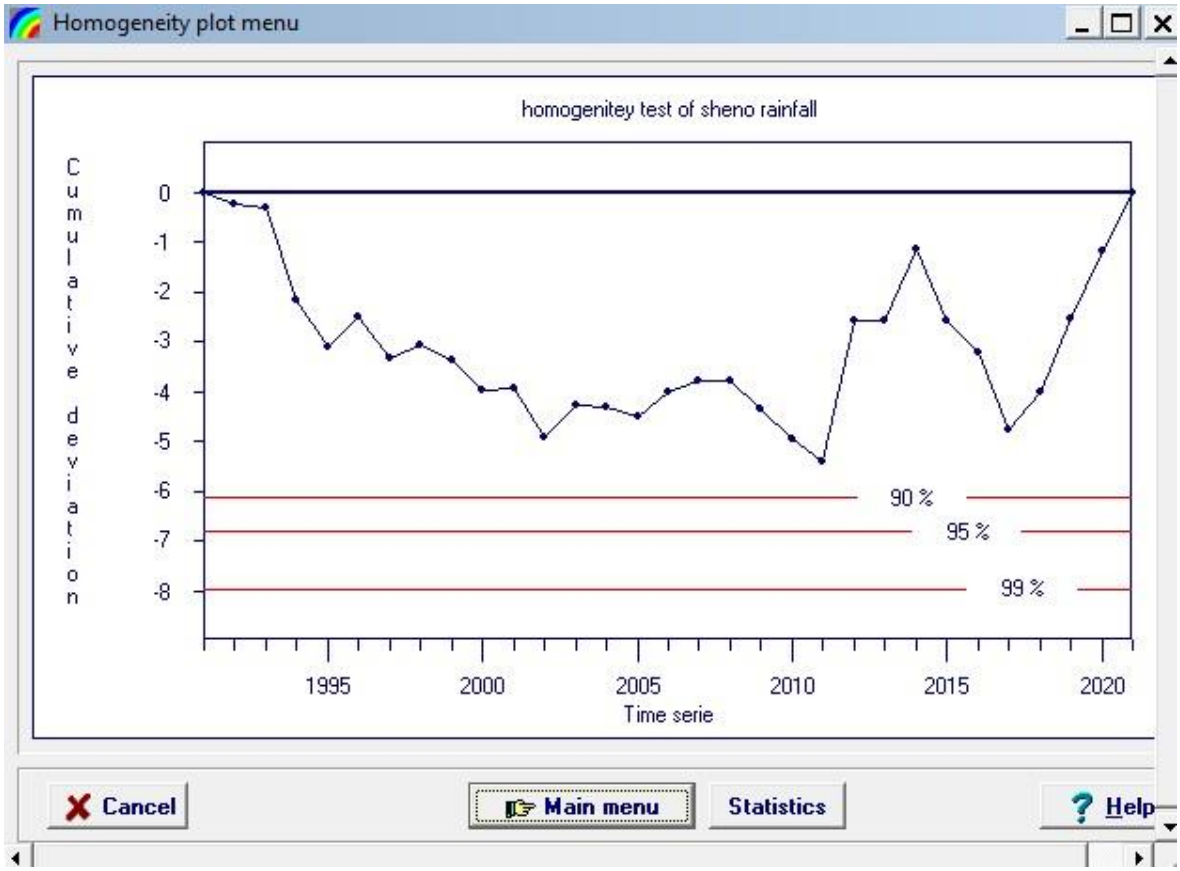

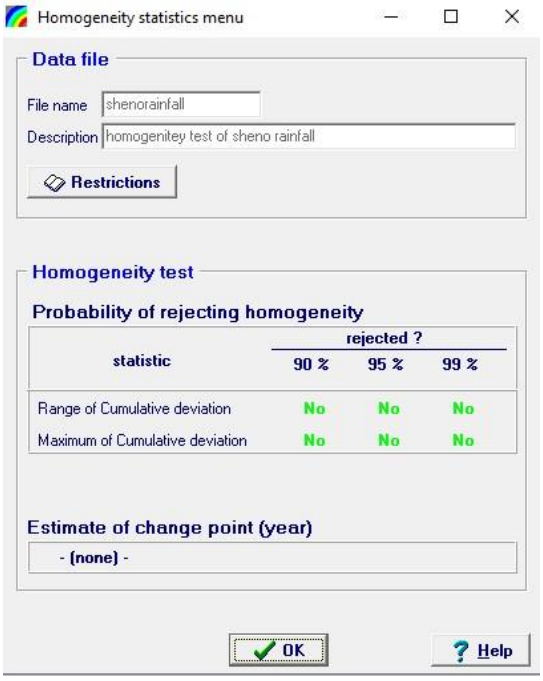

B. Kotu Gebey rainfall

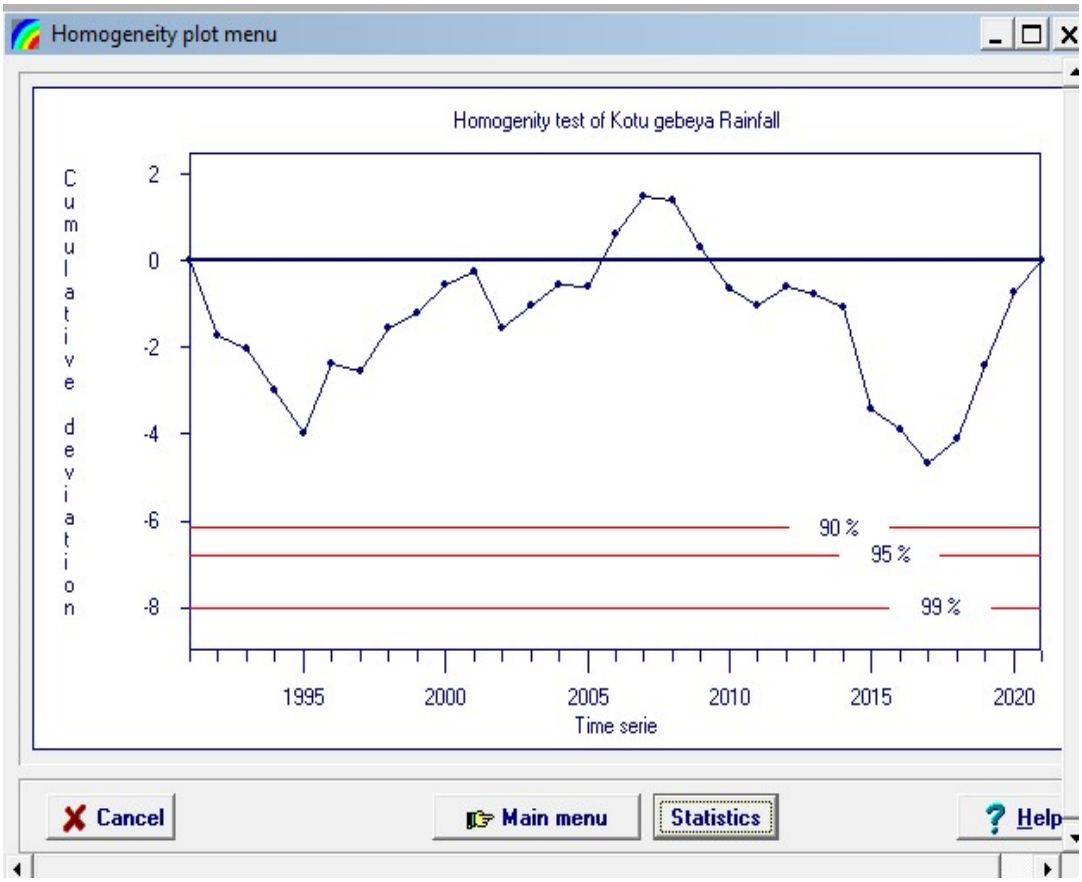

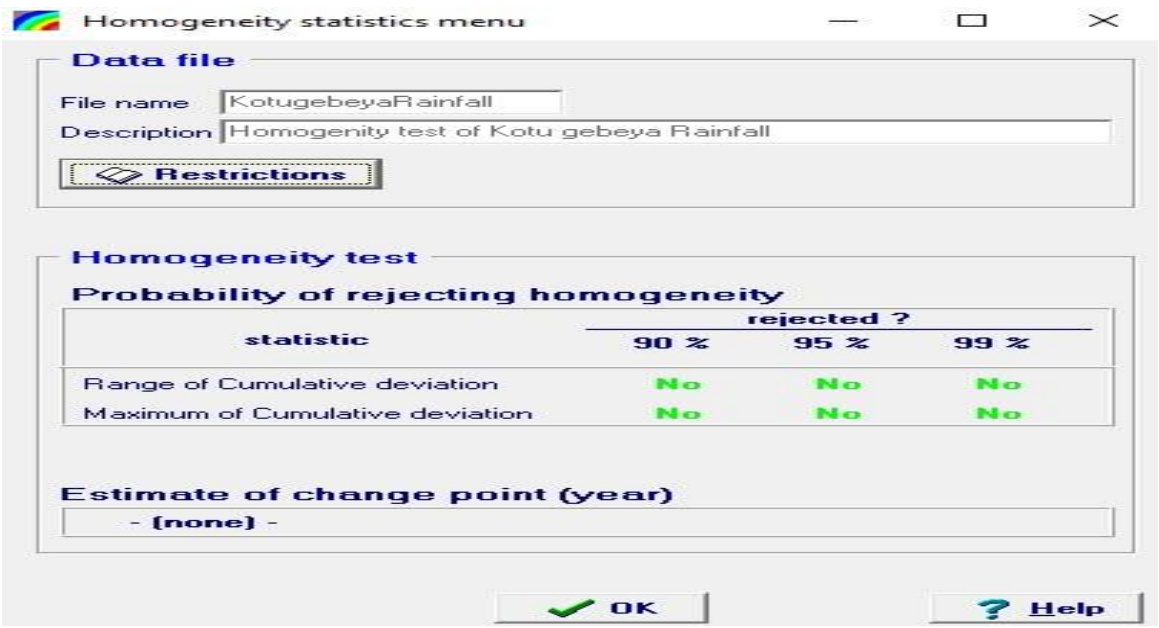

C. Lemi rainfall

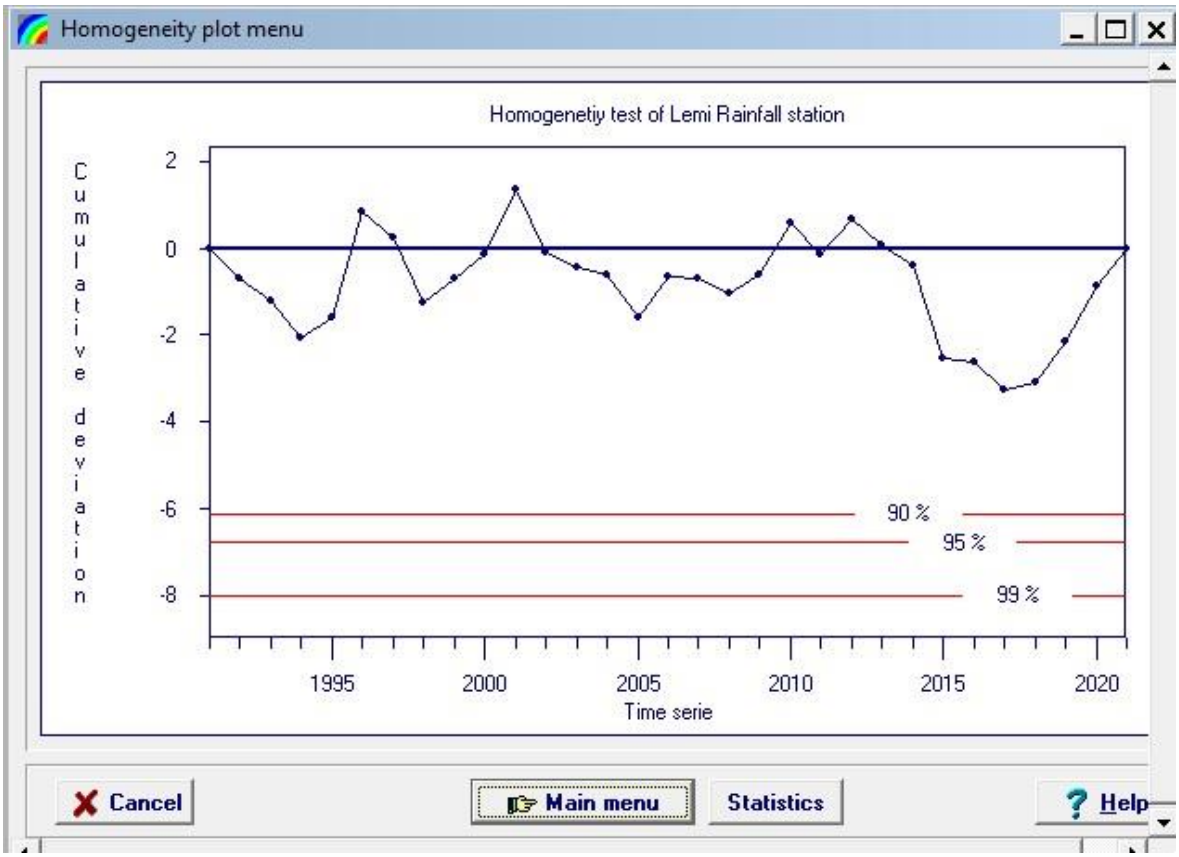

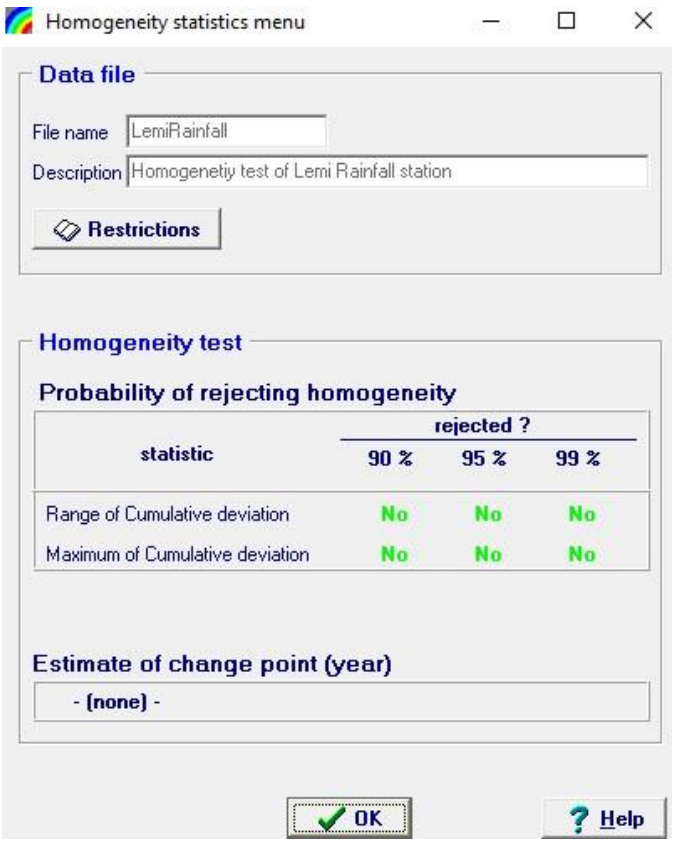

D. Mendida rainfall

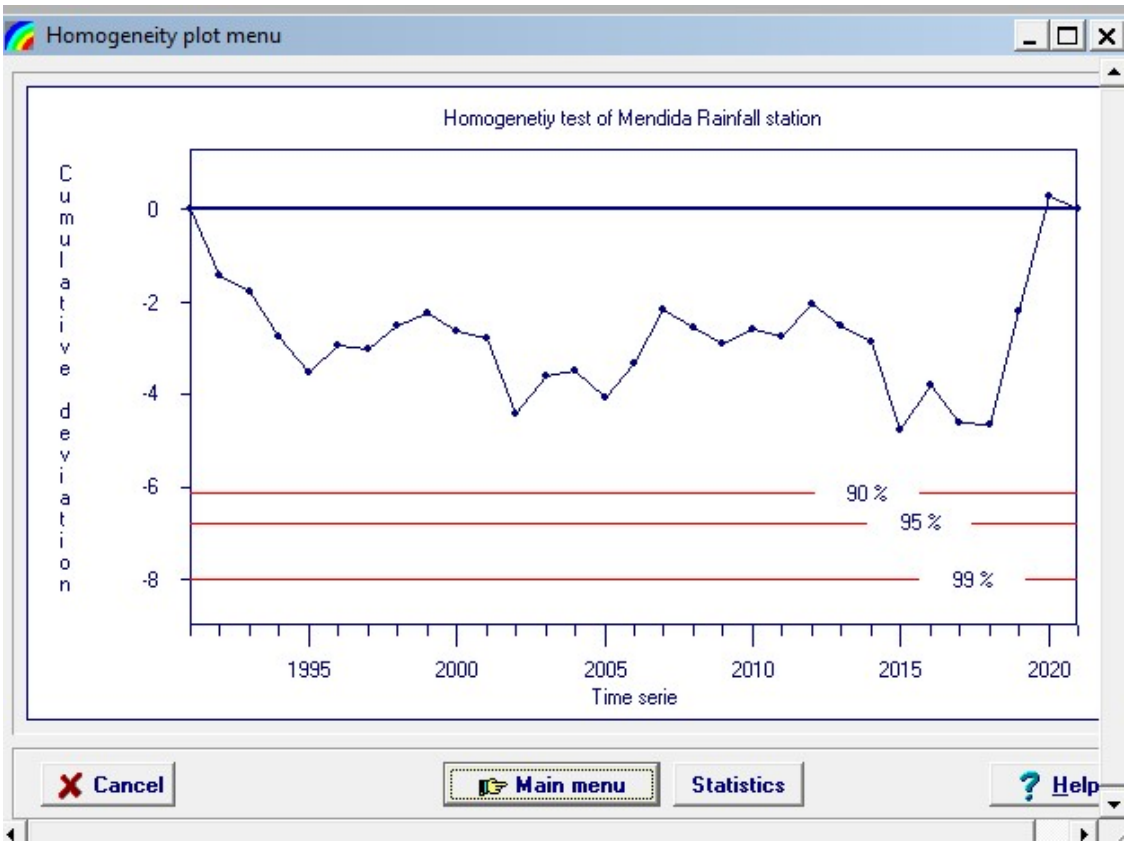

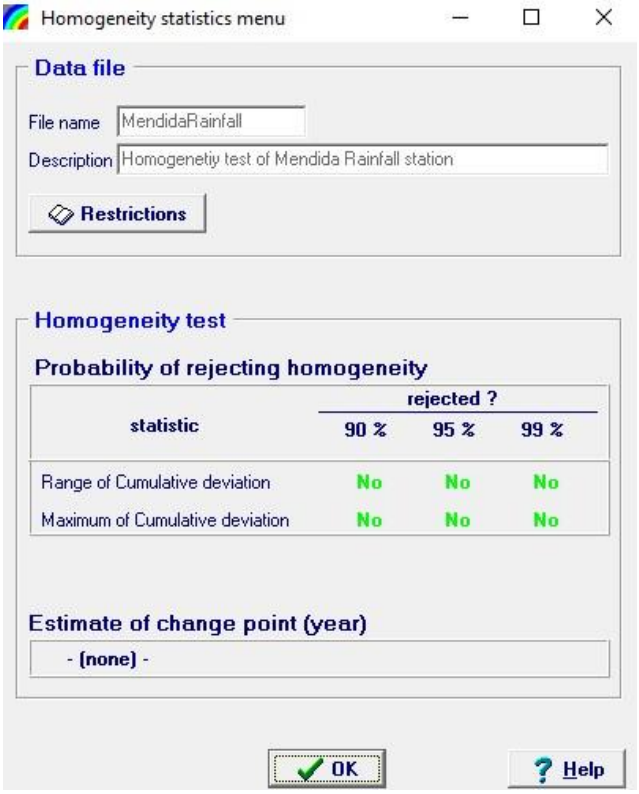

E. Sendafa rainfall

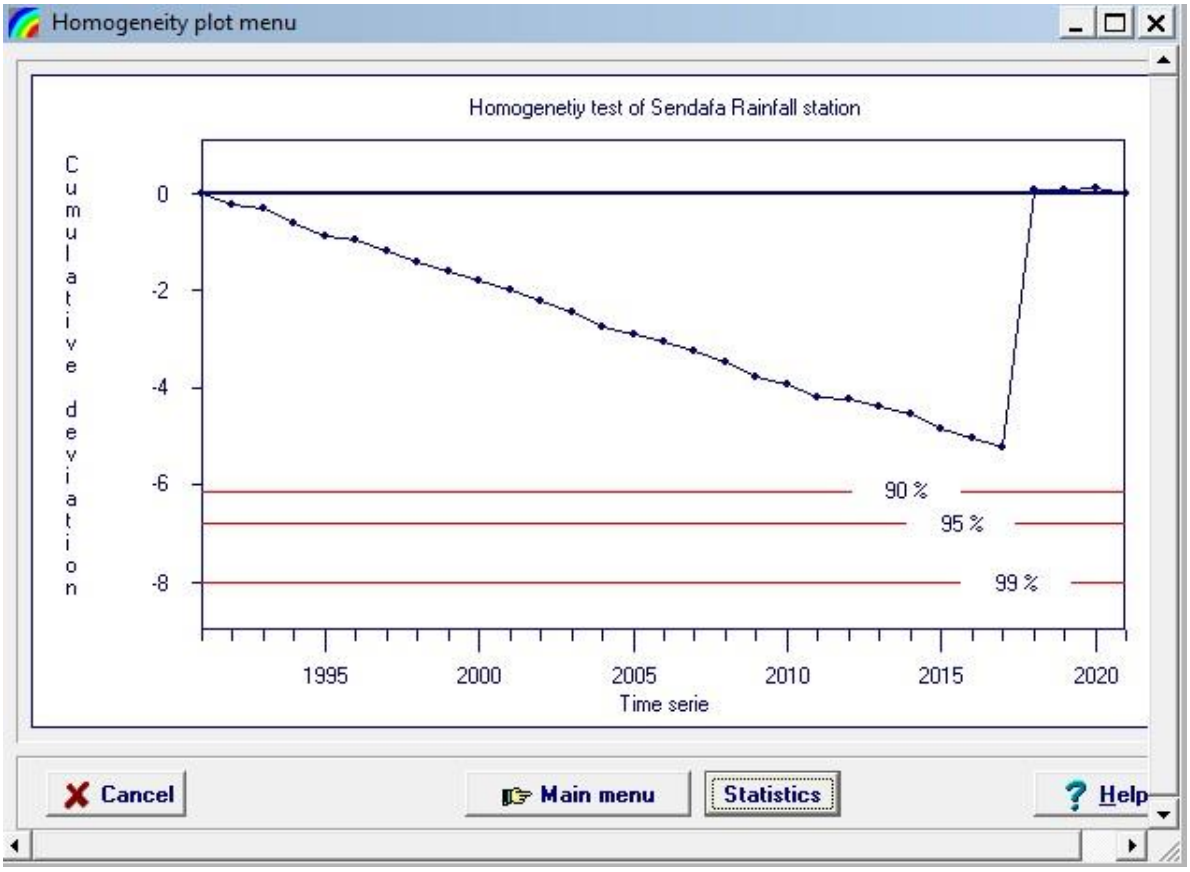

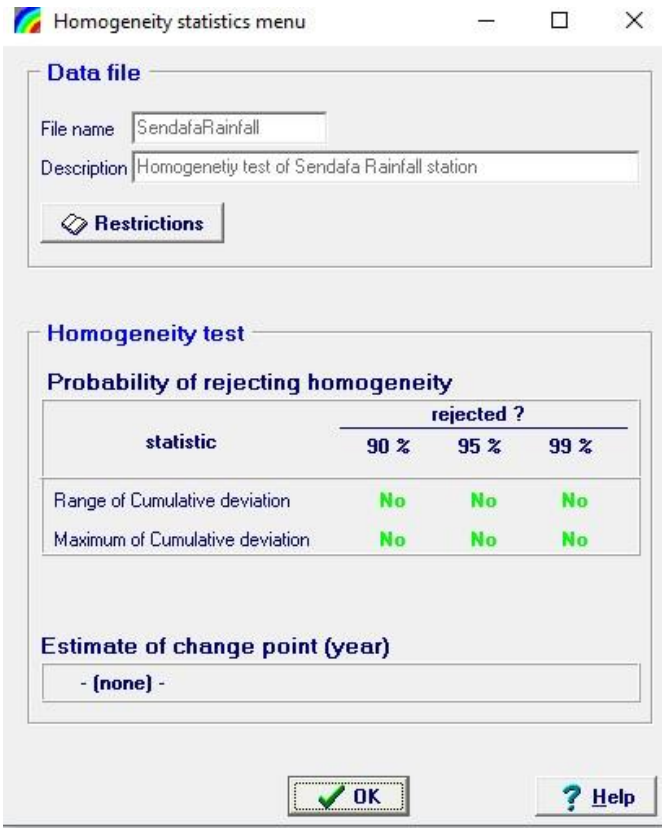

F. Stream flow of Robi Jida

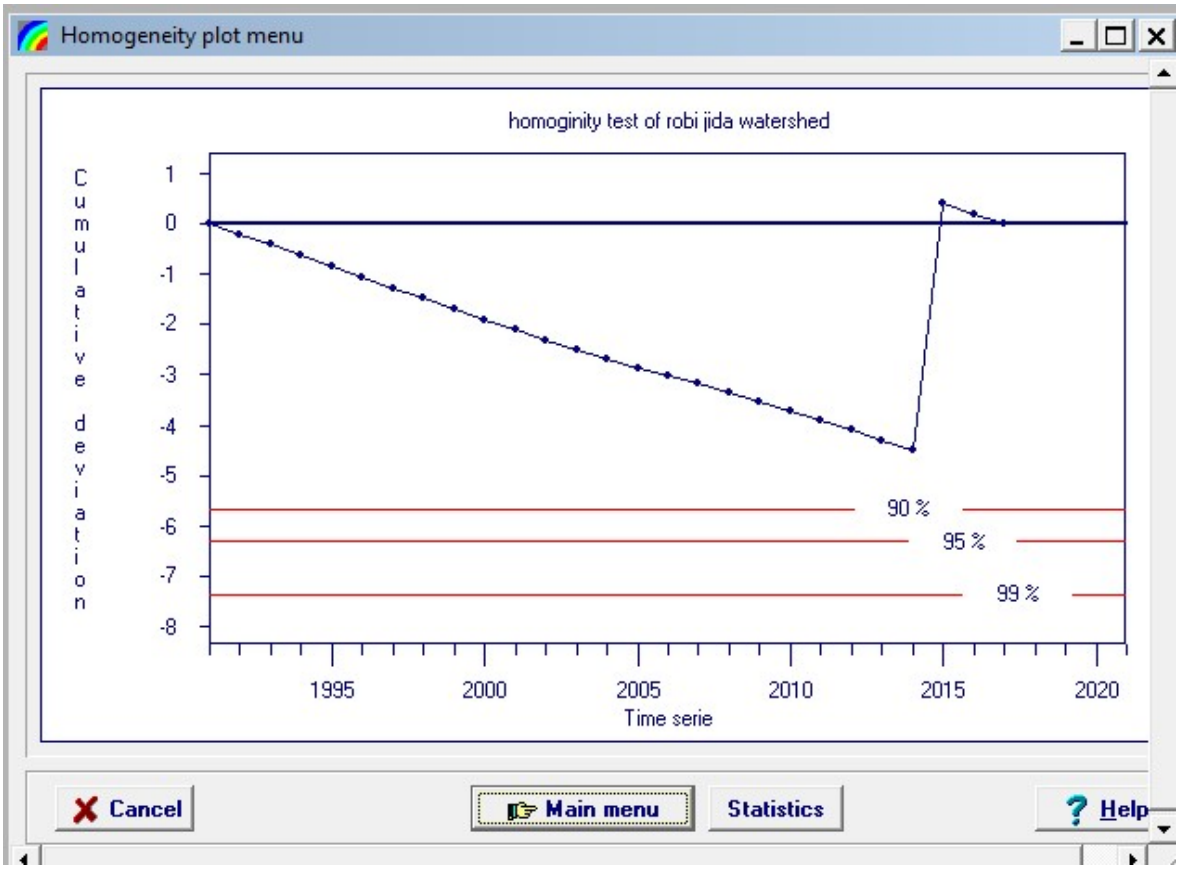

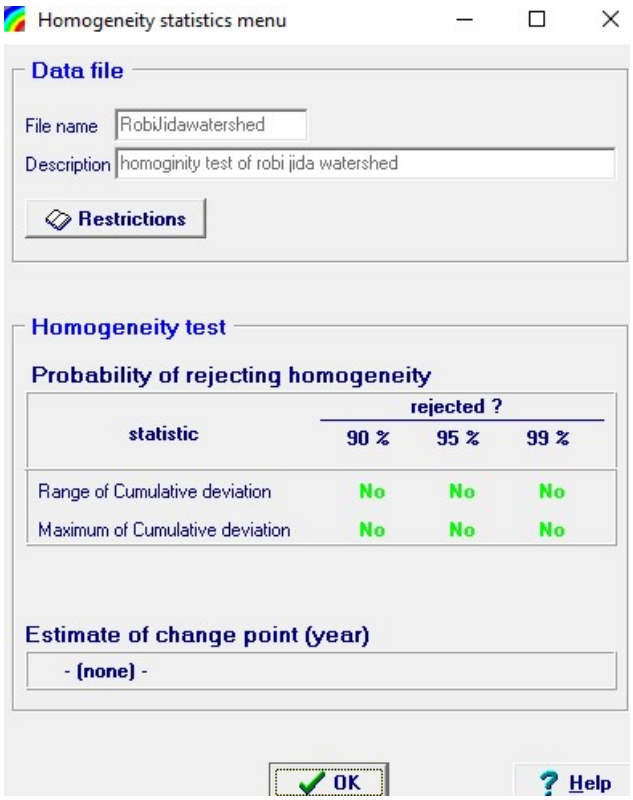

Table 7-6: Description of weather generator parameters and output.

Symbol	Description
TMPMX	Average or mean daily maximum air temperature for a month (^{0}C)
TMPMN	Average or mean daily minimum air temperature for a month (^{0}C)
TMPSTDMX	The standard deviation for daily maximum air temperature for a month (^{0}C)
TMPSTDMN	The standard deviation for daily minimum air temperature for a month (^{0}C)
PCPMM	Average or mean total monthly precipitation (mm H_2O
PCPSTD	The standard deviation for daily precipitation for a month (mm H_2O/day)
PCPSKW	The skew coefficient for daily precipitation in the month
PR_W1	Probability of a wet day following a dry day in the month
PR_W2	Probability of a wet day following a wet day in the month
PCPD	The average number of days of precipitation in the month
RAINHHM	Maximum 0.5 hour rainfall in entire period of record for month(mm H_2O)
SOLARAV	Average daily solar radiation for a month (MJ/m^2/day)
DEWPT	Average daily dew point temperature in month (^{0}C).
WNDAV	Average wind speed (m/s)

	Month											
Parameters	Jan	Feb	Mar	Apr	May	Jun	June	Aug	Sep	Oct	Nov	Dec
TMPMX	20	20.5	21	21.1	21.5	21	18.5	18.2	19	19.1	19	19
TMPMN	6.5	7.1	8	8.6	8.8	8.3	8	8.1	7.7	7.1	6.1	5.7
TMPSTDMX	1.3	1.8	1.8	1.7	1.6	1.7	1.6	1.4	1.1	1.2	1.3	1.4
TMPSTDMN	2	1.6	1.5	1.6	1.6	1.3	1.3	1.2	1.2	1.5	1.7	2
PCPMM	7.8	13.1	36	58.5	43.6	93	328	310	91	17.6	8.8	5.7
PCPSTD	1.4	2.5	3.3	4.7	4.2	5.7	11.2	11.1	5.3	2.2	1.9	1.3
PCPSKW	9.5	9.3	4.8	4	4.9	2.6	3.1	3.8	2.9	5.4	9.4	9.6
PR_W1	0.1	0.1	0.1	0.2	0.1	0.2	0.6	0.7	0.3	0.1	0	0
PR_W2	0.5	0.4	0.6	0.6	0.6	0.7	0.9	0.9	0.8	0.6	0.5	0.4
PCPD	3.3	2.9	7.9	10.5	7.6	14	27.5	27.7	16	4.4	2.4	1.6
RAINHHM	1.4	2.3	3.9	5.7	4.8	6.7	14	13.4	6.2	2.3	1.5	0.8
SOLARAV	15	16.2	17	16.6	16.7	15	13.4	13.8	15	16	15	15
DEWPT	63	59.1	63	70.8	67	65	77.4	80.9	79	71.8	68	66
WNDAV	3.2	3.4	3.4	3.3	3.4	2.8	2.5	2.3	2.6	3.7	3.6	3.3

Figure 7-2: Summary of stream flow sensitivity analysis by using the SUFI2 model.

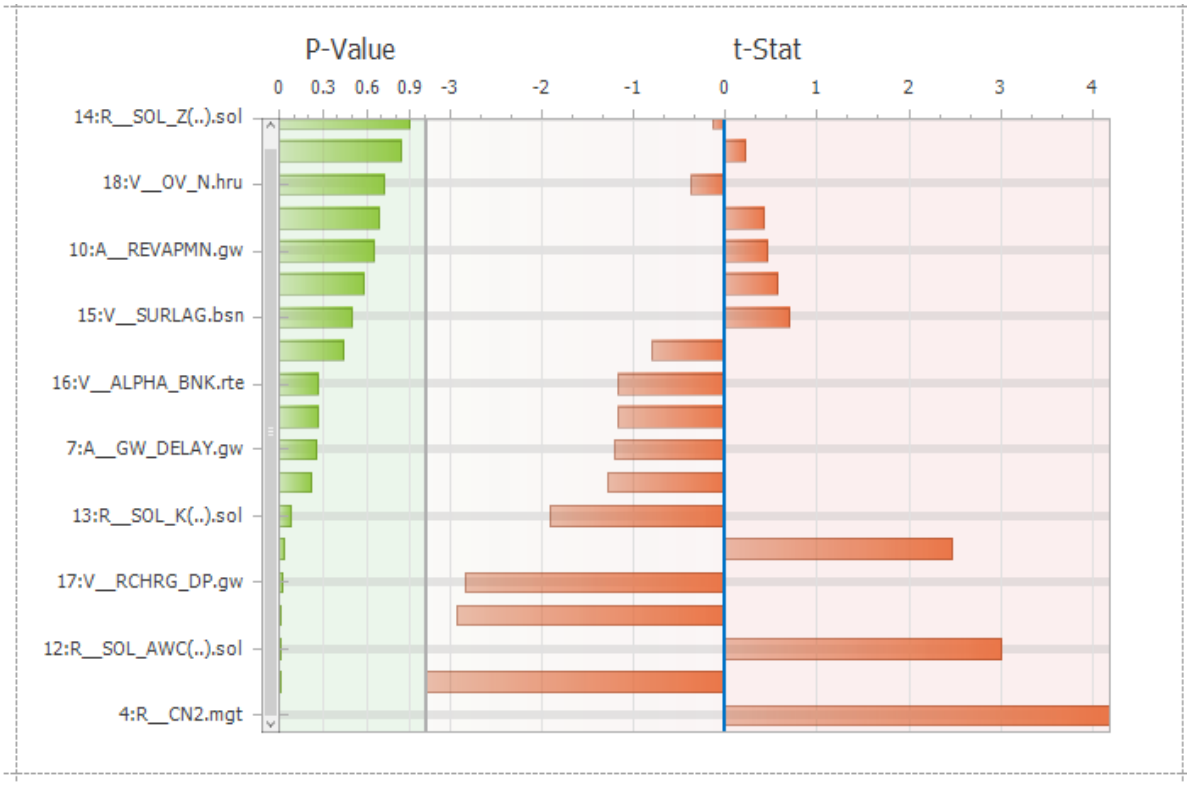

Figure 7-3: Summary statics of stream flow calibration using SUFI-2 results.

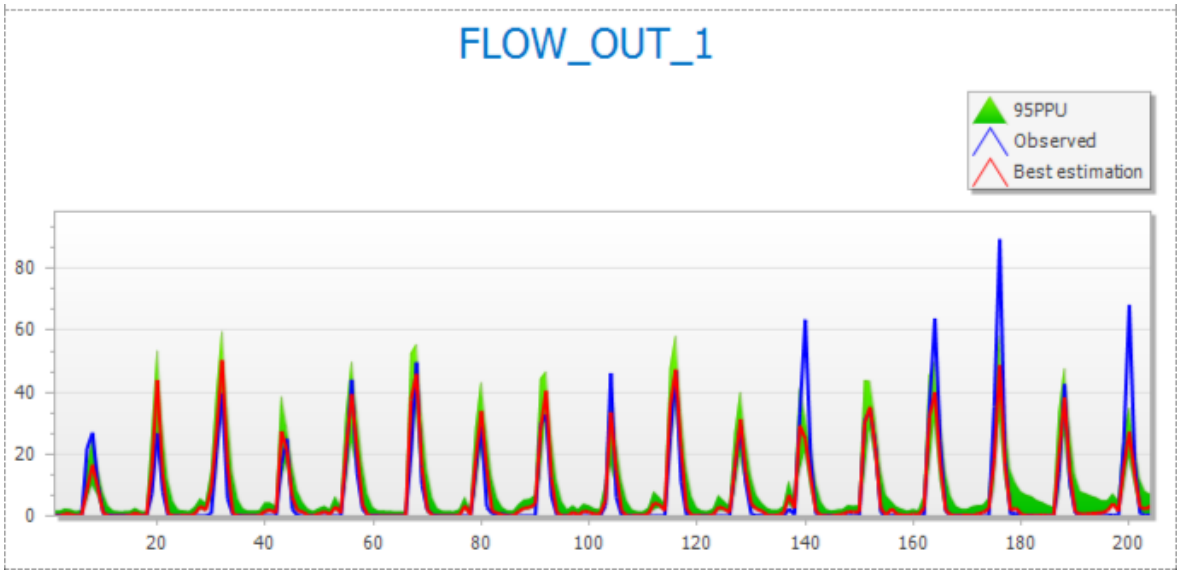

```
Goal_type= Nash_Sutcliff    No_sims= 500    Best_sim_no= 453    Best_goal = 7.970354e-001

Variable          p-factor  r-factor  R2    NS    bR2     MSE       SSQR      PBIAS  KGE   RSR   MNS   VOL_FR  ---  Mean_sim(Mean_obs)  S
FLOW_OUT_1        0.41      0.57      0.80  0.80  0.5931  4.2e+001  1.6e+001  -4.8   0.79  0.45  0.71  0.95           7.01(6.69)


---- Results for behavioral parameters ---
Behavioral threshold= 0.500000
Number of behavioral simulations = 491

Variable          p-factor  r-factor  R2    NS    bR2     MSE       SSQR      PBIAS  KGE   RSR   MNS   VOL_FR  ---  Mean_sim(Mean_obs)  S
FLOW_OUT_1        0.41      0.55      0.80  0.80  0.5931  4.2e+001  1.6e+001  -4.8   0.79  0.45  0.00  0.95           7.01(6.69)
```

Figure 7-4: Summary statics of stream flow validation using SUFI-2 results.

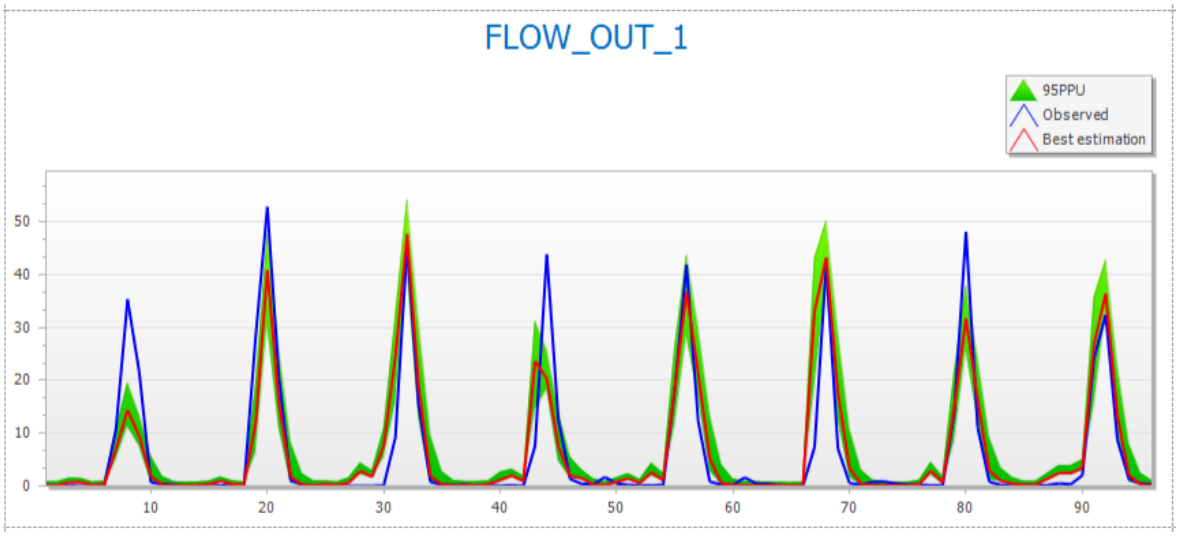


```
Goal_type= Nash_Sutcliff    No_sims= 100    Best_sim_no= 26    Best_goal = 7.686606e-001

Variable          p-factor  r-factor  R2    NS    bR2     MSE       SSQR      PBIAS  KGE   RSR   MNS   VOL_FR  ---  Mean_sim(Mean_obs)  S
FLOW_OUT_1        0.45      0.39      0.77  0.77  0.6000  3.6e+001  5.0e+000  -4.7   0.83  0.48  0.67  0.95           6.52(6.23)


---- Results for behavioral parameters ---
Behavioral threshold= 0.500000
Number of behavioral simulations = 100

Variable          p-factor  r-factor  R2    NS    bR2     MSE       SSQR      PBIAS  KGE   RSR   MNS   VOL_FR  ---  Mean_sim(Mean_obs)  S
FLOW_OUT_1        0.45      0.39      0.77  0.77  0.6000  3.6e+001  5.0e+000  -4.7   0.83  0.48  0.00  0.95           6.52(6.23)
```

Table7-7: Water balance of the Robi Jida watershed.

Year	PCP (mm)	PET (mm)	ET (mm)	SW (mm)	PERC (mm)	SUR_Q (mm)	GW_Q (mm)	WYLD (mm)	LAT_Q (mm)
1994	628.8	619.4	283.2	1378.7	231.4	115.6	0.0	118.8	2.6
1995	806.6	606.1	265.2	1352.3	284.7	258.2	0.0	261.2	2.5
1996	1069.9	581.3	343.6	1451.7	323.6	399.2	0.0	402.8	2.9
1997	805.9	595.6	319.7	1452.4	245.9	218.1	0.0	221.3	2.6
1998	1007.8	630.6	361.8	1455.6	335.2	329.5	0.0	332.8	2.8
1999	898.8	648.6	250.5	1272.8	281.9	362.4	0.0	365.9	2.8
2000	853.5	596.1	293.0	1378.7	288.7	257.6	0.0	260.9	2.7
2001	980.0	603.6	357.2	1534.9	307.9	321.1	0.0	324.6	2.9
2002	781.3	643.8	367.7	1371.7	198.0	209.2	0.0	212.1	2.4
2003	1098.5	607.4	351.4	1474.5	324.4	416.4	0.0	419.6	2.8
2004	954.0	629.3	375.6	1519.2	306.9	261.0	0.0	264.5	3.0
2005	933.8	612.3	336.7	1502.0	339.7	274.3	0.5	278.5	3.0
2006	1061.2	595.6	344.8	1473.6	348.7	334.8	1.4	340.0	3.1
2007	1010.9	618.8	341.4	1465.8	361.3	334.7	2.5	341.1	3.3
2008	968.3	638.8	315.4	1371.6	314.7	317.1	3.9	324.7	3.1
2009	833.1	649.2	284.5	1345.1	279.7	263.1	9.1	275.7	2.8
2010	873.8	623.7	406.6	1466.2	273.5	210.7	23.9	238.1	2.8
2011	862.8	630.9	368.7	1462.8	270.7	217.0	143.6	363.8	2.6
2012	1458.2	633.3	321.9	1478.8	505.9	636.5	256.1	896.9	3.6
2013	968.9	597.9	339.2	1384.6	380.1	239.6	306.0	550.1	3.6
2014	1204.7	615.6	360.3	1481.5	425.4	413.2	319.0	736.8	3.8
2015	678.1	669.4	326.2	1321.7	209.4	150.9	239.3	393.8	2.8
2016	872.5	623.8	360.0	1345.0	280.3	224.6	193.3	421.2	2.8
2017	661.4	625.7	330.3	1334.4	205.8	131.1	156.9	290.9	2.4
2018	1173.9	591.7	356.0	1444.4	420.7	375.9	215.2	594.8	3.1
2019	1300.4	632.8	423.6	1575.0	416.2	432.1	282.8	719.3	3.7
2020	1298.6	638.5	409.4	1558.2	430.1	483.4	324.7	813.0	4.0
2021	1217.6	676.9	346.9	1447.4	359.2	515.2	299.5	819.2	3.7
Average	973.7	622.7	340.7	1432.2	319.6	310.8	99.2	413.7	3.0

Figure 7-5: Summary of sediment yield sensitivity analysis by using the SUFI2 model.

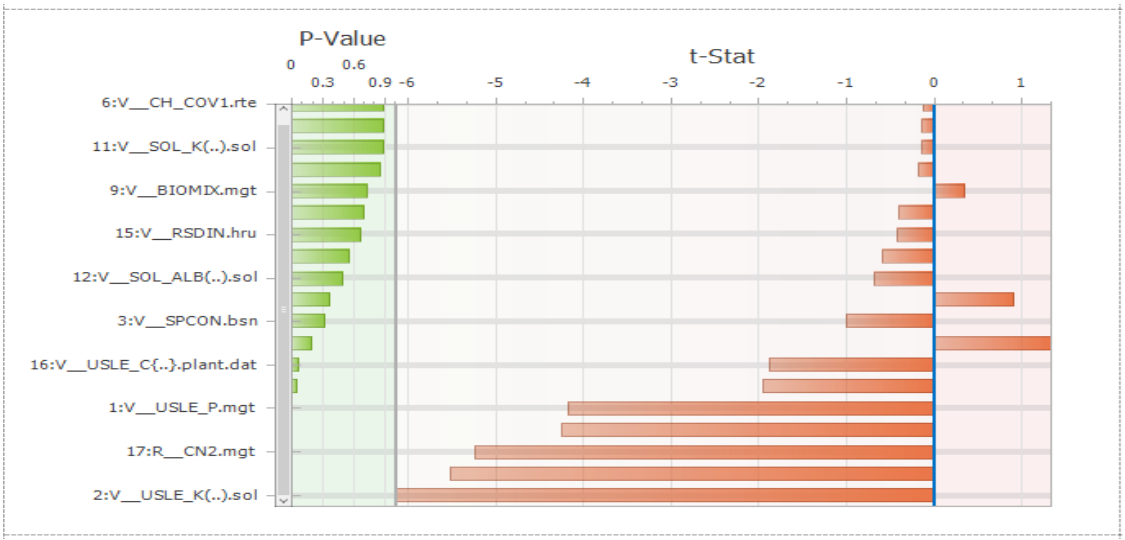

Figure 7-6: Summary statics of sediment calibration using SUFI-2 results.

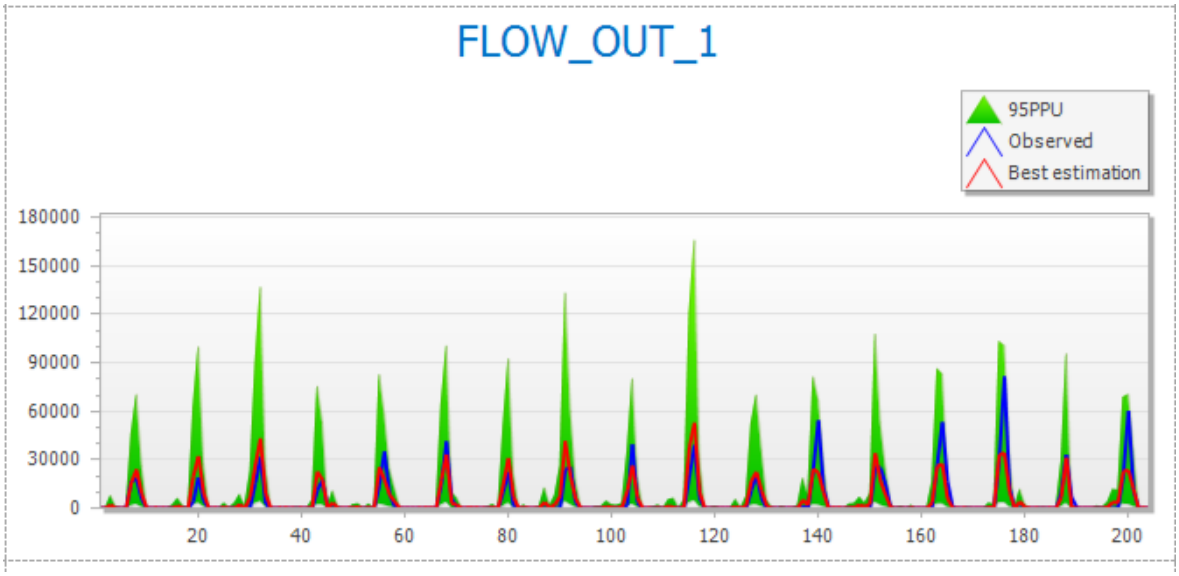

Goal_type= Nash_Sutcliff No_sims= 500 Best_sim_no= 24 Best_goal = 6.959938e-001

Variable	p-factor	r-factor	R2	NS	bR2	MSE	SSQR	PBIAS	KGE	RSR	MNS	VOL_FR	---	Mean_sim(Mean_obs)	S
FLOW_OUT_1	0.54	3.22	0.70	0.70	0.4635	4.3e+007	1.2e+007	1.1	0.74	0.55	0.67	1.01		5009.19(5065.44)	

---- Results for behavioral parameters ---
Behavioral threshold= 0.500000
Number of behavioral simulations = 100

Variable	p-factor	r-factor	R2	NS	bR2	MSE	SSQR	PBIAS	KGE	RSR	MNS	VOL_FR	---	Mean_sim(Mean_obs)	S
FLOW_OUT_1	0.51	0.41	0.70	0.70	0.4635	4.3e+007	1.2e+007	1.1	0.74	0.55	0.00	1.01		5009.19(5065.44)	

Figure 7-7: Summary statics of sediment validation using SUFI-2 results.

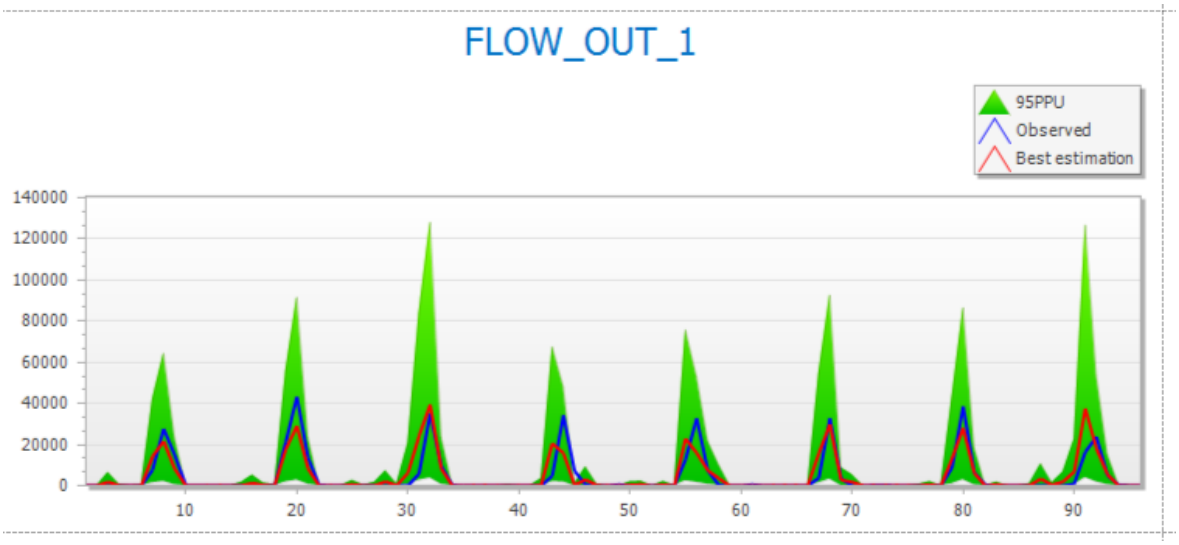

Goal_type= Nash_Sutcliff No_sims= 500 Best_sim_no= 468 Best_goal = 7.130306e-001

Variable	p-factor	r-factor	R2	NS	bR2	MSE	SSQR	PBIAS	KGE	RSR	MNS	VOL_FR	---	Mean_sim(Mean_obs)	S
FLOW_OUT_1	0.56	1.49	0.72	0.71	0.5562	2.7e+007	4.0e+006	-5.7	0.82	0.54	0.63	0.95		4685.39(4433.44)	

---- Results for behavioral parameters ---
Behavioral threshold= 0.500000
Number of behavioral simulations = 158

Variable	p-factor	r-factor	R2	NS	bR2	MSE	SSQR	PBIAS	KGE	RSR	MNS	VOL_FR	---	Mean_sim(Mean_obs)	S
FLOW_OUT_1	0.41	0.39	0.72	0.71	0.5562	2.7e+007	4.0e+006	-5.7	0.82	0.54	0.00	0.95		4685.39(4433.44)	